Universidad EAFIT

School of Sciences

Department of Mathematical Sciences

Thesis defended by **Diana Paola Lizarralde-Bejarano**

Defended on **25th August, 2021**

A thesis submitted in partial fulfillment of the requirements for the degree of Doctor of Philosophy in Mathematical Engineering from Universidad EAFIT

Academic Field **Mathematical Engineering**

Speciality **Biomathematics**

Interval analysis for handling uncertainty in epidemiological models

based on ODEs that simulate the transmission of infectious diseases with application to Dengue transmission

Thesis supervised by	María Eugenia Puerta Yepes	Supervisor
	Sair Arboleda	Co-Supervisor

Committee members

Referees	Azmy S. Ackleh	Professor at University of Louisiana
	María Lourdes Esteva Peralta	Professor at Universidad Autónoma de México (UNAM)
	Olga Lucía Quintero	Professor at Universidad EAFIT
Supervisors	María Eugenia Puerta Yepes	Professor at Universidad EAFIT
	Sair Arboleda	Senior Researcher at Universidad de Antioquia (UdeA)

Colophon

Doctoral dissertation entitled "Interval analysis for handling uncertainty in epidemiological models", written by Diana Paola Lizarralde-Bejarano, completed on 17th August, 2021, typeset with the document preparation system LaTeX 2_ε and the `yathesis` class.

Year: 2021
Title: Interval analysis for handling uncertainty in epidemiological models based on ODEs that simulate the transmission of infectious diseases with application to Dengue transmission

Author: Diana Paola Lizarralde-Bejarano
Print: Universidad EAFIT, Medellín, Colombia

To my dear Ruu and my lovely Agdis

Contents

Acknowledgements

First and foremost, I would like to thank my advisor, Maria Eugenia Puerta, for her help and support during this journey. I am incredibly thankful for all her comments, career advice, and the freedom she gave me during my Ph.D. I especially thank her for her constant support and calls during the COVID crisis during which I wrote this thesis.

This doctoral thesis would have been impossible without the kind help of my co-supervisor, Sair Arboleda, who shared invaluable biological insights and interpretations with me during the first stage of my Ph.D. I got inspired by her explanations, which I have used throughout my research.

I am most grateful to Prof. Kearfott for his mathematical insights and relevant comments in different matters concerning the topic of this thesis. I also owe special thanks to his wife, Ruth Mentley, for the gracious hospitality she extended to me during my research internship at the University of Louisiana at Lafayette in The United States. I was very fortunate to have a weekly discussion with Professor Hayriye Gulbudak in Lafayette. I learned so much from her.

I want to acknowledge the Department of Mathematical Science at Universidad EAFIT for giving me the opportunity to pursue my Ph.D. I owe special thanks to Olga Lucia Quintero for her persistence in matters concerning my Ph.D. Without her efforts in organising the doctorate program and the scholarship program that provided financial support, this thesis would not have been possible. In the same regard, I would also like to thank the Colombian Administrative

Department of Science, Technology, and Innovation (Colciencias) for providing me with additional financial support for these last four years of my project. I also would like to appreciate my professors María Gulnara Baldoquín, Juan Carlos Rivera, and Andrés Sicard-Ramírez at EAFIT for their insightful comments and valuable advice during the courses of my training component.

I am privileged to receive the company and support of my friends and office mates at EAFIT. I want to extend special thanks to Juan David Palacio and Camilo Rodriguez for supplying the endless amount of sugar and coffees during our working breaks to keep up my motivation. I am also grateful to Julian Ceballos and Andrés Duque for raising my tennis game and many other things. Thanks to Leandro Ariza, Alejandro Gómez, Santiago Lopez, Santiago Ortiz, Juan G. Paniagua, Andrés Perez and Andrés Yarce for the company and talks.

I would like to thank all my coauthors. I have enjoyed our exciting discussions. I would like to give a special mention to Alexandra Cataño and Daniel Rojas. I like to mention people of the weekly seminar at the math department, where I had the chance to share part of my research. I express my special thanks to Carlos Mario Vélez and Carlos Cadavid for their exciting comments and questions during my talks that enhanced the quality of thesis in many ways.

I am profoundly thankful to the Graham Linge family, especially for all their efforts for making my thesis writing bearable in charming and inspiring in Bergen. I cannot thank enough to Camila Pachecho and Diana Piedra for countless cooking and chatting sessions.

Above all, I would like to thank my family and all my friends. Their constant encouragement and support helped me sail through tough times during my Ph.D. I am forever indebted to Agda Tomasa, my mom Elsa Bejarano, my sister Andrea Lizarralde and her family, and my partner Jonathan Prieto Cubides and his family. Now, I know what matters in life.

Introduction

Outline of the current chapter

Recently, research in mathematical modeling has gained momentum due to its wide-spread application in various disciplines of science. In this thesis, we focus on mathematical epidemiology, particularly to treat uncertainty in the parameters and the initial conditions of models through interval analysis theory based on systems of differential equations (ODEs) that simulate the transmission of vector-borne diseases. This thesis considers dengue transmission disease as a case study.

In the formulation of ODES, it is relevant to examine the type of information that can collect and clearly delimit the objective or the question to be answered with these models. Based on this objective, we define the variables and parameters that are included in the model. The available information allows us to define the approximate parameters ranges and the initial condition ranges that make biological sense and answer the original question.

However, a major problem with this kind of application is dealing with

the uncertainty present in the process of measuring and obtaining information required to explain a real phenomenon. In particular, when we study the transmission of dengue diseases, it is possible to identify diverse uncertainty sources due to the inability to accurately and reliably measure all the quantities involved in the formulation of the model. For instance, these impossibilities can be (i) in measuring the transmission rates between humans and vectors; (ii) in accurately measuring the size of the vector populations in each developmental stage; (iii) in the measurement of vector mortality that only reflects mortality from natural causes and not from external causes since the latter cannot be simulated in the laboratory; and (iv) in measuring the recovery rate in humans.

On the other hand, according to the *World Health Organization* (WHO), there has been an increase in the number of dengue cases reported worldwide in recent years. This may be because the virus and the transmitting vectors have spread to new regions. Moreover, due to the existing difficulty in diagnosing this disease, it is possible that some cases are not classified correctly. Thus, the information handled by official entities not reliable.

For all the reasons mentioned above, it is crucial to model appropriate the uncertainty of both parameters and information without assuming additional hypotheses that cannot be verified. Moreover, it is necessary to validate and support the models with disease-specific data to obtain more trustworthy conclusions.

In this thesis, we intend to make a formal treatment of the parameters and initial conditions uncertainty of epidemiological mathematical models involved in the framework of the theory of interval analysis [69, 52, 100] by always maintaining the biological meaning of all values.

From the mathematical point of view, we will consider the initial value problem (IVP) in ODEs given by

$$\dot{y}(t) = f(t, y, \theta), \qquad y(t_0) = y_0, \tag{1}$$

where $t \in [t_0, t_f]$, $t_f > t_0$, $\theta \in \Theta$ is the p-dimensional vector of parameters, y is the n-dimensional vector of state variables, and y_0 is the n-dimensional vector of initial conditions. Furthermore, Θ and x_0 are interval vectors that represent the enclosures of the uncertainties of parameters and initial conditions, respectively. The purpose here is to obtain mathematically and computationally guaranteed enclosures for the vector of state variables y at all times, i.e. from t_0 to t_m, and compare these enclosures with the behavior of real data.

It is possible to define both the direct and the inverse problem from Equation (1) and the interval experimental data vector $X_i = (X_{i_1}, X_{i_2}, \ldots, X_{i_k})$, with $1 \leq i \leq n$, where n is the number of variables, and k denotes the number of measurements at different times. When the vector field f in Equation (1) is nonlinear,

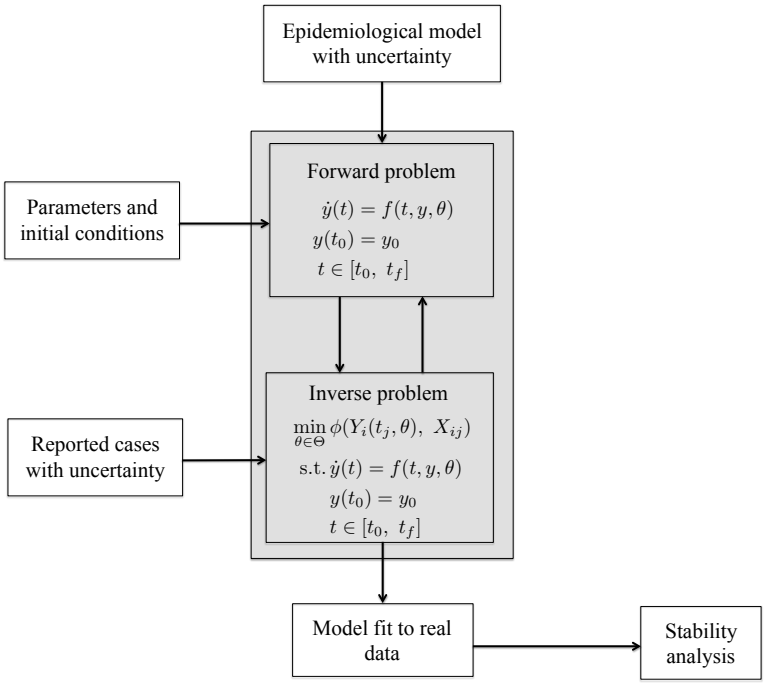

Figure 1 – **Problem statement**: Figure shows the input and output for the forward and the inverse problem considered in this thesis, and the connection between them.

the direct problem mainly consists of getting a numerical solution of this system. To compute these solutions, it is necessary to define initial parameters and initial

conditions considering the phenomenon's features and obtain mathematically reliable solutions. In this direction, a lot of work has been done for the case in which the initial conditions are real closed intervals, and there exist several available software packages to deal with this case. However, relatively little work has been done on the case in which parameters are given by intervals [52]. Here, we use the validated solver VSPODE (Validating Solver for Parametric ODEs) for parametric ODEs to obtain guaranteed enclosures on the solution of Equation (1) when we consider parameters and initial conditions as intervals. Deeper discussions on different methodologies, the main drawbacks such as overestimation caused by the dependency problem and wrapping effect and how they have been solved are mentioned in [72, 55, 74].

On the other hand, the inverse problem estimates the parameter's values that minimize the error between the data, and the model output as the actual data always contain some amount of noise. Some common ways that noise may arise are errors in digitizing information, measurement errors, and numerical round-off errors.

One of the strategies to solve this problem is through the formulation of an optimization problem, Equation (2), given by

$$\begin{aligned} &\min_{\theta \in \Theta} \phi(Y_i(t_j, \theta), X_{ij}) \\ &\text{s.t. } \dot{y} = f(t, y, \theta) \\ &\quad y(t_0, \theta) = y_0(\theta) \\ &\quad t \in [t_0, t_f] \end{aligned} \tag{2}$$

where ϕ is the objective function that measure the error, θ is a p-dimensional parameter vector, $Y_{ij} = Y_i(t_j, \theta)$ and X_{ij} are the solution of the ODEs and the experimental data for the variable i at the time t_j, respectively. Usually, ϕ is considered as the l_2-norm or Euclidian length to measure the fit. However, it

is not the only measure that can be applied. An alternative error measure that is better in many situations is the l_1-norm, since it is less sensitive to outliers, further discussion can be found in [4].

When parameters are real numbers, the optimization problem in Equation (2) can be solved by applying local search algorithms as the steepest descent method, the Gauss-Newton method, or the Levenberg-Marquard method. However, one of the greatest drawbacks of these methods is the huge dependence on the initial point. This makes it possible to fall into a local optimum easily. In particular, in biological systems, there are many local optima. This means that global optimization algorithms should be used to explore the parameter space but no assurance can be given that a global minima has been found. Such global methods are usually described using meta-heuristics. Some advantages of these methods are that they do not require much information about the problem to be solved, and it is not necessary to calculate derivatives of first or second order, which means that they can be applied to discontinuous problems. Among the most used meta-heuristics to solve Equation (2), are genetic algorithms, particle swarm optimization, and simulated annealing, as in [21, 86, 95]. Interval arithmetic is applied to obtain decision variables in a guaranteed way. In this context, interval algorithms, such as the Interval Newton method and the interval gradient method [39] allow obtaining verified solutions by exploiting the monotonicity and convexity characteristics of the functions by evaluating the first and second-order derivatives. In this way, it is possible to eliminate sub regions where it is guaranteed that there are no solutions. The regions with possible solutions are bisected to obtain narrower solutions, and the monotonicity and convexity criteria are applied again. For the case in which a closed expression is not known for the objective function, some authors have proposed to solve Equation (2) using a numerical verified solver for the dynamical system with the values obtained from solving the minimization problem. To define monotonicity and convexity

criteria, the ODEs are augmented with their first and second-order sensitivity equations [47].

In summary, this study was designed to incorporate uncertainty in parameters and initial conditions of epidemiological models that simulate the transmission of vector-borne diseases through the application of interval analysis, where the available information is not accurate and sufficient because of the characteristics of these diseases. To this end, we will perform local sensitivity analysis and structural identifiability analysis to select the parameters and initial conditions, to which we will incorporate the uncertainty due to the lack of information and due to lack of measurement precision.

Finally, it is important to mention that as part of the formulation of a suitable mathematical model to simulate the transmission of vector-borne diseases, it is important to (i) clarify the objective and question to answer with the model. (ii) consider the available information to define initial biological ranges for parameters and initial conditions. (iii) perform structural identifiability analysis to select models that can produce uniqueness in the parameter estimation' solution when we assume noise-free data. (iv) includes uncertainty in a coherent way with the information, preferably without adding extra hypotheses. (v) choose as much as possible the best set of parameters that solve the parameter estimation problem, taking into account the biological interpretation of these solutions.

Considering all the facts and approaches mentioned above, we expect to increase these mathematical models' reliability to comprehend these phenomena better.

Goals

Main goal

The main aim of this study is to formulate and solve an optimization model based on interval analysis to handle the uncertainty present in the mathematical modeling of infectious disease transmission with an application to dengue using differential equations systems.

Specific goals

- Formulate the structure of the ODEs to understand the transmission of an infectious disease with parameters defined in the real interval space $\mathbb{IR}^p$.
- Determine a strategy to solve numerically epidemiological models formulated in the previous item where the parameters and initial conditions might belong to $\mathbb{IR}^p$.
- Estimate each mathematical model's parameters and compare them with the expected biological values so that models have more biological meaning.
- Identify the stability regions of the formulated models' equilibrium points to understand the transmission of infectious disease by constructing Lyapunov's functions depending on the parameters of the models mentioned.

Outline and contributions of the thesis

The following thesis is further divided into Chapter 1 that includes the necessary background in epidemiological models and stability theory which will be further used in Chapters 3 and 6. We will also present the basic concepts of interval

analysis and the reasons to consider uncertainty in ODEs and how to incorporate it here.

In Chapter 3, we introduce three different models that simulate dengue transmission diseases. From the biological point of view, the main difference among these models is how we represent the transitions in the vector population. From the mathematical perspective, the main difference is the dimension of the parameter space and the space of the state variables. Additionally, we present the data used during this research, precisely the number of reported dengue cases per epidemiological week, and the biological ranges of the model's parameters obtained from the results of experimental assays with vector populations.

The main goal of this chapter is to provide a criterion to decide which model performs better considering the available information and the model structure. To do so, we calculated the *basic reproductive number* (R_0) and performed the structural identifiability analysis for each model. As the infected subsystem is the same for the three models, then the corresponding R_0 does not vary. Moreover, the elasticity results of R_0 show that the transmission rates, the recovery rate, and the mortality rate in mosquitoes are the most relevant parameters in producing secondary infections. On the other hand, we found that the vector initial conditions and the parameters that describe the vector development are not identifiable from the cumulative number of reported cases. The previous facts make it possible to determine the uncertain parameters that will be further used in the next chapter to simulate dengue transmission in Itagüí and Neiva.
Chapter 4 presents the strategy used to solve the forward problem in Equation (1) when we consider some parameters and initial conditions to be real closed intervals. This strategy is based on applying the Interval Taylor Series (ITS) and the formulation of Taylor models that depend on parameters and initial conditions. As usual, when a guaranteed solution is computed, the first phase of the numerical algorithm verifies the solution's existence and uniqueness. The

second phase is in charge of computing a tighter enclosure for the solution. A new Taylor polynomial is proposed to achieve this goal where the remainder is not enclosed in an interval but a parallelepiped. This approach is implemented in the VSPODE software, which is used in this study. Complete details of the algorithm are given by the authors in [52].

This chapter's main result is first to define the uncertain quantities (parameters and initial conditions) concerning the results of elasticity and structural identifiability analysis. Second, to obtain mathematically and computationally verified solutions for the model of seven variables that simulate dengue transmission disease. These solutions were computed for meaningful biological scenarios as the presence of larger mosquito populations and admitting uncertainty in relevant parameters that can not be measure accurately. Finally, we contrast the results obtained with actual dengue case data for the Colombian cities of Itagüí and Neiva. In this way, we have a broader picture, in which we consider the worst and the best cases of the studied phenomenon.

Chapter 5 presents the algorithm used to solve the inverse problem described in Equation (2) when the uncertainty in parameters is considered. Furthermore, the definitions of strong and weak compatibility were adapted for ODEs to introduce a qualitative measure of compatibility between the interval data and the model's output.

The main result of this chapter is the formulation of the new algorithm PISA (Parameter Interval Search Algorithm) to estimate interval parameters. In the algorithm's formulation, we exploit the biological features of our case study to eliminate the regions where reasonable solutions are not found. For instance, considering the exponential growth at the outbreak's beginning in each municipality, we assume the average number of infected secondary humans greater or equal to one ($R_{0_H} \geq 1$). This assumption agrees with the definition of an epidemic outbreak for these cities. PISA applies this reasoning in F1 to eliminate

regions without biological sense. Then, to define a monotonicity criterion, we establish a set of directions in which the cumulative number of infected human increase. These directions are determined by considering the results from the elasticities of R_0. We proceed in this way since it was impossible to calculate the enclosure for the gradient of the objective function for our case study without increasing the system's dimension. Under these considerations, PISA was successfully applied to estimate the most sensitive interval-valued parameters for Itagüí and Neiva. Furthermore, we regard the stability results that allow us to determine which equilibrium point emerges according to the value of R_0. Thus, we can define the uncertainty level in initial conditions such that the model trajectories tend to the same equilibrium. With this in mind, we compute the compatibility measure to determine how much the estimated parameters and the initial conditions explain additional noise in the data.

In Chapter 6, the strategy proposed by Parrilo in [84] to compute polynomial Lyapunov's function is presented. These results are classical in systems and control theory but not well known in the community of mathematical epidemiology. This approach is relatively new in solving a semidefinite optimization problem. Moreover, there are already tools that allow computing these functions automatically for fixed parameter values. Following this approach, we proved the stability of both equilibrium points for the dengue transmission model of seven state variables. Additionally, for the interval-valued parameters estimated by PISA, we conclude that Model 3.3 has one unique globally stable equilibrium point, the diseases-free point.

Conclusions and directions for further research are given in Section 6.5.

We list below the publications, conference abstracts and some manuscripts that are in preparation:

- Lizarralde-Bejarano, Diana Paola, Arboleda-Sánchez, Sair, and Puerta-Yepes, María Eugenia. Stability analysis of nonlinear systems using opti-

mization techniques. International Conference on Applied Mathematics and Informatics, ICAMI 2017. Conference, pp. 86.

- Catano-Lopez, Alexandra, Rojas-Diaz, Daniel, Laniado, Henry, Arboleda-Sánchez, Sair, Puerta-Yepes, María Eugenia, and Lizarralde-Bejarano, Diana Paola. An alternative model An alternative model to explain the vectorial capacity using as example *Aedes aegypti* case in dengue transmission. Heliyon 5.10 (2019). DOI: 10.1016/j.heliyon.2019.e02577

- Lizarralde-Bejarano, Diana Paola, Rojas-Díaz, Daniel, Arboleda-Sánchez, Sair, and Puerta-Yepes, María Eugenia. Sensitivity, uncertainty and identifiability analyses to define a dengue transmission model with real data of an endemic municipality of Colombia. PLoS ONE 15.3 (2020). DOI: 10.1371/journal.pone.0229668.

- Lizarralde-Bejarano, Diana Paola and Puerta-Yepes, María Eugenia. Ch. 4: Canal endémico in: Modelos matemáticos y estadísticos para el pronóstico y entendimiento de enfermedades transmitidas por vectores, a partir de datos reales. Caso de estudio para dengue en Colombia. Submitted, pp. 41-50.

- Lizarralde-Bejarano, Diana Paola and Puerta-Yepes, María Eugenia. Ch. 5: Modelos matemáticos basados en sistemas de ecuaciones diferenciales in: Modelos matemáticos y estadísticos para el pronóstico y entendimiento de enfermedades transmitidas por vectores, a partir de datos reales. Caso de estudio para dengue en Colombia. Submitted, pp. 51-69.

- Lizarralde-Bejarano, Diana Paola, Gulbudak, Hayriye, Kearfott, Ralph Baker, and Puerta-Yepes, María Eugenia. Modeling two dengue outbreaks in Colombia considering interval uncertainty in parameters and initial conditions. Submitted.

- Lizarralde-Bejarano, Diana Paola, Prieto-Cubides, Jonathan, Kearfott, Ralph Baker, and Puerta-Yepes, María Eugenia. Parameter estimation considering interval uncertainty. In preparation.

In addition, an academic internship was done in the Department of Mathematics, University of Louisiana at Lafayette, U.S.A.

Bibliography of the current chapter

[4] Richard C Aster, Brian Borchers, and Clifford H Thurber. Parameter estimation and inverse problems. Elsevier, 2018 (cit. on pp. 7, 119).

[21] Yamille Del Valle, Ganesh Kumar Venayagamoorthy, Salman Mohagheghi, Jean-Carlos Hernandez, and Ronald G Harley. Particle swarm optimization: basic concepts, variants and applications in power systems. IEEE Transactions on evolutionary computation 12.2 (2008), pp. 171–195 (cit. on p. 7).

[39] Eldon Hansen and G William Walster. Global optimization using interval analysis: revised and expanded. Vol. 264. CRC Press, 2003 (cit. on pp. 7, 143).

[47] Michel Kieffer and Eric Walter. Guaranteed estimation of the parameters of nonlinear continuous-time models: Contributions of interval analysis. International Journal of Adaptive Control and Signal Processing 25.3 (2011), pp. 191–207 (cit. on pp. 8, 143).

[52] Youdong Lin and Mark A. Stadtherr. Validated solutions of initial value problems for parametric ODEs. Applied Numerical Mathematics 57.10 (2007), pp. 1145–1162. DOI: https://doi.org/10.1016/j.apnum.2006.10.006 (cit. on pp. 4, 6, 11, 92, 117, 118, 143).

[55] Rudolf J Lohner. On the ubiquity of the wrapping effect in the computation of error bounds. In: Perspectives on enclosure methods. Springer, 2001, pp. 201–216 (cit. on pp. 6, 36, 37, 90).

[69] Ramon E Moore, R Baker Kearfott, and Michael J Cloud. Introduction to Interval Analysis. Siam, 2009 (cit. on pp. 4, 29).

[72] Nedialko S Nedialkov, Kenneth R Jackson, and George F Corliss. Validated solutions of initial value problems for ordinary differential equations. Applied Mathematics and Computation 105.1 (1999), pp. 21–68 (cit. on pp. 6, 35, 90, 93, 110, 143).

[74] Markus Neher, Kenneth R Jackson, and Nedialko S Nedialkov. On Taylor model based integration of ODEs. SIAM Journal on Numerical Analysis 45.1 (2007), pp. 236–262 (cit. on pp. 6, 91).

[84] Pablo A Parrilo. Structured semidefinite programs and semialgebraic geometry methods in robustness and optimization. California Institute of Technology, 2000 (cit. on pp. 12, 148–150).

[86] M Peifer and J Timmer. Parameter estimation in ordinary differential equations for biochemical processes using the method of multiple shooting. IET Systems Biology 1.2 (2007), pp. 78–88 (cit. on p. 7).

[95] Aymée de los Angeles Marrero Severo, Liuva M Pedroso Rodríguez, and Jorge Barrios Ginart. Algoritmos evolutivos en la solución de problemas de estimación de parámetros. Revista de Matemática: Teoría y Aplicaciones 13.2 (2006), pp. 139–150 (cit. on p. 7).

[100] Luciano Stefanini and Barnabas Bede. Generalized Hukuhara differentiability of interval-valued functions and interval differential equations. Nonlinear Analysis: Theory, Methods and Applications 71.3-4 (2009), pp. 1311–1328 (cit. on p. 4).

Chapter 1

Background

Outline of the current chapter

1.1 Abstract

In this chapter, we cover the preliminary materials required in the development of this thesis. in Section 1.2 we present a brief review of state-of-art epidemiological models based on ODEs, the general characteristics of these models, and how to calculate the *Basic Reproductive Number*. Then, we present our case study (dengue transmission) and how we compute the interval ranges for model parameters based on the results from experimental assays. A quick introduction of interval arithmetic, interval-valued functions, and an explanation of two of the principal reasons for the overestimation in interval arithmetic computations are also mentioned in Section 1.3. Finally, we compiled some definitions and results about stability theory in the Lyapunov sense.

1.2 Epidemiological models

Recently, there has been an increasing interest in understanding and identifying the main factors involved in the transmission and spread of infectious diseases through different strategies, such as as the formulation of models based on Ordinary Differential Equations systems (ODEs), the construction of risk maps considering external factors (social and environmental) [109, 101, 82], the analysis of development features of vector population through experimental assays [87, 10], and the formulation of statistical models that consider information from social media [59].

The focus of this chapter is on ODE models, which are formulated as Initial Value Problems (IVPs). This approach provides a key instrument to understand, explain, and determine when an outbreak of the disease occurs [42].

1.2.1 State-of-art

One of the first applications of mathematical models to epidemiology was the work carried out by Bernoulli in 1760 to explain the spread of smallpox. Later, in 1906, Hammer established that the course of an epidemic depends on the rate of contact between susceptible and infected individuals. This result is known as the *mass action law* [11], and it is an assumption that has considered through the years in the formulation of several compartmental models [93]. However, it was not until 1911 when Ronald Ross deduced from a compartmental model that to control the malaria transmission, it was sufficient to reduce the number of infected mosquitoes below a *threshold*. A few years later, McDonald in his work on malaria, named this threshold value *basic reproductive number*, R_0. The Basic Reproductive Number (R_0) is defined as the expected number of new cases of an infection produced by a typical infected individual in a wholly susceptible population over the full course of the infectious period [11]. In mathematical epidemiology, this number is one of the most important concepts since it is a threshold parameter that helps us to determine if the disease dies out ($R_0 < 1$) or if the disease persists ($R_0 > 1$).

In the Ross-McDonald model, the proportion of infected mosquitoes, x increases when the proportion of susceptible females feed on the blood of an infectious human, y, thereby becoming an infected mosquito with a transmission rate β, that depends on (a) the mosquitoes biting rate per time unit, (b) the probability of infection of a susceptible mosquito when biting an infected human, and (c) the proportion of infected humans, y. The proportion of infected mosquitoes decreases at rate μ, where μ is the natural mortality rate for mosquitoes.

Similarly, the proportion of infected humans, y increases when a proportion of infected females feed on the blood of a susceptible human, y, thereby be-

coming an infected mosquito with a transmission rate α, that depends on (a) the probability of infection of a susceptible human by infected mosquito biting, and (b) the number of female mosquitoes per human. Finally, the proportion of infected humans decreases at rate γ, where γ is the recovery rate for humans ($1/\gamma$ is the duration of the recovery period).

The model based on these assumptions is given by the following system of differential equations:

$$\begin{aligned} \frac{dx}{dt} &= \beta y(1-x) - \mu x \\ \frac{dy}{dt} &= \alpha x(1-y) - \gamma y \end{aligned} \tag{1.1}$$

The threshold associated with this model is given by $R_0 = \frac{\beta\alpha}{\gamma\mu}$.

Finally, in 1927 Kermack and McKendrick formulated a compartmental model based on differential equations to explain the occurrence of an epidemic [46]. This model follows the simple rule input-output and considers the size of the population constant during the epidemic. The total population is divided in three compartments, Susceptible, S, Infected, I, and Recovered, R. The model based on these assumptions is given by:

$$\begin{aligned} \frac{dS}{dt} &= -\beta \frac{I}{H} S \\ \frac{dI}{dt} &= \beta \frac{I}{H} S - \gamma I \\ \frac{dR}{dt} &= \gamma I \end{aligned} \tag{1.2}$$

where the basic reproductive number is $R_0 = \frac{\beta}{\gamma}$. These two models have established the foundations in the formulation of new compartmental models for understanding and studying the dynamics of different diseases such as smallpox, measles, dengue, and HIV-AIDS to name a few [20, 2, 33]. As a result, in the recent years, there has been an exponential growth in the formulation of several epidemiological models to understand transmission, evaluate control strategies,

vaccination strategies, and spread of a particular disease [3, 93, 98, 44].

At this point, it is important to highlight that the formulation of models depend on the specific questions to be answered. For example, a model that only wants to understand the transmission of a certain disease can be different from a model that helps to propose different strategies of control, and these, in turn, will be different from a model that wants to analyze the spread of a disease from one population to another.

For instance, the model introduced in [110] was proposed to describe the transmission dynamic of Dengue virus, and the established control strategies over mosquito's population. Hence, the model included all developmental stages of the vector (eggs, larvae, and pupae) which corresponds to the first three equations. The following three equations corresponds to adult population of mosquitoes (susceptible, exposed, and infected), and the last four corresponds to human population (susceptible, exposed, infected and recovered). The parameters which represent control are μ_l', μ_p', μ_w' which have to be interpreted as the additional mortality rates produced in larvae, pupae and adult mosquitoes as a consequence of application of chemical (larvicides, fumigations) in each stage of

the vector.

$$\begin{aligned}
\frac{dE}{dt} &= \phi\left(1-\frac{E(t)}{C'}\right)W(t) - (\sigma_e+\mu_e)E(t)\\
\frac{dL}{dt} &= \sigma_e E(t) - (\sigma_l+\mu_l+\mu_l')L(t)\\
\frac{dP}{dt} &= \sigma_l L(t) - (\sigma_p+\mu_p+\mu_p')P(t)\\
\frac{dW_1}{dt} &= \sigma_p P(t) - \left[\beta_w\frac{I(t)}{N}+\mu_w+\mu_w'\right]W_1(t)\\
\frac{dW_2}{dt} &= \beta_w\frac{I(t)}{N}W_1(t) - (\gamma_w+\mu_w+\mu_w')W_2(t)\\
\frac{dW_3}{dt} &= \gamma_w W_2(t) - (\mu_w+\mu_w')W_3(t)\\
\frac{ds}{dt} &= \mu_h - \left[\beta_h\frac{W_3(t)}{W(t)}+\mu_h\right]s(t)\\
\frac{de}{dt} &= \beta_h\frac{W_3(t)}{W(t)}s(t) - (\gamma_h+\mu_h)e(t)\\
\frac{di}{dt} &= \gamma_h e(t) - (\sigma_h+\mu_h)i(t)\\
\frac{dr}{dt} &= \sigma_h i(t) - \mu_h r(t)
\end{aligned} \tag{1.3}$$

In [81], it is shown that an endemic SIR model may be sufficient to simulate the transmission of Dengue in some populations i.e. it is not always necessary to consider explicitly mosquito population as in Model 1.4.

$$\begin{aligned}
\frac{dH_S}{dt} &= B_H - \beta\frac{H_I}{H}H_S - \mu_H H_S\\
\frac{dH_I}{dt} &= \beta\frac{H_I}{H}H_S - (\gamma_H+\mu_H)H_I\\
\frac{dH_R}{dt} &= \gamma H_I - \mu_H H_R
\end{aligned} \tag{1.4}$$

In recent years, the dispersion and transmission of one disease from one place to another have taken the strength of the formulation of meta-population models [5]. These consist of dividing the populations into several sub-populations, leading to the formulation of a model for each sub-population taking into account the mobility of one group to the other. For example, in Model 1.5, two

patches are considered; in each patch there is a population N_1 and N_2, respectively. An epidemic SIR model was formulated for each patch, where the parameters are different for each population, and the p_{ij} is defined as the fraction of the time that the individuals of the i patch are in the patch j. The details of the model are described in [11].

$$\begin{aligned}
S_1' &= -\beta_1 p_{11} S_1 \left[p11 \frac{I_1}{N_1} + p_{21} \frac{I_2}{N_2} \right] - \beta_2 p_{12} S_1 \left[p12 \frac{I_1}{N_1} + p_{22} \frac{I_2}{N_2} \right] \\
I_1' &= \beta_1 p_{11} S_1 \left[p11 \frac{I_1}{N_1} + p_{21} \frac{I_2}{N_2} \right] + \beta_2 p_{12} S_1 \left[p12 \frac{I_1}{N_1} + p_{22} \frac{I_2}{N_2} \right] - \gamma_1 I_1 \\
S_2' &= -\beta_1 p_{21} S_2 \left[p11 \frac{I_1}{N_1} + p_{21} \frac{I_2}{N_2} \right] - \beta_2 p_{22} S_2 \left[p12 \frac{I_1}{N_1} + p_{22} \frac{I_2}{N_2} \right] \\
I_2' &= \beta_1 p_{21} S_2 \left[p11 \frac{I_1}{N_1} + p_{21} \frac{I_2}{N_2} \right] + \beta_2 p_{22} S_2 \left[p12 \frac{I_1}{N_1} + p_{22} \frac{I_2}{N_2} \right] - \gamma_2 I_2
\end{aligned} \tag{1.5}$$

Thus, depending on the question formulated, a model can be more complex than others. This fact is reflected in the number of variables and the number of parameters to estimate, as observed in Models 1.3 to 1.5.

1.2.2 General aspects of models

Epidemiological models considered in this research will be based on non-linear ODEs, $\dot{x}(t) = f(x(t))$, where f is a polynomial. The formulation of these compartmental models follows the same rules of the balance equations, "input minus output".

These compartments allow to split the populations into different states, for example, susceptible, infected, and recovered in Model 1.2. Nevertheless, the systems that will be analyzed in this work will have the same polynomial structure. The vector field of these systems are polynomials up to degree two or rational functions when populations change along the time. For instance, in Model 1.3, if we consider N and $W(t)$ constants in the time, we are in presence of a polynomial system, but if N, and $W(t)$ change in the time, then the vector

field in Model 1.3 will not be polynomial.

Additionally, all interactions between several compartments follow the mass action law which establishes that the number of infectious contacts for time unit is directly proportional to the number of contacts between infectious (denoted by I) and susceptible (denoted by S) individual. Mathematically, we can express the mass action law as follows

$$\#\text{ of infectious contacts} = k\,S\,I$$

where, k is the constant of proportionality that can be decomposed as the product between the successful transmission probability of the virus from one infected individual to a susceptible individual, and the number of contacts per individual.

In this case study, a suitable range or interval of values with biological meaning for the state variables, parameters and initial conditions can be found in our models since all of these quantities are bounded beforehand. Finally, it is possible to define *the basic reproductive number*, R_0, for each model in terms of the model parameters. Eventually, from the value of R_0 it is possible to determine the occurrence or non-occurrence of an outbreak.

1.2.3 Basic Reproductive Number

The Basic Reproductive Number (R_0), is defined as the expected number of new cases of an infection produced by a typical infected individual in a wholly susceptible population over the full course of the infectious period [11]. In mathematical epidemiology, this number is one of the most important concepts, since it is a threshold parameter that helps us to determine if the disease dies out ($R_0 < 1$) or if the disease persists ($R_0 > 1$).

Several strategies have been proposed to calculate R_0. However, for a fixed model, the R_0 values calculated with the different strategies may differ. This

shows the difficulty in accurately calculating the number of secondary infections within an entirely susceptible population [99]. Here, to compute R_0, we applied the *Next Generation Matrix* (NGM) around the disease-free equilibrium point following the strategy presented in [23]. We outline the strategy to calculate R_0 in the following steps.

1. Identify the *ODE* system that describes the production of new infections and changes in state among infected individuals. The set of such equations are hereafter referred to as the infected subsystem in this study.

2. Linearize the infected subsystem of nonlinear ODEs about the infection-free steady state. A matrix can describe this linear system. Here, we refer to this matrix as the Jacobian matrix of the infected system and we denote it by J.

3. Rewrite the matrix J as $T + \Sigma$, where T is the *transmission part*, describing the production of new infections, and Σ is the *transition part*, describing changes in state (including removal by death or the acquisition of immunity).

4. Finally, we compute the dominant eigenvalue, or more precisely the spectral radius ρ of the matrix $\mathbf{K} = -T\Sigma^{-1}$. The matrix $\mathbf{K}$ is called the *next-generation matrix* (NGM) and R_0 the dominant eigenvalue of this matrix [22].

This approach provides the geometric mean of the number of infections per generation [40].

1.2.4 Case study: Dengue transmission

Dengue is a viral disease transmitted by the bite of infected female *Aedes* mosquito. There are four distinct closely related serotypes of the virus that

cause dengue (DEN-1, DEN-2, DEN-3 and DEN-4). Dengue is present in tropical and subtropical climates throughout the planet, especially in urban and semi-urban areas. Symptoms appear between 3 or 14 days (average 4 – 7 days) after an infective bite [79]. *Aedes aegypti* is the principal vector who transmits Dengue virus. The transmission cycle begins with a human infected by any serotype that was bitten by a female mosquito. After a period of incubation of the virus that lasts between four and ten days, an infected mosquito can transmit the pathogen throughout life. The symptomatic and asymptomatic persons are the main carriers and multipliers of the virus [78]. After the first symptoms, infected people can transmit the virus to mosquitoes for four or five days but no more than twelve days.

The *Aedes aegypti* lives in urban habitats and reproduces mainly in artificial containers. Unlike other mosquitoes, *Aedes aegypti* feeds during the day; the bites intensify in the morning and in the evening, before it gets dark. In each feeding period, the female mosquito can bite many people. The four serotypes of the virus can circulate simultaneously in the same region [80]. Besides, the infection by one of the four serotypes mentioned above generates a permanent immunity to the human only for that serotypes and a temporary immunity for the other ones. Consequently, during their life, a person can suffer all the serotypes of the dengue virus.

In the study of the dengue transmission, different compartmental models have been formulated. For instance, in [81] a *sir* model was formulated that considered birth and mortality rate as equal. In this paper, the *sir* model was used to simulate the epidemic of hemorrhagic dengue that occurred in Thailand between January 1984 and March 1985. On the other hand, to establish control strategies to limit the number of infected humans in a dengue epidemic, in [19] a model type Ross-McDonald was formulated and fitted to the dengue outbreak occurred in Cali, Colombia during 2013.

Other compartmental models include both populations involved in the transmission process (mosquitoes and human population) [29, 33], variable populations [28], and several serotypes [30]. These models have been analyzed qualitatively through the calculation of R_0 and the stability analysis of the equilibrium points that allows to determine regions of stability for different scenarios as the coexistence of different serotypes. Models have also been proposed that include a compartment for the aquatic phase in addition to the adult population of mosquitoes and humans [89]. In these models, the R_0 is also calculated from the available information through the calculation of the force of infection, while in [111, 32] models are formulated that include a compartment for each stage of development of the vector (egg, larva, pupa). These studies stress on the importance of the influence of the temperature in the entomological parameters and are evaluated in the occurrence or non-occurrence of an epidemic outbreak.

Other factors that have been considered to understand the dynamics of dengue is the vertical transmission in the vector population [31]. This hypothesis has gained momentum to explain the endemic state of the disease in some regions [1]. Furthermore, in recent years models have been formulated to evaluate different vaccination strategies [17, 44] and to assess the impact of biological controls; more specifically the behaviour of the vector population when interacting with mosquitoes with Wolbachia and how this impacts the number of cases of the disease [13, 43].

Finally, according to vector biology and the results presented in [57] about the increase in the mortality rate after the vector was infected, Professor Carlos Marío Vélez and his students (Alexandra Cataño, Camilo Londoño, and Daniel Rojas) in the framework of the project No. 111572553478 of COLCIENCIAS formulated a model following the concepts presented in [110]. Furthermore, they included in the model a new parameter α, which represents the increase in the mortality rate after the vector was infected that is in the compartmental

of infectious mosquitoes. Moreover, the evaluation of control-vector strategies could result in a new model.

1.2.5 Parameter and initial condition ranges

One of the greatest difficulties to work with ODEs in mathematical epidemiology, is to establish ranges of values for the parameters and initial conditions. These ranges help to define the feasible region to the optimization problem (parameter estimation) taking into account the differences between development rates of vector populations [88].

For this case study, laboratory data is available. Along these lines, we can define the initial ranges for some parameters and initial conditions of dengue transmission models. Within the parameters we found: (a) parameters to simulate the transition from one to another compartment (transition parameters) and (b) parameters to simulate the mortality rate in each compartment (mortality parameters).

For the transition parameters, we consider a cohort of individuals in a determined compartmental, A. We represent it by $u(s)$. If a fraction α leaves the compartmental A per unit of time, then

$$u'(s) = \alpha u(s)$$
$$u(s) = u(0)e^{-\alpha s}.$$

Thus, the average rate an individual spends in the compartment A follows an exponential distribution with expected value $1/\alpha$, where α is defined as the *period of time in A*.

For mortality parameters, we formulate the initial value problem (IVP) for

each compartmental

$$P'(t) = -\mu P(t)$$
$$P(0) = P_0$$

which has a solution $P(t) = P_0 e^{-\mu t}$, where μ represents the mortality rate. To establish the initial condition P_0 for each compartment, the modeler has to consider the available information and experimental assays results.

1.3 Introductory material to interval analysis

In this section, we introduce the basics of interval analysis that we will use later. The results presented in this section are based on [68, 69].

1.3.1 Interval arithmetic

Interval-arithmetic is largely attributed to Ramon Moore in the 1960s. He developed it to account for rounding errors linked to mathematical calculations rigorously. The object on which this theory is constructed is the set of closed intervals in $\mathbb{R}$.

$$\mathbb{IR} = \{X = [\underline{X}, \overline{X}] \mid \underline{X} \leq \overline{X},\ \underline{X}, \overline{X} \in \mathbb{R}\}. \tag{1.6}$$

Two intervals X and Y are equal if $\underline{X} = \underline{Y}$ and $\overline{X} = \overline{Y}$. Also, we say X is *degenerate* if $\underline{X} = \overline{X}$, thus, the real number X can be identified by a degenerate interval $[X, X]$.

Let $X = [\underline{X}, \overline{X}]$ and $Y = [\underline{Y}, \overline{Y}] \in \mathbb{IR}$, the interval-arithmetic operations are defined as follows:

1. $X + Y = [\underline{X} + \underline{Y}, \overline{X} + \overline{Y}]$.

2. $-X = [-\overline{X}, -\underline{X}]$.

3. $X - Y = X + (-Y) = [\underline{X} - \overline{Y}, \overline{X} - \underline{Y}]$.

4. $X \cdot Y = [\min\{S\}, \max\{S\}]$, where $S = \{\underline{X}\,\underline{Y}, \underline{X}\,\overline{Y}, \overline{X}\,\underline{Y}, \overline{X}\,\overline{Y}\}$.

5. $1/Y = [1/\overline{Y}, 1/\underline{Y}]$ such that $0 \notin Y$.

6. $X/Y = X \cdot 1/Y = \{x/y \,|\, x \in X,\ y \in Y\}$ such that $0 \notin Y$.

Addition and multiplication in $\mathbb{IR}$ are associative and commutative, but only sub-distributive: $(X * (Y + Z) \subseteq (X * Y) + (X * Z))$. The interval $[0, 0]$ plays the role of neutral element, while the interval $[1, 1]$ has the same role for multiplication. However, in general, for an arbitrary interval X there exists neither an additive nor multiplicative inverse, that is, $X - X = 0$ and $X * 1/X = 1$ are not satisfied. Thus, $(\mathbb{IR}, +, \cdot)$ is a monoid. We also define the following quantities for an interval $X = [\underline{X}, \overline{X}]$:

1. The width $w(X) = X - X$.

2. The absolute value or magnitude $|X| = \max\{|\underline{X}|, |\overline{X}|\}$.

3. The midpoint $m(X) = \frac{1}{2}(\overline{X} + \underline{X})$.

4. The ratio $rad(X) = \overline{X} - m(x)$.

From these measurements, it is possible to express each interval X as

$$X = [\underline{X}, \overline{X}] = m(X) + [-rad(x), rad(X)]. \tag{1.7}$$

We can even define an order relation between intervals as follows:

1. Let $X, Y \in \mathcal{I}$. $X < Y$ means that $\overline{X} < \underline{Y}$. This order relation is transitive.

2. Another transitive order relation on $\mathcal{I}$ is the set inclusion: $X \subseteq Y$ if and only if $\underline{Y} \leq \underline{X}$ and $\overline{X} \leq \overline{Y}$. Since it is not possible to compare all intervals between them, the set inclusion just defines a *partial order* in $\mathbb{IR}$.

1.3.2 Interval vectors and matrices

The interval definition, their properties and operation can be extended naturally to n-dimensional real interval vectors, $\mathbb{IR}^n$ and the set of $n \times m$ real interval matrices, $\mathbb{IR}^{n\times m}$. To perform the arithmetic operations between interval vectors and matrices we follow the same formulas as in the scalar case, but replacing the scalars by intervals.

Example 1.3.1. Consider the matrix $\mathbf{A} \in \mathbb{IR}^{3\times 2}$ and $\mathbf{X} \in \mathbb{IR}^2$ given by:

$$\mathbf{A} = \begin{pmatrix} [1,2] & [-3,-2] \\ [3,4] & [1,2] \\ [-2,-1] & [-1,1] \end{pmatrix} \text{ and } \mathbf{X} = \begin{pmatrix} [1,3] \\ [-1,2] \end{pmatrix} \tag{1.8}$$

then,

$$\mathbf{AX} = \begin{pmatrix} [1,2][1,3] + [-3,-2][-1,2] \\ [3,4][1,3] + [1,2][-1,2] \\ [-2,-1][1,3] + [-1,1][-1,2] \end{pmatrix} = \begin{pmatrix} [-5,10] \\ [1,16] \\ [-8,1] \end{pmatrix}.$$

For two matrices (or vectors) $\mathbf{A}$ and $\mathbf{B} \in \mathbb{IR}^{n\times m}$, we say that $\mathbf{A} \subseteq \mathbf{B}$ if and only if $[A_{ij}] \subseteq [B_{ij}]$ for each component ij of the matrix (or vector). Additionally, we can define the width, the midpoint, and the magnitude as follows.

1. The width of an interval matrix (or vector) $\mathbf{A}$ is given by the maximum width of their components

$$w(\mathbf{A}) = \max_{i,j} w(A_{ij})$$

2. The midpoint of an interval matrix (or vector) $\mathbf{A}$ is the real matrix (or vector) formed by the midpoint of each component

$$m(\mathbf{A})_{ij} = m(A_{ij})$$

3. For a vector **X** the maximum norm is given by

$$\| \mathbf{X} \| = \max_{1 \leq i \leq n} \{|X_i|\}.$$

4. For a matrix **A** the maximum norm is given by

$$\| \mathbf{A} \| = \max_{1 \leq i \leq n} \sum_{j=1}^{m} \{|A_{ij}|\}.$$

Example 1.3.2. For the interval matrix in Equation (1.8), we have:

$$\begin{aligned} w(\mathbf{A}) &= \max\{w([1,2]), w(-3,-2), w(3,4), w(-2,-1), w([-1,1])\} \\ &= 2 \end{aligned}$$

$$m(\mathbf{A}) = \begin{pmatrix} m([1,2]) & m([-3,-2]) \\ m([3,4]) & m([1,2]) \\ m([-2,-1]) & m([-1,-1]) \end{pmatrix} = \frac{1}{2} \begin{pmatrix} 3 & -5 \\ 7 & 3 \\ -3 & 0 \end{pmatrix}$$

$$\begin{aligned} \| \mathbf{A} \| &= \max\{|A_{11}| + |A_{12}|, |A_{21}| + |A_{22}|, |A_{31}| + |A_{32}|\} \\ &= \max\{|[1,2]| + |[-3,2]|, |[3,4]| + |[1,2]|, |[-2,-1]| + |[-1,1]|\} \\ &= 6 \end{aligned}$$

A distance measure between two interval vectors

Definition 1.3.1. A real-valued function d over a set S is a metric if for any x and $y \in S$ the following statements hold:

1. $d(x,y) = 0$ if and only if $x = y$
2. $d(x,y) = d(y,x)$
3. $d(x,y) \leq d(x,z) + d(z,y)$ for any $z \in S$

In this way, (S,d) is a metric space.

To determine the dissimilarities between two intervals we will consider the Hausdorff distance, which was initially proposed to measure the dissimilarity between two sets of a metric space. The definition of Hausdorff distance d_H between two sets $\mathcal{A}$ and $\mathcal{B}$ in $\mathbb{R}^n$ is given by

$$d_H(\mathcal{A},\mathcal{B}) = \max\left\{\sup_{a\in\mathcal{A}}\inf_{b\in\mathcal{B}} \| a-b \|, \sup_{b\in\mathcal{B}}\inf_{a\in\mathcal{A}} \| a-b \|\right\} \tag{1.9}$$

Then, the Hausdorff distance, d_H, between two intervals $X = [\underline{x},\overline{x}]$ and $Y = [\underline{y},\overline{y}] \in \mathbb{IR}$, is

$$\begin{aligned} d_H(X,Y) &= \max\{|\underline{x}-\underline{y}|, |\overline{x}-\overline{y}|\} \\ &= |m(X)-m(Y)| + |rad(X)-rad(Y)| \end{aligned} \tag{1.10}$$

Then for X and $Y \in \mathbb{IR}^n$ we have

$$d_H(X,Y) = \left\{\sum_{i=1}^{n} |d_H(X_i,Y_i)|^{\alpha}\right\}^{1/\alpha} \tag{1.11}$$

where, $\alpha > 0$.

Considering $\alpha = 1$ in Equation (1.11), we get

$$\begin{aligned} d_H(X,Y) &= \sum_{i=1}^{n} |d_H(X_i,Y_i)| \\ &= \sum_{i=1}^{n} |\max\{|\overline{x_i},\overline{y_i}|, |\underline{x_i},\underline{y_i}|\}| \\ &= \sum_{i=1}^{n} \max\{|\overline{x_i},\overline{y_i}|, |\underline{x_i},\underline{y_i}|\} \\ &= \sum_{i=1}^{n} |m(X_i)-m(Y_i)| + |rad(X_i)-rad(Y_i)|. \end{aligned} \tag{1.12}$$

For $\alpha = 2$ in Equation (1.11), we get

$$\begin{aligned} d_H(X,Y) &= \sqrt{\sum_{i=1}^{n} |\, d_H(X_i,Y_i)|^2} \\ &= \sqrt{\sum_{i=1}^{n} |\max\{|\overline{x_i} - \overline{y_i}|, |\underline{x_i} - \underline{y_i}|\}|^2} \\ &= \sqrt{\sum_{i=1}^{n} ||m(X_i) - m(Y_i)| + |rad(X_i) - rad(Y_i)||^2} \end{aligned} \tag{1.13}$$

In this manner, it is possible to define all the elements of local analysis, such as limits, sequences, continuity, convergence, differentiability, and integrability over the metric space $(\mathbb{IR}^n, d_H)$.

1.3.3 Interval-valued functions

An interval-valued function F can be defined as an *interval extension* of a real-valued function f, such that $\{f(x)|x \in X\} \subseteq F(X)$ and $F(X) = f(x)$ for degenerate intervals $X = [x,x]$. Moreover, for a real function $f : \mathbb{R}^n \to \mathbb{R}$ and an interval vector $\mathbf{X}$, it is possible to compute $F(\mathbf{X})$ by (1) replacing each occurrence of each real variable with the corresponding interval, (2) replacing the standard functions (e.g., e^x, $\cos x$, among others) with enclosures of their ranges, and (3) performing interval arithmetic operations instead of the real operations. However, in general, $f(\mathbf{X})$ is not unique, since it depends on how the function is expressed.

Example 1.3.3. Consider the function $f(x) = \frac{x}{1+x}$ with $x \in [1,2]$. The range of f over $[1,2]$ is $[\frac{1}{2}, \frac{2}{3}]$. Now consider two different interval extensions for this function

$$F(X) = \frac{X}{1+X}, X = [\underline{X}, \overline{X}]$$
$$G(X) = \frac{1}{1+\frac{1}{X}}, X = [\underline{X}, \overline{X}]$$

If X is a real number these two expressions are equivalent, otherwise, they are not when X is an interval

$$F([1,2]) = \frac{[1,2]}{1+[1,2]} = [\frac{1}{3},1]$$
$$G([1,2]) = \frac{1}{1+\frac{1}{[1,2]}} = [\frac{1}{2},\frac{2}{3}]$$

From these calculations, we observe that the natural interval-extension F overestimate the range of the function f, while the interval-extension G not.

In general, an interval extension $F(X_1, X_2, \ldots, X_3)$ of a real-valued function $f(x_1, x_2, \ldots, x_3)$ is only an upper approximation to the range of f, since there are multiple occurrences of some variables x_i in the formal expressions of f. In fact, a challenge in some applications is how to express f to obtain the narrowest possible interval extension $F(X)$ [72].

1.3.4 Taylor series

The approximation of degree N by Taylor series for a function $x(t)$ is given by

$$x(t) = \sum_{k=0}^{n-1} (x)_k (t-t_0)^k + R_N([\,t_0, t\,]) \tag{1.14}$$

where, $R_N([\,t_0, t\,]) = (x)_N(s)(t-t_0)^N$ for all $s \in [\,t_0, t\,]$. To calculate these coefficients more efficiently computationally are defined recursively as

$$(x_j)_i = \frac{x^{(i)}(t_j)}{i!} \tag{1.15}$$

where, $x^{(i)}(t)$ corresponds to the ith derivative of $x(t)$. Then, if we consider the initial value problem given by an interval, Y_j

$$y'(t) = f(y), \qquad y(t_j) = y_j \in Y_j$$

Taylor coefficients would be given by

$$
\begin{aligned}
(Y_j)_0 &= Y_j \\
(Y_j)_1 &= f^{(1)}(Y_j) = f(Y_j) \\
(Y_j)_i &= f^{(i)}(Y_j) = \frac{1}{i}\left(\frac{\partial f^{(i-1)}}{\partial y} f\right)(Y_j) \qquad \text{for } i \geq 2
\end{aligned}
$$

and therefore we could construct in Equation (1.14) for functions defined in $\mathbb{IR}^n$.

1.3.5 Dependency problem and wrapping effect

Interval methods are affected by overestimation. This overestimation is often caused by the *dependency problem* and the *wrapping effect*. The dependency problem is the failure of interval arithmetic to identify different occurrences of the same variable, as illustrated in the previous example in Example 1.3.3. Meanwhile, the wrapping effect appears when intermediate results of a computation and the solutions are enclosed by intervals [55].

Example 1.3.4. The wrapping effect is clearly illustrated by Neher's example [73]. Consider the function

$$
\begin{aligned}
f : \mathbb{R}^2 &\to \mathbb{R}^2 \\
(x, y) &\to \frac{\sqrt{2}}{2}(x + y, y - x)
\end{aligned}
$$

The image of f applied to the square with vertices $(0,0)$, $(0,\sqrt{2})$, $(\sqrt{2},0)$, and $(\sqrt{2},\sqrt{2})$ is the rotated square with corners $(0,0)$, $(1,1)$, $(1,-1)$, and $(2,0)$. Nevertheless, if we consider the natural extension of f, given by

$$
F(X, Y) = \frac{\sqrt{2}}{2}(X + Y, Y - X)
$$

the image of the square $X \times Y$ where, $X = Y = [0, \sqrt{2}]$ is the square $[0,2] \times [-1,1]$

(see Figure 1.1).

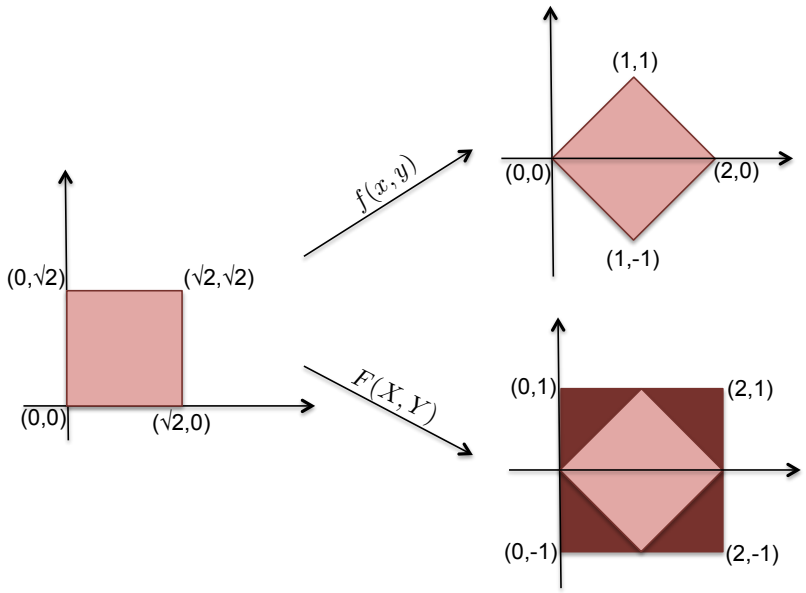

Figure 1.1 – **Wrapping-effect:** Images of f and F of the square with vertices $(0,0)$, $(0,\sqrt{2})$, $(\sqrt{2},0)$, and $(\sqrt{2},\sqrt{2})$.

Different approaches have been proposed to reduce the overestimation caused by these two problems. For instance, these include rearranging expression evaluation, coordinate transformations (considering orthogonal and non-orthogonal matrices), and the use of Taylor models [55].

1.4 Stability theory

It is not always possible to obtain an analytic solution for nonlinear ODEs. For this reason, it is necessary to carry out a qualitative analysis of these systems. Particularly, it is crucial to examine how the trajectories change around the equilibrium points. This analysis is known as *stability analysis*. One can classify the equilibrium points as hyperbolic or non-hyperbolic according to the eigenvalues of the Jacobian matrix. If the system only has hyperbolic points, the *linearization*

method will provide all the necessary information[1]. Otherwise, it is possible to apply *the direct method of Lyapunov* to determine the stability of an equilibrium point. As the ODEs that simulate the transmission of infectious diseases have hyperbolic and non-hyperbolic points, we prove the stability of these in the Lyapunov sense.

In this section, we introduce the basics of stability theory in Lyapunov's sense. We are mostly took these definitions and theorems from [38, 61].

1.5 Lyapunov stability

Definition 1.5.1. An equilibrium point $\mathbf{x}^*$ of the system $\dot{\mathbf{x}} = \mathbf{f}(\mathbf{x})$ is said to be *hyperbolic* if all eigenvalues, λ's, of the Jacobian matrix around this point ($D\mathbf{f}(\mathbf{x}^*)$) have nonzero real part. Otherwise $\mathbf{x}^*$ is said to be *non-hyperbolic*.

Definition 1.5.2. A scalar function $\mathcal{V}(\mathbf{x})$ such that $\mathcal{V} : \mathbb{R}^n \to \mathbb{R}$ is called *radially unbounded* if

$$\mathcal{V}(\mathbf{x}) \to \infty \quad \| \mathbf{x} \| \to \infty.$$

Definition 1.5.3. Let $\mathcal{V}$ be a continuous scalar function, that is, $\mathcal{V} : \mathbb{R}^n \to \mathbb{R}$. The function $\mathcal{V}$ is called *positive definite* on the entire space if

- $\mathcal{V}(\mathbf{x}^*) = 0$.
- $\mathcal{V}(\mathbf{x}) > 0$ for $\mathbf{x} \neq \mathbf{x}^*$,

where $\mathbf{x}^*$ is an equilibrium of the autonomous system $\dot{\mathbf{x}} = \mathbf{f}(\mathbf{x})$. We define the orbital derivative of $\mathcal{V}(\mathbf{x})$ along the solutions of the ODEs as

$$\dot{\mathcal{V}}(\mathbf{x}) = \nabla V(\mathbf{x}) \cdot \mathbf{f}(\mathbf{x})$$

[1] This is guaranteed by the Grobman-Hartman theorem [38].

Theorem 1.5.1. *[Lyapunov's stability theorem] If a function $\mathcal{V}(\boldsymbol{x})$ is globally positively definite and radially unbounded, and its time derivative is globally negative,*

$$\dot{\mathcal{V}}(\boldsymbol{x}) < 0 \quad \boldsymbol{x} \neq \boldsymbol{x}^*,$$

then the equilibrium $\boldsymbol{x}^*$ is globally stable.

A function $\mathcal{V}$ that satisfies the conditions of the previous Theorem 1.5.1 is called a *Lyapunov function*.

The following result is an extension of the previous theorem and is useful when one can only establish the non-negativity of the orbital derivative.

Theorem 1.5.2 (Krasovkii-Lasalle theorem)**.** *Consider the system $\dot{\boldsymbol{x}} = \boldsymbol{f}(\boldsymbol{x})$ where $\boldsymbol{x}^*$ is an equilibrium point. Suppose that there exist a continuously differentiable function $\mathcal{V} : \mathbb{R}^n \to \mathbb{R}$. Also, assume that this function is globally positively definite and radially unbounded and that satisfies*

$$\dot{\mathcal{V}}(\boldsymbol{x}) \leq 0 \quad \textit{for all } t, \quad \textit{and all} \quad \boldsymbol{x} \in \mathbb{R}^n.$$

Define the invariant set

$$\mathcal{I} = \{\boldsymbol{x} \in \mathbb{R}^n \mid \dot{\mathcal{V}}(\boldsymbol{x}) = 0\}.$$

If $\mathcal{I} = \{\boldsymbol{x}^*\}$, then $\boldsymbol{x}^*$ is globally stable.

Bibliography of the current chapter

[1] Ben Adams and Michael Boots. How important is vertical transmission in mosquitoes for the persistence of dengue? Insights from a mathematical model. Epidemics 2.1 (2010), pp. 1–10 (cit. on p. 27).

[2] Roy M Anderson. The role of mathematical models in the study of HIV transmission and the epidemiology of AIDS. Journal of Acquired Immune Deficiency Syndromes 1.3 (1988), pp. 241–256 (cit. on p. 20).

[3] Mathieu Andraud, Niel Hens, Christiaan Marais, and Philippe Beutels. Dynamic epidemiological models for dengue transmission: a systematic review of structural approaches. PloS one 7.11 (2012), e49085 (cit. on p. 21).

[5] Frank Ball et al. Seven challenges for metapopulation models of epidemics, including households models. Epidemics 10 (2015), pp. 63–67 (cit. on p. 22).

[10] Oliver J Brady et al. Modelling adult Aedes aegypti and Aedes albopictus survival at different temperatures in laboratory and field settings. Parasites & Vectors 6.1 (2013), p. 351. DOI: 10.1186/1756-3305-6-351 (cit. on p. 18).

[11] Fred Brauer. Mathematical epidemiology: Past, present, and future. Infectious Disease Modelling 2.2 (2017), pp. 113–127. DOI: https://doi.org/10.1016/j.idm.2017.02.001 (cit. on pp. 19, 23, 24).

[13] JS Brownstein, E Hett, and SL ONeill. The potential of virulent Wolbachia to modulate disease transmission by insects. Journal of invertebrate pathology 84.1 (2003), pp. 24–29 (cit. on p. 27).

[17] Laurent Coudeville and Geoff P Garnett. Transmission dynamics of the four dengue serotypes in southern Vietnam and the potential impact of vaccination. PloS one 7.12 (2012), e51244 (cit. on pp. 27, 81).

[19] Michel De Lara and Lilian Sofia Sepulveda Salcedo. Viable control of an epidemiological model. Mathematical biosciences 280 (2016), pp. 24–37 (cit. on pp. 26, 81).

[20] Sara Del Valle, Herbert Hethcote, James M Hyman, and Carlos Castillo-Chavez. Effects of behavioral changes in a smallpox attack model. Mathematical biosciences 195.2 (2005), pp. 228–251 (cit. on p. 20).

[22] O. Diekmann, J. A.P. Heesterbeek, and J. A.J. Metz. On the definition and the computation of the basic reproduction ratio R_0 in models for infectious diseases in heterogeneous populations. Journal of Mathematical Biology 28.4 (1990), pp. 365–382. DOI: https://doi.org/10.1007/BF00178324 (cit. on pp. 25, 83).

[23] O. Diekmann, J.A.P. Heesterbeek, and M.G. Roberts. The construction of next-generation matrices for compartmental epidemic models. Journal of the Royal Society Interface 7.47 (2010), pp. 873–885. DOI: https://doi.org/10.1098/rsif.2009.0386 (cit. on pp. 25, 83).

[28] Lourdes Esteva and Cristobal Vargas. A model for dengue disease with variable human population. Journal of Mathematical Biology 38.3 (1999), pp. 220–240. DOI: https://doi.org/10.1007/s002850050147 (cit. on pp. 27, 59).

[29] Lourdes Esteva and Cristobal Vargas. Analysis of a dengue disease transmission model. Mathematical Biosciences 150.2 (1998), pp. 131–151. DOI: https://doi.org/10.1016/S0025-5564(98)10003-2 (cit. on pp. 27, 62).

[30] Lourdes Esteva and Cristobal Vargas. Coexistence of different serotypes of dengue virus. Journal of Mathematical Biology 46.1 (2003), pp. 31–47 (cit. on pp. 27, 83).

[31] Lourdes Esteva and Cristobal Vargas. Influence of vertical and mechanical transmission on the dynamics of dengue disease. Mathematical biosciences 167.1 (2000), pp. 51–64 (cit. on p. 27).

[32] Lourdes Esteva and Hyun Mo Yang. Assessing the effects of temperature and dengue virus load on dengue transmission. Journal of Biological Systems 23.04 (2015), p. 1550027. DOI: https://doi.org/10.1142/S0218339015500278 (cit. on pp. 27, 83).

[33] Zhilan Feng and Jorge X Velasco-Hernández. Competitive exclusion in a vector-host model for the dengue fever. Journal of mathematical biology 35.5 (1997), pp. 523–544 (cit. on pp. 20, 27).

[38] Jack K Hale and Hüseyin Koçak. Dynamics and bifurcations. Vol. 3. Springer Science & Business Media, 2012 (cit. on p. 38).

[40] J A P Heesterbeek. A brief history of R_0 and a recipe for its calculation. Acta Biotheoretica 50.3 (2002), pp. 189–204. DOI: https://doi.org/10.1023/A:1016599411804 (cit. on p. 25).

[42] Herbert W Hethcote. The basic epidemiology models: models, expressions for R_0, parameter estimation, and applications. In: Mathematical understanding of infectious disease dynamics. World Scientific, 2009, pp. 1–61. DOI: https://doi.org/10.1142/9789812834836_0001 (cit. on pp. 18, 45, 79).

[43] Harriet Hughes and Nicholas F Britton. Modelling the use of Wolbachia to control dengue fever transmission. Bulletin of mathematical biology 75.5 (2013), pp. 796–818 (cit. on p. 27).

[44] Michael A Johansson, Joachim Hombach, and Derek AT Cummings. Models of the impact of dengue vaccines: a review of current research and potential approaches. Vaccine 29.35 (2011), pp. 5860–5868 (cit. on pp. 21, 27).

[46] William O Kermack and Anderson G McKendrick. A contribution to the mathematical theory of epidemics. In: Proceedings of the Royal Society of London A: Mathematical, Physical and Engineering Sciences. Vol. 115. 772. The Royal Society. 1927, pp. 700–721 (cit. on p. 20).

[55] Rudolf J Lohner. On the ubiquity of the wrapping effect in the computation of error bounds. In: Perspectives on enclosure methods. Springer, 2001, pp. 201–216 (cit. on pp. 6, 36, 37, 90).

[57] Rafael Maciel-de-Freitas, Jacob C Koella, and Ricardo Lourenço-de-Oliveira. Lower survival rate, longevity and fecundity of Aedes aegypti (Diptera: Culicidae) females orally challenged with dengue virus serotype 2. Transactions of the Royal Society of Tropical Medicine and Hygiene 105.8 (2011), pp. 452–458 (cit. on p. 27).

[59] Cecilia de Almeida Marques-Toledo et al. Dengue prediction by the web: Tweets are a useful tool for estimating and forecasting Dengue at country and city level. PLOS Neglected Tropical Diseases 11.7 (July 2017), pp. 1–20. DOI: https://doi.org/10.1371/journal.pntd.0005729 (cit. on p. 18).

[61] Maia Martcheva. "Ch.7: Analysis of Complex ODE Epidemic Models: Global Stability". In: *An Introduction to Mathematical Epidemiology*. Springer US, 2015, pp. 149–181. DOI: https://doi.org/10.1007/978-1-4899-7612-3_7 (cit. on p. 38).

[68] Ramon E Moore, Fritz Bierbaum, and Klaus-Peter Schwiertz. Methods and applications of interval analysis. 2 (1979) (cit. on p. 29).

[69] Ramon E Moore, R Baker Kearfott, and Michael J Cloud. Introduction to Interval Analysis. Siam, 2009 (cit. on pp. 4, 29).

[72] Nedialko S Nedialkov, Kenneth R Jackson, and George F Corliss. Validated solutions of initial value problems for ordinary differential equations. Applied Mathematics and Computation 105.1 (1999), pp. 21–68 (cit. on pp. 6, 35, 90, 93, 110, 143).

[73] Markus Neher. From interval analysis to Taylor models-an Overview. In: Proc. IMACS. 2005 (cit. on p. 36).

[78] Oms. Dengue y dengue grave. May 2016. URL: http://www.who.int/mediacentre/factsheets/fs117/es/ (cit. on p. 26).

[79] World Health Organization et al. Dengue: Guías para el diagnóstico, tratamiento, prevención y control: nueva edición. Tech. rep. Ginebra: Organización Mundial de la Salud, May 2009 (cit. on pp. 26, 66).

[80] Julio César Padilla, Diana Patricia Rojas, and Roberto Sáenz Gómez. Dengue en Colombia: epidemiología de la reemergencia a la hiperendemia. Guías de Impresión Ltda., 2012 (cit. on p. 26).

[81] Abhishek Pandey, Anuj Mubayi, and Jan Medlock. Comparing vector-host and SIR models for dengue transmission. Mathematical biosciences 246.2 (2013), pp. 252–259 (cit. on pp. 22, 26).

[82] Mayra Elizabeth Parra-Amaya, María Eugenia Puerta-Yepes, Diana Paola Lizarralde-Bejarano, and Sair Arboleda-Sánchez. Early detection for dengue using Local Indicator of Spatial Association (LISA) analysis. Diseases 4.2 (2016), p. 16. DOI: https://doi.org/10.3390/diseases4020016 (cit. on p. 18).

[87] Víctor Hugo Peña-García, Omar Triana-Chávez, and Sair Arboleda-Sánchez. Estimating Effects of Temperature on Dengue Transmission in Colombian Cities. Annals of Global Health 83.3 (2017). Current Topics in Global Health, pp. 509–518. DOI: https://doi.org/10.1016/j.aogh.2017.10.011 (cit. on p. 18).

[88] Víctor Hugo Peña-García, Omar Triana-Chávez, Ana María Mejía-Jaramillo, Francisco J Díaz, Andrés Gómez-Palacio, and Sair Arboleda-Sánchez. Infection Rates by Dengue Virus in Mosquitoes and the Influence of Temperature May Be Related to Different Endemicity Patterns in Three Colombian Cities. International Journal of Environmental Research and Public Health 13.7 (2016), p. 734. DOI: https://doi.org/10.3390/ijerph13070734 (cit. on pp. 28, 111).

[89] Suani Tavares Rubim de Pinho, Claudia P Ferreira, Lourdes Esteva, FR Barreto, VC Morato e Silva, and MGL Teixeira. Modelling the dynamics of dengue real epidemics. Philosophical Transactions of the Royal Society A: Mathematical, Physical and Engineering Sciences 368.1933 (2010), pp. 5679–5693 (cit. on pp. 27, 81).

[93] Robert C Reiner et al. A systematic review of mathematical models of mosquito-borne pathogen transmission: 1970–2010. Journal of The Royal Society Interface 10.81 (2013), p. 20120921 (cit. on pp. 19, 21).

[98] Boris Shulgin, Lewi Stone, and Zvia Agur. Pulse vaccination strategy in the SIR epidemic model. Bulletin of mathematical biology 60.6 (1998), pp. 1123–1148 (cit. on p. 21).

[99] Robert J. Smith, Jing Li, and Daniel Blakeley. The failure of R_0. Computational and Mathematical Methods in Medicine 2011 (2011). DOI: https://doi.org/10.1155/2011/527610 (cit. on pp. 25, 162).

[101] Anna M Stewart-Ibarra et al. Spatiotemporal clustering, climate periodicity, and social-ecological risk factors for dengue during an outbreak in Machala, Ecuador, in 2010. BMC Infectious Diseases 14.1 (2014), p. 610. DOI: https://doi.org/10.1186/s12879-014-0610-4 (cit. on p. 18).

[109] Tzai-Hung Wen, Neal H. Lin, Chun-Hung Lin, Chwan-Chuen King, and Ming-Daw Su. Spatial mapping of temporal risk characteristics to improve environmental health risk identification: A case study of a dengue epidemic in Taiwan. Science of the Total Environment 367.2 (2006), pp. 631–640. DOI: https://doi.org/10.1016/j.scitotenv.2006.02.009 (cit. on p. 18).

[110] Hyun Mo Yang and Cláudia Pio Ferreira. Assessing the effects of vector control on dengue transmission. Applied Mathematics and Computation 198.1 (2008), pp. 401–413 (cit. on pp. 21, 27).

[111] Hyun Mo Yang, Maria de Lourdes da Graca Macoris, Karen Cristina Galvani, and Maria Teresa Macoris Andrighetti. Follow up estimation of Aedes aegypti entomological parameters and mathematical modellings. Biosystems 103.3 (2011), pp. 360–371 (cit. on p. 27).

Chapter 2

Uncertainty

Outline of the current chapter

2.1 Abstract

Uncertainty is present in all measurement processes and modeling real phenomena. Frequently, available information is not 100% reliable or accurate. In this chapter, we briefly present different strategies to include uncertainty in epidemiological models given by ODEs. Moreover, taking into account that the knowledge and information are limited for our case study (dengue transmission),

we present a justification of why we will model the uncertainty through interval analysis.

2.2 Problem statement

To explain an actual phenomenon requires measuring and getting information, which frequently contains some uncertainty levels. One source of this may be the lack of knowledge about the study phenomenon, which makes it difficult in the modeling process to determine which characteristics should be included or excluded in the study. Other sources of uncertainty include the impossibility of obtaining measurements of some relevant factors, collecting information over long periods, etc. [65]. Thus, uncertainty must be correctly considered as long as its effects are present in the decision-making process. Up to the year 1960, statistics and probability theory were the known methods that could model uncertainty [113]. Currently, it is possible to find other theories capable of dealing with this (e.g. fuzzy set theory and interval arithmetic).

In the case of vector-borne diseases such as West Nile virus, Malaria, Zika, and Dengue, there is uncertainty due to the inability to accurately and reliably measure transmission rates, vector populations, and the recovery rate in humans. Usually, these characteristics are included in the modeling process as parameters or initial conditions. This information is necessary to build more reliable models that allow us to understand the dynamics of this type of disease and thus be able to propose appropriate control strategies. However, in contrast to other sciences where it is possible to carry out several experiments to obtain information and test hypotheses, such experiments are often impossible, unethical or expensive when modeling the spread of infectious diseases in human populations [42].

For instance, the experimental assays with vector populations involve imprecision, some degree of approximation, or uncertainty to various degrees, since it

is not possible to include all external aspects involved in development process in the laboratory. For example, consider an experiment where three replicas with vector population are carried out. Suppose that each experiment starts with 100 eggs, and we measure the percentage of eggs hatching for this vector population. Then, this measurement can be stated in different ways as follows (a) between 86 and 92 percent, (b) about 89 percent, or (c) has a mean value of 89 and a standard deviation of 2 percent and follows a normal distribution. Depending on the nature of imprecision, the analysis of the system can be conducted using interval analysis, fuzzy theory, or a probabilistic approach [91].

2.3 Uncertain parameters and initial conditions in epidemiological models

To the best of our knowledge, ODEs in mathematical epidemiology have included uncertainty in their parameters via fuzzy theory, a probabilistic approach [7, 6, 12] and to a lesser extent through the application of interval analysis [25].

To use fuzzy theory, it is necessary to define the range of the uncertain parameter and a preference function (or membership function see Definition 2.4.1), which allows the researcher to describe the desirability of using different values within the range. Frequently, this definition depends on the expert's estimation. On the other hand, to apply the probabilistic approach, we must know the specified probability distribution that follows the uncertain parameter. Finally, if all the uncertain parameter has upper and lower bounds, we can use interval analysis. These strategies help to get insights into transmission dynamics when the population distribution is heterogeneous. However, in general, to apply the fuzzy or the probabilistic approach; we have to formulate some additional hypotheses on parameter behavior or additional information about them. For instance, in [56], those authors assume that parameters as the duration of the in-

fectious period in humans, the biting rate, the mosquito to human transmission rate, and human to mosquito transmission rate follow a uniform distribution. While the extrinsic incubation period follows a triangular distribution. In contrast with this work, the authors of [12] assume that the latent and infection periods are random and independent variables following a gamma probability distribution[1].

On the other hand, within the fuzzy transmission models in [6] an SIS model was formulated

$$\frac{dS}{dt} = -\beta SI + \gamma I$$
$$\frac{dI}{dt} = \beta SI - \gamma I$$

where, β (the transmission rate), and γ (the recovery rate) are given by functions that depend on the amount of virus, v. To define appropriate membership functions it is necessary knowing the minimum value of virus v_{min} such that a susceptible individual becomes an infected individual.

$$\beta(v) = \begin{cases} 1, & \text{if } v_M < v \leq v_{max}, \\ \frac{v - v_{min}}{v_M - v_{min}}, & \text{if } v_{min} < v \leq v_M \\ 0, & \text{otherwise.} \end{cases}$$
$$\gamma(v) = \frac{(\gamma_0 - 1)}{v_{max}} v + 1$$

where, γ_0 represents the minimum recovery time.

It is worth pointing out that it is impossible to know the exact distribution for the model parameters in many applications. In this scenario, it is reasonable

[1] The probability density function for the gamma distribution is given by:

$$f(x; \alpha, \beta) = \frac{\beta^\alpha x^{\alpha-1} e^{-x\beta}}{\Gamma(\alpha)}, \text{ with } x > 0$$

to assign equal probabilities to all the alternatives. This can be done by using interval analysis. In recent years, there are advances in the field of application of interval analysis for uncertainty analysis. For example, the technique for error analysis presented in [94]; the proposed system for modeling uncertainty by intervals using the product of these [70]; and strategies to model the uncertainty parameters of nonlinear vibration systems through intervals to analyze the output of the system [90].

2.4 Strategy to reduce fuzzy uncertainty to interval uncertainty

A fuzzy set concerns with the idea of flexibility over the concept of belongingness [63, 77]. In 1965, Zadeh proposed a *membership degree*, according to which an element could partially belong to a given set.

Definition 2.4.1. Given a non-empty set X, a *fuzzy set* of X is a pair (A, μ_A) where $A \subseteq X$ and $\mu_A : X \to [0,1]$. One refers to μ_A as the *membership function* of A.

Definition 2.4.2. Given a fuzzy set (A, μ_A), its *support*, denoted by $S(A)$, is the open set formed by elements in X with positive membership degree in A.

$$S(A) = \{x : x \in X, \mu_A(x) > 0\}. \tag{2.1}$$

We write $\overline{S(A)}$ to refer to the closure of $S(A)$, i.e. the closed set formed by $S(A)$ along with its limit points.

For convenience, we freely confuse (A, μ_A), A and μ_A. Thus, we may refer to μ_A as the fuzzy set. For each x in A, the value $\mu_A(x)$ indicates the membership degree of the element x in A. If X is $\mathbb{R}$ in Definition 2.4.1, we refer to A as a *fuzzy number*. Fuzzy numbers are commonly used to describe the expressions of the expert, such as “around of”, “small”, “medium”, “approximately equal to a”, etc.

It is clear from Definition 2.4.1 that two fuzzy sets can only be referred as equal whenever their membership functions coincide pointwise. Given two fuzzy sets, A and B, we have that $A = B$, if and only if, $\mu_A = \mu_B$. Thus, a fuzzy set is completely determined by its membership function. We now examine an alternative charactherisation of these membership functions in terms of α-cuts.

Definition 2.4.3. An *α-cut* is a set of all elements that belong to a fuzzy set with at least α degree. We denote by $[A]_\alpha$, the α-cut of the fuzzy set A.

$$[A]_\alpha = \{x \in X \,|\, \mu_A(x) \geq \alpha\}.$$

Notably, if A is a fuzzy number, then all its α-cuts are closed intervals on $\mathbb{R}$ [63]. One can alternatively represent a membership function of a fuzzy set by the aggregation of their α-cuts. Using this α-cut charactherization for membership functions, one can describe the relation between computing under fuzzy uncertainty and interval uncertainty, for the particular case of fuzzy numbers, of special interest in this document. To this end, one needs the *extension principle* which allows us to extend concepts from classical set theory to fuzzy set theory in the following way [114].

Definition 2.4.4. Let X be the cartesian product of universes $X = X_1 \times \cdots \times X_n$, and $A_1, \ldots, A_n$ be n fuzzy sets in $X_1, \ldots, X_n$, respectively. Given a mapping f from X to Y, the *extended* fuzzy set of X in Y by f, denoted by $f(X)$, is formed by the set $f(A)$ defined as $\{f(x_1, \ldots, x_n) \,|\, x_i \in A_i, i = 1, \ldots, n\}$, along with the membership function $\mu_{f(X)}(y)$ defined as in Equation (2.2).

$$\mu_{f(X)}(y) = \begin{cases} \sup\limits_{(x_1,\ldots,x_n) \in f^{-1}(y)} \min(\mu_{A_1}(x_1), \ldots, \mu_{A_n}(x_n)) & \text{if } f^{-1}(y) \neq \emptyset \\ 0 & \text{otherwise} \end{cases} \tag{2.2}$$

where $f^{-1}(y)$ denotes the set of all points $(x_1,\ldots,x_n) \in X$ such that $y = f(x_1,\ldots,x_n)$.

To illustrate the aforementioned relation between fuzzy and interval uncertainty, let $f : \mathbb{R} \to \mathbb{R}$ be a continuous function, and $A_1,\ldots,A_n \in \mathcal{P}(\mathbb{R})$ be fuzzy numbers such that $\mu_{A_i}(x_i)$ is a continuous functions for i from 1 to n.

We will show that

$$[f(A_1,\ldots,A_n)]_\alpha = f([A_1]_\alpha,\ldots,[A_n]_\alpha). \tag{2.3}$$

That is, the α-cut $[f(A_1,\ldots,A_n)]_\alpha$ is equal to the range of possible values of $f(x_1,\ldots,x_n)$ where x_i ranges over $[A_i]_\alpha$ for i from 1 to n.

To this end, in [76], Nguyen proved that it suffices to show that for all $y \in \mathbb{R}$,

$$\sup_{(x_1,\ldots,x_n)\in f^{-1}(y)} \{\min(\mu_{A_1}(x_1),\ldots,\mu_{A_n}(x_n))\}$$

is attained, to state that Equation (2.3) holds. Let us prove then that such a condition holds in our case.

Let $\phi(x_1,\ldots,x_n)$ be $\min(\mu_{A_1}(x_1),\ldots,\mu_{A_n}(x_n))$. One can prove that the function ϕ is continuous, as each function $\mu_{A_i}(x_i)$ is continuous. Note also that $\phi(x_1,\ldots,x_n) \geq 0$, since, again, each $\mu_{A_i}(x_i) \geq 0$. Thus,

$$\sup_{(x_1,\ldots,x_n)\in f^{-1}(y)} \phi(x_1,\ldots,x_n) = \sup_{(x_1,\ldots,x_n)\in f^{-1}(y)\cap \overline{S}} \phi(x_1,\ldots,x_n)$$

since $\phi = 0$ outside of $\overline{S}$ where $\overline{S} = \overline{S(A_1)} \times \cdots \times \overline{S(A_n)}$.

By Tychonoff's theorem, one proves that $\overline{S}$ is compact, as it is a product of n compact sets with respect to the product topology. Then, $\overline{S}$ is a closed and bounded set. On the other hand, the set formed by the preimages of y by f, $f^{-1}(y)$, is closed by continuity of f. Then $f^{-1}(y) \cap \overline{S}$ is compact since the intersection of two closed sets is closed and bounded because $f^{-1}(y) \cap \overline{S} \subseteq \overline{S}$. Consequently, ϕ reaches its maximum on the compact set $f^{-1}(y) \cap \overline{S}$ for all $y \in \mathbb{R}$.

2.5 Interval uncertainty

In some cases, it is not possible to know the exact probabilistic distribution of the measurement errors. Moreover, many distributions can be agreeable with the knowledge of the measurement of errors. Under this scenario, one wants to select the distribution with the least possible amount of information. *"If a random variable has the density probability function $\rho(x)$, the amount of information it bears is usually described by the* ***entropy****"* [49].

$$S = -\int_{-\infty}^{\infty} \rho(x) \ln \rho(x)\, dx,$$

where, the entropy gives a measure of how chaotic the probabilistic distribution is. Thus, one should select the probability distribution $\rho(x)$ with the largest entropy. This consideration is known as the *maximum entropy approach*.

Theorem 2.5.1. *The uniform distribution is the maximum entropy distribution on any interval* $[\underline{a}, \overline{a}]$.

Proof. From [49]:

Consider a probability density function $\rho(x)$ on the given interval, i.e., that $\rho(x) = 0$ for $x \notin [\underline{a}, \overline{a}]$. The idea here is to maximize the entropy

$$S = -\int_{-\infty}^{\infty} \rho(x) \ln \rho(x)\, dx = -\int_{\underline{a}}^{\overline{a}} \rho(x) \ln \rho(x)\, dx$$

under the constraint that

$$\int_{\underline{a}}^{\overline{a}} \rho(x)\, dx = 1.$$

To do so, we apply the Lagrange multipliers method to reduce the one variable constraint optimization problem to an unconstraint problem of two variables.

Thus we have the Lagrange function:

$$L[\rho] = -\int_{\underline{a}}^{\overline{a}} \rho(x)\ln\rho(x)\ dx + \lambda\int_{\underline{a}}^{\overline{a}} \rho(x) - 1\ dx$$

where λ is a Lagrange multiplier. As $\rho(x)$ is a function, L is a functional. Then, to optimize L we follow the same strategy to deduce the Euler-Lagrange equation from the calculus of variations. To do so, we consider the parametrization of all the distribution functions defined on the interval $[\underline{a},\overline{a}]$:

$$\overline{\rho}(x) = \rho(x) + \epsilon\eta(x)$$

where $\rho(x)$ is the stationary distribution function, ϵ is a small real number, and $\eta(x)$ is any arbitrary distribution function on the given interval.

Now, for a fixed ρ and η, different values of ϵ give different values of $L[\overline{\rho}]$. Thus, the rate of change of the functional is:

$$\begin{aligned}
\frac{d}{d\epsilon}L[\overline{\rho}] &= \left(\frac{d}{d\epsilon}\int_{\underline{a}}^{\overline{a}} -\rho(x)\ln\rho(x)\ dx + \lambda\int_{\underline{a}}^{\overline{a}} \rho(x) - 1\ dx\right) \\
&= \int_{\underline{a}}^{\overline{a}} \frac{d}{d\epsilon}(-\rho(x)\ln\rho(x) + \lambda\rho(x) - \lambda)dx \\
&= \int_{\underline{a}}^{\overline{a}} (-\eta\ln\rho(x) - \eta + \lambda\eta)dx \\
&= \int_{\underline{a}}^{\overline{a}} -\eta(\ln\rho(x) + 1 - \lambda)dx
\end{aligned}$$

η is not zero since it is an arbitrary function, so we conclude that $\ln\rho(x) + 1 - \lambda$, hence $\rho(x) = \exp(\lambda - 1)$. The probability density has the same value for all $x \in [\underline{a},\overline{a}]$. Therefore, the maximum entropy distribution without any extra information is the uniform distribution. □

This result follows the judgement to choose a uniform distribution for errors when one does not have reasons or information to suppose that one value is more probable than another.

On the other hand, there are usually three sources of error while performing numerical computations with real numbers:

- *Input errors* usually occur for some human mistakes. For instance, in the measurement process or when a person mistypes a value on the computer.
- *Truncation errors* arise when we approximate a continuous or infinite operation by a computable discrete one.
- *Rounding errors* arise when we perform arithmetic operations between real numbers on a machine. This happens because of the inexactness in the representation of real numbers.

All these errors arise when we process the experimental results on a computer since usually, the results are given by some real number. To handle all these errors, we can use the interval arithmetic [18].

2.6 Conclusions

According to the type of information obtained from experimental assays (see Tables 3.1–3.2 in Sec 3.3 of the next chapter), we consider that for transmission of vector-borne diseases, an efficient and a reliable way to account for uncertainty is through interval analysis. Unlike applications based on probability and fuzzy theory, interval analysis does not attempt to infer an uncertainty structure of the model-output based on an uncertainty structure assumed for the model-input.

Bibliography of the current chapter

[6] L. C. Barros, R. C. Bassanezi, R. Z. G. Oliveira, and M. B. F. Leite. A disease evolution model with uncertain parameters. In: Proceedings Joint 9th IFSA World Congress and 20th NAFIPS International Conference (Cat. No. 01TH8569). Vol. 3. IEEE. 2001, pp. 1626–1630. DOI: https://doi.org/10.1109/NAFIPS.2001.943794 (cit. on pp. 46, 47, 110).

[7] L.C.DE Barros, M.B.Ferreira Leite, and R.C Bassanezi. The SI epidemiological models with a fuzzy transmission parameter. Computers & Mathematics with Applications 45.10 (2003), pp. 1619–1628. DOI: https://doi.org/10.1016/S0898-1221(03)00141-X (cit. on pp. 46, 110).

[12] Tom Britton and David Lindenstrand. Epidemic modelling: Aspects where stochasticity matters. Mathematical Biosciences 222.2 (2009), pp. 109–116. DOI: https://doi.org/10.1016/j.mbs.2009.10.001 (cit. on pp. 46, 47, 110).

[18] Hend Dawood. Interval mathematics as a potential weapon against uncertainty. In: Mathematics of uncertainty modeling in the analysis of engineering and science problems. IGI Global, 2014, pp. 1–38 (cit. on p. 53).

[25] Joshua Enszer and Mark Stadtherr. Verified Solution Method for Population Epidemiology Models with Uncertainty. International Journal of Applied Mathematics and Computer Science 19.3 (2009), pp. 501–512. DOI: https://doi.org/10.2478/v10006-009-0040-4 (cit. on pp. 46, 90, 92, 110, 168).

[42] Herbert W Hethcote. The basic epidemiology models: models, expressions for R_0, parameter estimation, and applications. In: Mathematical understanding of infectious disease dynamics. World Scientific, 2009, pp. 1–61. DOI: https://doi.org/10.1142/9789812834836_0001 (cit. on pp. 18, 45, 79).

[49] Vladik Kreinovich and Sergey P Shary. Interval methods for data fitting under uncertainty: a probabilistic treatment (2015) (cit. on p. 51).

[56] Paula Mendes Luz, Cláudia Torres Codeço, Eduardo Massad, and Claudio José Struchiner. Uncertainties regarding dengue modeling in Rio de Janeiro, Brazil. Memórias do Instituto Oswaldo Cruz 98.7 (2003), pp. 871–878 (cit. on p. 46).

[63] Eduardo Massad, Neli Regina Siqueira Ortega, Laecio Carvalho de Barros, and Claudio José Struchiner. Fuzzy Logic in Action: Applications in Epidemiology and Beyond. Springer Berlin Heidelberg, 2008. DOI: 10.1007/978-3-540-69094-8 (cit. on pp. 48, 49).

[65] Wasim Maziak. Is uncertainty in complex disease epidemiology resolvable? Emerging Themes in Epidemiology 12.1 (2015), p. 7. DOI: https://doi.org/10.1186/s12982-015-0028-5 (cit. on p. 45).

[70] SM Mousavi, R Tavakkoli-Moghaddam, H Hashemi, and SMH Mojtahedi. A novel approach based on non-parametric resampling with interval analysis for large engineering project risks. Safety science 49.10 (2011), pp. 1340–1348 (cit. on p. 48).

[76] Hung T Nguyen. A note on the extension principle for fuzzy sets. Journal of Mathematical Analysis and Applications 64.2 (June 1978), pp. 369–380. DOI: 10.1016/0022-247x(78)90045-8 (cit. on p. 50).

[77] Hung T. Nguyen, Vladik Kreinovich, Berlin Wu, and Gang Xiang. Computing Statistics under Interval and Fuzzy Uncertainty. Springer Berlin Heidelberg, 2012. DOI: 10.1007/978-3-642-24905-1 (cit. on p. 48).

[90] Zhiping Qiu, Lihong Ma, and Xiaojun Wang. Non-probabilistic interval analysis method for dynamic response analysis of nonlinear systems with uncertainty. Journal of Sound and Vibration 319.1-2 (2009), pp. 531–540 (cit. on p. 48).

[91] Singiresu S Rao and L Berke. Analysis of uncertain structural systems using interval analysis. AIAA journal 35.4 (1997), pp. 727–735 (cit. on p. 46).

[94] Edward J Rothwell and Michael J Cloud. Automatic error analysis using intervals. IEEE Transactions on Education 55.1 (2012), pp. 9–15 (cit. on p. 48).

[113] H.-J. Zimmermann. An application-oriented view of modeling uncertainty. European Journal of Operational Research 122.2 (2000), pp. 190–198. DOI: https://doi.org/10.1016/S0377-2217(99)00228-3 (cit. on pp. 45, 110).

[114] H.-J. Zimmermann. The Extension Principle and Applications. In: Fuzzy Set Theory — and Its Applications. Springer Netherlands, 1991, pp. 53–67. DOI: 10.1007/978-94-015-7949-0_5 (cit. on p. 49).

Chapter 3

Epidemiological models

Outline of the current chapter

3.1 Abstract

Several models have been formulated to simulate the transmission of dengue diseases. Here we presented three different models. One includes all the development stages of the vector (eggs-larvae-pupae) explicitly. The second considers collective these development stages in one compartmental (the aquatic phase), and the third one considers a constant recruitment rate in the vector adult population. The latter simplifies the previous one since we define the recruitment rate as the equilibrium point of the aquatic population. In this way, it was possible to consider the biological ranges of the parameters involved in the vector development. Then, to establish the biological range of the recruitment rate for each municipality, we use interval arithmetic.

This chapter's primary goal is to study the impact of modeling assumptions reflected in each model's number of parameters and state variables. In this way, we aim to evaluate the structure, complexity, trustworthiness, and suitability of three models on the dynamics of dengue in two municipalities of Colombia. To achieve this aim, we calculated the Basic Reproductive Number (R_0), performed the locally structural identifiability analysis, and calculated the elasticities values of R_0 for each model.

The results from these analyses showed that the simplest model was the most appropriate and reliable. Therefore, explicitly incorporating the development stages of the vector population may not be necessary for modeling dengue transmission when the only available information is the cumulative number of reported dengue cases.

3.2 Formulation of Dengue transmission models

As mentioned in Chapter 1, dengue virus has four serotypes (DENV-1, DENV-2, DENV-3 and DENV-4). However, since the record of the number of cases produced by each serotype is not available for Colombia, the models presented here only consider transmission by one of them.

We considered the three epidemiological models introduced in [54]. These models included compartments for both the populations involved in the dengue transmission process. The main difference between these models is the number of state variables and parameters that allow us to capture different aspects of the vector's development in all their life stages. For all the models, we use M to denote the size of mosquito population, which can vary over time, and H to denote the size of the total human population, which is considered to remain constant (birth and death rate equal to μ_h) over the studied time period of maximum one year.

3.2.1 Model considering all development stages of the vector (eggs-larvae-pupae-adult)

For vector population, we considered the aquatic immature stage (egg E, larva L, and pupa P) and the adult phase, M (for females mosquitoes only); the last was divided into three sub-populations, representing susceptible M_s, exposed M_e, and infectious M_i mosquitoes. Analogously, for human population, we considered four sub-populations, namely susceptible H_s, exposed H_e, infectious H_i, and recovered H_r humans.

In the model, the development of mosquito begins with the number of eggs E at time t, which increases with the per capita oviposition rate $\delta(1 - E/C)$, where δ is the intrinsic oviposition rate per capita, and C is the carrying capacity of the environment. The number of eggs decreases based on the transition rate from

eggs to larvae γ_e and the eggs mortality rate μ_e. The number of larvae L at time t increases with the transition rate from eggs to larvae γ_e and decreases with the transition rate from larvae to pupae γ_l and larvae mortality rate μ_l. Likewise, the number of pupae P at time t increases with the transition rate from larvae to pupae γ_l and decreases with the transition rate from pupae to adults γ_p and the pupae mortality rate μ_p. In this manner, the population of adult mosquitoes, including females and males, increases at a rate γ_p. Because DENV transmission only involves female mosquitoes, we included the parameter f, representing the fraction of female mosquitoes produced during the hatching of all eggs. Thus, the population of susceptible females M_s increases at rate $f\gamma_p$, because we removed the number of males $\gamma_p(1-f)P$ that completed the development cycle.

In both populations, the flow from the susceptible to the exposed compartment depends on the proportion of infected in each population (H_i/H and M_i/M) and the transmission coefficients (β_h and β_m). Here, we assumed the transmission coefficients to be the product of the mosquito's biting rate and the transmission probabilities. Once extrinsic and intrinsic incubation periods are completed, the exposed mosquitoes and humans become infected at a rate of θ_m and θ_h, respectively. Finally, infected humans recover at a rate of γ_h, while mosquitoes remain infected for the rest of their lives [28]. Figure 3.1 shows all transitions described above. Based on the above assumptions, the dynamics of

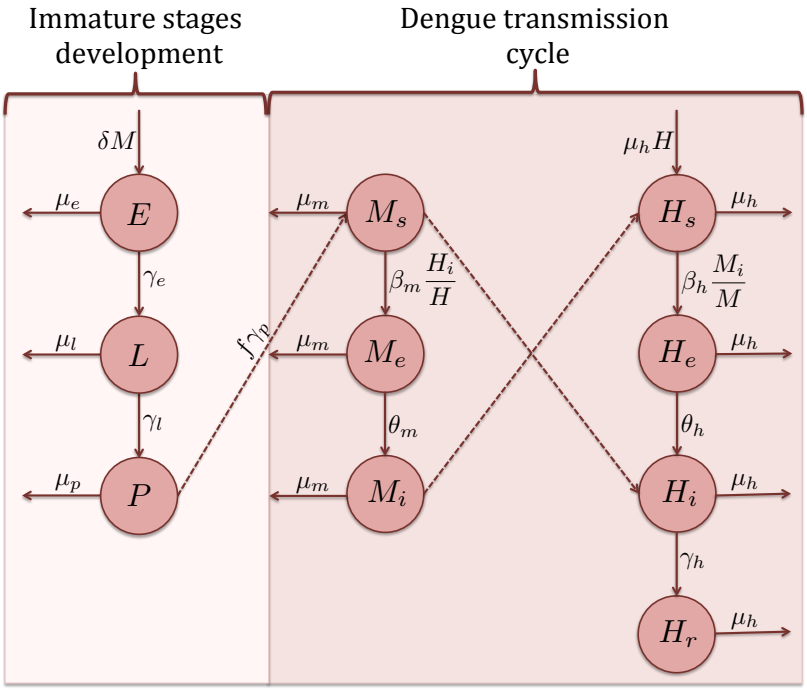

Figure 3.1 – **Dengue transmission model: all stages of vector were included.** Flow diagram summarizing the transitions from one compartment to another in Model 3.1 is shown. It is assumed that the population is divided into immature stages (mosquito), adult females (mosquito), and humans.

dengue transmission is given by the following system of differential equations:

$$
\begin{aligned}
\frac{dE}{dt} &= \delta\left(1-\frac{E}{C}\right)M - (\gamma_e+\mu_e)E \\
\frac{dL}{dt} &= \gamma_e E - (\gamma_l+\mu_l)L \\
\frac{dP}{dt} &= \gamma_l L - (\gamma_p+\mu_p)P \\
\frac{dM_s}{dt} &= f\gamma_p P - \beta_m \frac{H_i}{H} M_s - \mu_m M_s \\
\frac{dM_e}{dt} &= \beta_m \frac{H_i}{H} M_s - (\theta_m+\mu_m)M_e \\
\frac{dM_i}{dt} &= \theta_m M_e - \mu_m M_i \\
\frac{dH_s}{dt} &= \mu_h H - \beta_h \frac{M_i}{M} H_s - \mu_h H_s \\
\frac{dH_e}{dt} &= \beta_h \frac{M_i}{M} H_s - (\theta_h+\mu_h)H_e \\
\frac{dH_i}{dt} &= \theta_h H_e - (\gamma_h+\mu_h)H_i \\
\frac{dH_r}{dt} &= \gamma_h H_i - \mu_h H_r
\end{aligned}
\tag{3.1}
$$

3.2.2 Model considering one aquatic phase for the vector

In contrast with the previous model, this model considers the larval and pupal stages collectively as the aquatic phase A, which increases with the effective per capita oviposition rate $\rho(1 - A/C)$, with $\rho = k\delta$, where δ is the intrinsic oviposition rate per capita, and k is the fraction of eggs hatching to larvae. The aquatic phase decreases according to the transition rate from the aquatic phase to the adult phase γ_m and the mortality rate in the aquatic phase μ_a. Similarly to Model 3.1, the population of susceptible females M_s increases at rate $f\gamma_m$. Figure 3.2 shows all transitions described above and the flow of dengue transmission between populations. Based on the above assumptions, the

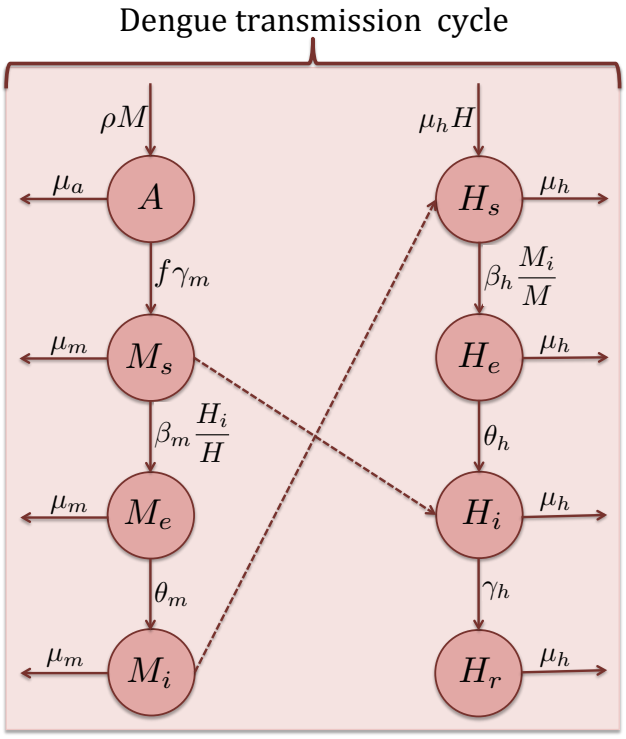

Figure 3.2 – **Dengue transmission model considering one aquatic phase for the vector.** Flow diagram summarizing the transitions from one compartment to another in Model 3.2 is shown. It is assumed that the population is divided into one aquatic stage (mosquito), adult females (mosquito), and humans.

dynamics of dengue transmission is given by the following system of differential equations:

$$\begin{aligned}
\frac{dA}{dt} &= \rho\left(1-\frac{A}{C}\right)M-(\gamma_m+\mu_a)A\\
\frac{dM_s}{dt} &= f\gamma_m A-\beta_m\frac{H_i}{H}M_s-\mu_m M_s\\
\frac{dM_e}{dt} &= \beta_m\frac{H_i}{H}M_s-(\theta_m+\mu_m)M_e\\
\frac{dM_i}{dt} &= \theta_m M_e-\mu_m M_i\\
\frac{dH_s}{dt} &= \mu_h H-\beta_h\frac{M_i}{M}H_s-\mu_h H_s\\
\frac{dH_e}{dt} &= \beta_h\frac{M_i}{M}H_s-(\theta_h+\mu_h)H_e\\
\frac{dH_i}{dt} &= \theta_h H_e-(\gamma_h+\mu_h)H_i\\
\frac{dH_r}{dt} &= \gamma_h H_i-\mu_h H_r
\end{aligned} \tag{3.2}$$

3.2.3 Model without considering development stages of the vector

Finally, for Model 3.3 we only considered the adult population of female mosquitoes. In this model, the behaviour of the aquatic phase of the vector population is captured in one parameter, Λ, which is interpreted as the recruitment rate. In this way, the population of females mosquito increases at a constant rate independent of the actual number of adult mosquitoes. This assumption seems reasonable since only a fraction of a large reservoir of eggs and larvae matures to females, and this process does not depend directly on the size of the female mosquito population [29].

To establish an appropriate biological range for this parameter, we define $\Lambda = f\gamma_m A^*$ with $A^* = C\left(1-\frac{1}{R_M}\right)$ and $R_M = \frac{\rho f\gamma_m}{\mu_m(\gamma_m+\mu_a)}$, where R_m is the number of secondary females produced by only one female (the offspring), and A^* is the equilibrium value of the aquatic phase in which mosquitoes are present

in Model 3.2. Thus, we take into account parameters that describe the transition and mortality from the aquatic phase to the adult phase of the vector $(\rho, \gamma_m, \mu_a, \mu_m, f)$.

Figure 3.3 shows the flow of dengue transmission between populations. Based

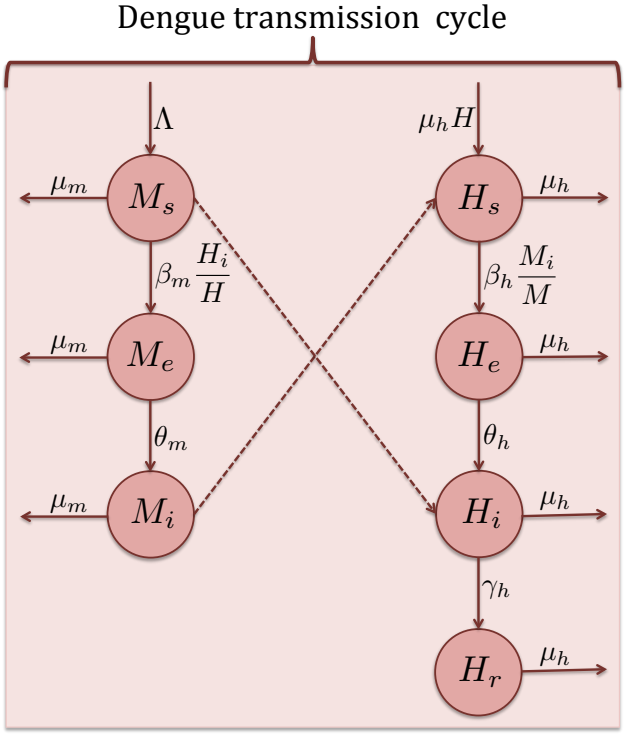

Figure 3.3 – **Dengue transmission model without considering development stages of the vector.** Flow diagram summarizing the transitions from one compartment to another in Model 3.3 is shown.

on the above assumptions, the dynamics of dengue transmission is given by the

following system of differential equations:

$$\begin{aligned}
\frac{dM_s}{dt} &= \Lambda - \beta_m \frac{H_i}{H} M_s - \mu_m M_s \\
\frac{dM_e}{dt} &= \beta_m \frac{H_i}{H} M_s - (\theta_m + \mu_m) M_e \\
\frac{dM_i}{dt} &= \theta_m M_e - \mu_m M_i \\
\frac{dH_s}{dt} &= \mu_h H - \beta_h \frac{M_i}{M} H_s - \mu_h H_s \\
\frac{dH_e}{dt} &= \beta_h \frac{M_i}{M} H_s - (\theta_h + \mu_h) H_e \\
\frac{dH_i}{dt} &= \theta_h H_e - (\gamma_h + \mu_h) H_i \\
\frac{dH_r}{dt} &= \gamma_h H_i - \mu_h H_r
\end{aligned} \tag{3.3}$$

3.3 Data and parameters ranges

3.3.1 Data

We consider data from 2016 dengue outbreaks in the municipalities of Itagüí (Antioquia, Colombia) and Neiva (Huila, Colombia). The information of the reported dengue cases was obtained from the *National Public Health Surveillance System* (SIVIGILA by its Spanish initials) (http://portalsivigila.ins.gov.co/sivigila/documentos/Docs_1.php). The outbreak in Itagüí lasted 60 epidemiological weeks, beginning in epidemiological week 51 of 2015 (with 10 reported cases) and ending in epidemiological week 6 of 2016 (with 4 reported cases). The total number of dengue cases reported during this period was 2915 (see Figure 3.4). Meanwhile, the outbreak in Neiva lasted 24 epidemiological weeks, beginning in the epidemiological week 38 of 2016 (with 16 reported cases) and ending in the epidemiological week 9 of 2017 (with 7 reported cases). The total number of dengue cases reported during this period was 687 (see Figure 3.5).

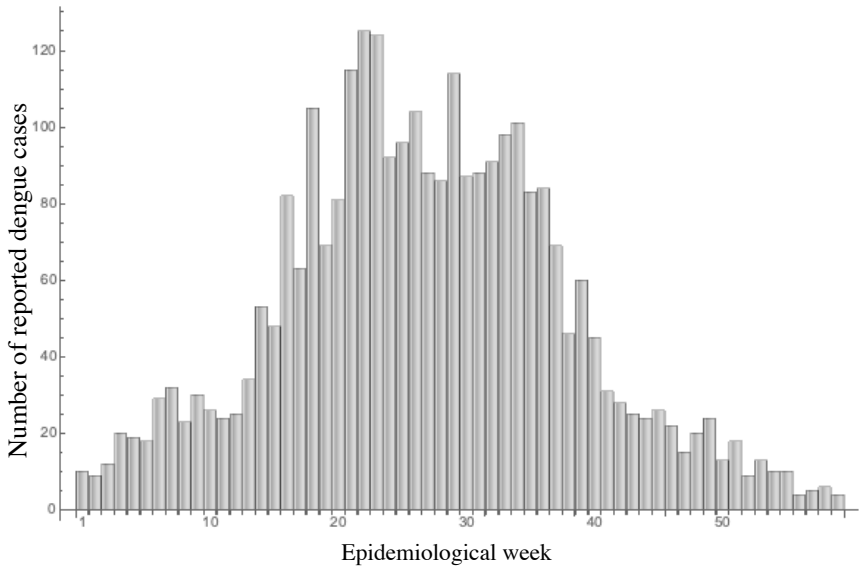

Figure 3.4 – **Number of reported dengue cases for Itagüí:** Bar chart showing the reported dengue cases from epidemiological week 51 of 2015 to epidemiological week 6 of 2016.

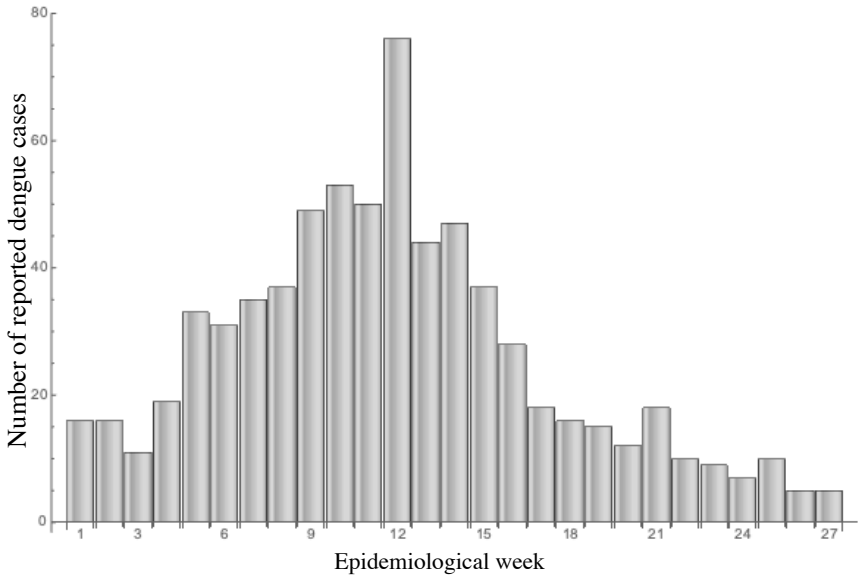

Figure 3.5 – **Number of reported dengue cases for Neiva:** Bar chart showing the reported dengue cases from epidemiological week 38 of 2016 to epidemiological week 9 of 2017.

3.3.2 Parameters

To define the biological ranges for transition and mortality parameters for vector populations, we used the results of life tables created from experiments performed in the BCEI laboratory (Grupo de Biología y Control de Enfermedades infecciosas de la Universidad de Antioquia) between 2017 and 2019, with mosquito populations of Itagüí and Neiva. However, we extended intervals for mortality rate (μ_m) since these ranges were calculated under experimental conditions and did not consider external factors (as fumigation) that can increase it. Finally, to compute the range of Λ we applied interval arithmetic. For a deeper description of the experimental protocol, we refer the reader to [53].

On the other hand, the information about the size of human population for each municipality was taken from the National Administrative Department of Statistics (DANE by its Spanish initials). Meanwhile, ranges of values for intrinsic incubation period (θ_h), extrinsic incubation period (θ_m), and recovery rate (γ_h) were calculated considering the average duration of each period ($1/\theta_h$, $1/\theta_m$) and ($1/\gamma_h$) according to [79]. Ranges for parameters and initial conditions for each municipality are summarized in Table 3.1 and 3.2, respectively.

3.4 Equilibrium points of the models

To analyze the dynamics of models (3.1) and (3.2), we first investigated the dynamic of the vector population of each model. Then we examined the steady states of all three models among humans. To do this, we assumed that all model parameters do not depend on time.

Table 3.1 – **Parameters used in the simulations of models (3.1)-(3.3) for Itagüí and Neiva, their biological descriptions, and their values range.**

Param.	Meaning	Itagüí		Neiva	
		Rang./day	Rang./week	Rang./day	Rang./week
δ	Per capita oviposition rate	[13, 60]	[13, 240]	[16, 32]	[16, 128]
γ_e	Transition rate from eggs to larvae	[0.2, 0.5]	[1.4, 3.5]	[0.2, 0.5]	[1.4, 3.5]
μ_e	Mortality rate in eggs	[0, 0.012]	[0, 0.83]	[0.008, 0.02]	[0.06, 0.14]
γ_l	Transition rate from larvae to pupae	[0.14, 0.17]	[1, 1.17]	[0.125, 0.2]	[0.88, 1.4]
μ_l	Mortality rate in larvae	[0.001, 0.03]	[0.01, 0.2]	[0.017, 0.04]	[0.12, 0.26]
γ_p	Transition rate from pupae to adults	[0.33, 1]	[2.33, 7]	[0.33, 1]	[2.33, 7]
μ_p	Mortality rate in pupae	[0, 0.04]	[0, 0.3]	[0, 0.04]	[0, 0.3]
ρ	Effective per capita oviposition rate	[12, 60]	[12, 240]	[14, 29]	[14, 128]
γ_m	Transition rate from the aquatic phase to the adult phase	[0.11, 0.13]	[0.77, 0.88]	[0.11, 0.13]	[0.77, 0.88]
μ_a	Mortality rate in the aquatic phase	[0.001, 0.027]	[0.008, 0.19]	[0.015, 0.028]	[0.11, 0.19]
C	Carrying capacity of the environment	[6400, 95000]	[6400, 95000]	[6400, 95000]	[6400, 95000]
f	Fraction of female mosquitoes hatched from all eggs	[0.39, 0.51]	[0.39, 0.51]	[0.32, 0.45]	[0.32, 0.45]
Λ	Recruitment rate	[273, 6297]	[1779, 42612]	[223, 5550]	[1454, 37529]
H	Size of human population	248036	248036	324466	324466
μ_m	Mortality rate in the adult phase	[0.011, 0.016]	[0.008, 0.26]	[0.02, 0.027]	[0.14, 0.45]
μ_h	Birth and death rate of the human population	0.000032	0.00023	0.000015	0.00011
β_m	Transmission rate from human to mosquito	[0, 4]	[0, 4]	[0, 4]	[0, 4]
β_h	Transmission rate from mosquito to human	[0, 4]	[0, 4]	[0, 4]	[0, 4]
θ_m	Transition rate from exposed to infected mosquito	[0.08, 0.13]	[0.58, 0.88]	[0.08, 0.13]	[0.58, 0.88]
θ_h	Transition rate from exposed to infected human	[0.1, 0.25]	[0.7, 1.75]	[0.1, 0.25]	[0.7, 1.75]
γ_h	Recovery rate	[0.07, 0.25]	[0.5, 1.75]	[0.07, 0.25]	[0.5, 1.75]

Table 3.2 – **Initial conditions used in the simulations of Model 3.3 for Neiva and Itagüí, their biological descriptions, and their values ranges.**

Initial condition	Meaning	Itagüí	Neiva
$E(0)$	Eggs	$[0,100000]$	$[0,100000]$
$L(0)$	Larvae	$[0,100000]$	$[0,100000]$
$P(0)$	Pupae	$[0,100000]$	$[0,100000]$
$A(0)$	Aquatic phase	$[0,100000]$	$[0,100000]$
$M_s(0)$	For susceptible mosquitoes	$[0,5000000]$	$[0,5000000]$
$M_e(0)$	For exposed mosquitoes	$[0,200]$	$[0,200]$
$M_i(0)$	For infectious mosquitoes	$[0,200]$	$[0,200]$
$H_s(0)$	For susceptible humans	$[198429,247912]$	$[259573,324294]$
$H_e(0)$	For exposed humans	$[21,84]$	$[27,108]$
$H_i(0)$	For infectious humans	$[10,40]$	$[16,64]$
$H_r(0)$	For recovered humans	$[0,49576]$	$[0,64850]$

3.4.1 Model 3.1

Since $M(t) = M_s(t) + M_e(t) + M_i(t)$, we see from the first six equations of (3.1) that vector dynamics from egg stage to adult stage is given by:

$$\begin{aligned}
\frac{dE}{dt} &= \delta\left(1 - \frac{E}{C}\right)M - (\gamma_e + \mu_e)E \\
\frac{dL}{dt} &= \gamma_e E - (\gamma_l + \mu_l)L \\
\frac{dP}{dt} &= \gamma_l L - (\gamma_p + \mu_p)P \\
\frac{dM}{dt} &= f\gamma_p P - \mu_m M
\end{aligned} \tag{3.4}$$

Mosquito dynamics: The system (3.4) has two equilibrium points; the mosquito-free state and the state in which mosquitoes are present denoted by

$$P_0 = (0,0,0,0)$$

$$P_1 = (E^*, L^*, P^*, M^*)$$

respectively, where

$$
\begin{aligned}
E^* &= C\left(1 - \frac{1}{R_M}\right) \\
L^* &= \frac{\gamma_e}{(\gamma_l + \mu_l)} E^* \\
P^* &= \frac{\gamma_l}{(\gamma_p + \mu_p)} \frac{\gamma_e}{(\gamma_l + \mu_l)} E^* \\
M_s^* = M^* &= \frac{f\gamma_p}{\mu_m} \frac{\gamma_l}{(\gamma_p + \mu_p)} \frac{\gamma_e}{(\gamma_l + \mu_l)} E^*
\end{aligned}
$$

where, $R_M = \frac{f\gamma_p}{\mu_m} \frac{\gamma_l}{(\gamma_p+\mu_p)} \frac{\gamma_e}{(\gamma_l+\mu_l)} \frac{\delta}{(\gamma_e+\mu_e)}$. This point is biologically acceptable when $R_M > 1$. Moreover, R_M can be biologically interpreted as the number of secondary mosquitoes produced by a single female (*the basic offspring number*). Now, we analyze the steady-state among humans for Model 3.1. These points are given by the constant solutions of the following algebraic system and

$$
\begin{aligned}
\delta\left(1 - \frac{E}{C}\right) M - (\gamma_e + \mu_e) E &= 0 \\
\gamma_e E - (\gamma_l + \mu_l) L &= 0 \\
\gamma_l L - (\gamma_p + \mu_p) P &= 0 \\
f\gamma_p P - \beta_m \frac{H_i}{H} M_s - \mu_m M_s &= 0 \\
\beta_m \frac{H_i}{H} M_s - (\theta_m + \mu_m) M_e &= 0 \\
\theta_m M_e - \mu_m M_i &= 0 \\
\mu_h H - \beta_h \frac{M_i}{M} H_s - \mu_h H_s &= 0 \\
\beta_h \frac{M_i}{M} H_s - (\theta_h + \mu_h) H_e &= 0 \\
\theta_h H_e - (\gamma_h + \mu_h) H_i &= 0 \\
\gamma_h H_i - \mu_h H_r &= 0
\end{aligned}
$$

Human population free of mosquitoes: The null (with respect to mosquito) equilibrium point is given by $E = 0$, $L = 0$, $P = 0$, $M_s = 0$, $M_e = 0$, $M_i = 0$, $H_s = H$,

$H_e == 0$, $H_i = 0$, and $H_r = 0$.

Human population infested with mosquito but free of dengue: The trivial (with respect to the disease) equilibrium point is given by

$$\begin{aligned}
E^* &= C\left(1 - \frac{1}{R_M}\right) \\
L^* &= \frac{\gamma_e}{(\gamma_l + \mu_l)} E^* \\
P^* &= \frac{\gamma_l}{(\gamma_p + \mu_p)} \frac{\gamma_e}{(\gamma_l + \mu_l)} E^* \\
M_s^* = M^* &= \frac{f\gamma_p}{\mu_m} \frac{\gamma_l}{(\gamma_p + \mu_p)} \frac{\gamma_e}{(\gamma_l + \mu_l)} E^* \\
M_e^* &= M_i^* = 0 \\
H_s^* &= H \\
H_e^* &= H_i^* = H_r^* = 0
\end{aligned} \tag{3.5}$$

where, $R_M = \frac{f\gamma_p}{\mu_m} \frac{\gamma_l}{(\gamma_p+\mu_p)} \frac{\gamma_e}{(\gamma_l+\mu_l)} \frac{\delta}{(\gamma_e+\mu_e)}$. This point is biologically acceptable when $R_M > 1$.

Dengue prevalent in human population: This non-trivial equilibrium point is given by

$$\begin{aligned}
E^* &= C\left(1 - \frac{1}{R_M}\right) \\
L^* &= \frac{\gamma_e}{(\gamma_l + \mu_l)} \cdot C\left(1 - \frac{1}{R_M}\right) \\
P^* &= \frac{\gamma_l}{(\gamma_p + \mu_p)} \cdot \frac{\gamma_e}{(\gamma_l + \mu_l)} \cdot C\left(1 - \frac{1}{R_M}\right) \\
M_s^* &= \frac{HC\mu_m(\gamma_e + \mu_e)(R_M - 1)}{\delta(\beta_m H_i^* + \mu_m H)} \\
M_e^* &= \frac{HC\mu_m(\gamma_e + \mu_e)(R_m - 1)}{\delta(\beta_m H_i^* + \mu_m H)} \cdot \frac{\beta_m}{(\theta_m + \mu_m)} \cdot \frac{H_i^*}{H} \\
M_i^* &= \frac{HC\mu_m(\gamma_e + \mu_e)(R_M - 1)}{\delta(\beta_m H_i^* + \mu_m H)} \cdot \frac{\beta_m \theta_m}{\mu_m(\theta_m + \mu_m)} \cdot \frac{H_i^*}{H} \\
H_s^* &= \frac{\mu_h(\theta_m + \mu_m)H(\mu_m H + \beta_m H_i^*)}{\beta_m H_i^*(\beta_h \theta_m + \mu_h(\theta_m + \mu_m)) + (\theta_m + \mu_m)\mu_h \mu_m H}
\end{aligned}$$

$$H_e^* = \frac{(\gamma_h + \mu_h)}{\theta_h} H_i^*$$
$$H_r^* = \frac{\gamma_h}{\mu_m} H_i^*$$

where, the number of infected humans H_i^* is

$$H_i^* = \frac{\beta_h \beta_m \theta_m \theta_h \mu_h H - (\theta_h + \mu_h)(\gamma_h + \mu_h)(\theta_m + \mu_m)\mu_h \mu_m H}{\beta_m (\theta_h + \mu_h)(\gamma_h + \mu_h)(\beta_h \theta_m + \mu_h(\theta_m + \mu_m))}$$

3.4.2 Model 3.2

Since $M(t) = M_s(t) + M_e(t) + M_i(t)$, we see from the first four equations of Model 3.2 that mosquito dynamics from vector population is given by

$$\begin{aligned} \frac{dA}{dt} &= \rho\left(1 - \frac{A}{C}\right)M - (\gamma_m + \mu_a)A \\ \frac{dM}{dt} &= f\gamma_m A - \mu_m M \end{aligned} \tag{3.6}$$

Then, to analyze the dynamic of Model 3.2, we first examined the dynamic of Model 3.6.

Mosquito dynamics: Model 3.6 has two equilibrium points; the mosquito-free state and the state in which mosquitoes are present denoted by

$$P_0 = (0, 0, 0, 0)$$
$$P_1 = (A^*, M^*)$$

respectively, where

$$A^* = C\left(1 - \frac{1}{R_M}\right)$$
$$M_s^* = M^* = \frac{f\gamma_m}{\mu_m} A^*$$

where, $R_M = \frac{f\gamma_m \rho}{\mu_m(\gamma_m + \mu_a)}$. This point is biologically acceptable when $R_M > 1$. More-

over, R_M can be biologically interpreted as the number of secondary mosquitoes produced by a single female (*the basic offspring number*).

Now, we consider the corresponding autonomous modeling to obtain a steady-state among humans for Model 3.2. One can get these points by equating the derivatives to zero

$$\begin{aligned}
\rho\left(1-\frac{A}{C}\right)M-(\gamma_m+\mu_a)A&=0\\
f\gamma_m A-\beta_m\frac{H_i}{H}M_s-\mu_m M_s&=0\\
\beta_m\frac{H_i}{H}M_s-(\theta_m+\mu_m)M_e&=0\\
\theta_m M_e-\mu_m M_i&=0\\
\mu_h H-\beta_h\frac{M_i}{M}H_s-\mu_h H_s&=0\\
\beta_h\frac{M_i}{M}H_s-(\theta_h+\mu_h)H_e&=0\\
\theta_h H_e-(\gamma_h+\mu_h)H_i&=0\\
\gamma_h H_i-\mu_h H_r&=0
\end{aligned}$$

Human population free of mosquitoes: The null (with respect to mosquito) equilibrium point is given by

$$\begin{aligned}
A=M_s=M_e=M_i&=0\\
H_s&=H\\
H_e=H_i=H_r&=0
\end{aligned}$$

Human population infested with mosquito but free of dengue: The trivial

(with respect to the disease) equilibrium point is given by

$$\begin{aligned} A^* &= C\left(1 - \frac{1}{R_M}\right) \\ M_s^* &= M^* = \frac{f\gamma_m}{\mu_m} A^* \\ M_e^* &= M_i^* = 0 \\ H_s^* &= H \\ H_e^* &= H_i^* = H_r^* = 0 \end{aligned} \tag{3.7}$$

Dengue prevalent in human population: This non-trivial equilibrium point is given by

$$\begin{aligned} A^* &= C\left(1 - \frac{1}{R_M}\right) \\ M_s^* &= \frac{HC\mu_m(\gamma_m + \mu_a)(R_M - 1)}{\rho(\beta_m H_i^* + \mu_m H)} \\ M_e^* &= \frac{HC\mu_m(\gamma_m + \mu_a)(R_M - 1)}{\rho(\beta_m H_i^* + \mu_m H)} \cdot \frac{\beta_m}{(\theta_m + \mu_m)} \cdot \frac{H_i^*}{H} \\ M_i^* &= \frac{HC\mu_m(\gamma_m + \mu_a)(R_M - 1)}{\rho(\beta_m H_i^* + \mu_m H)} \cdot \frac{\beta_m \theta_m}{\mu_m(\theta_m + \mu_m)} \cdot \frac{H_i^*}{H} \\ H_s^* &= \frac{\mu_h H(\theta_m + \mu_m)(\mu_m H + \beta_m H_i^*)}{\beta_h \beta_m \theta_m H_i^* + \mu_h(\theta_m + \mu_m)(\mu_m H + \beta_m H_i^*)} \\ H_e^* &= \frac{(\gamma_h + \mu_h)}{\theta_h} H_i^* \\ H_r^* &= \frac{\gamma_h}{\mu_m} H_i^* \end{aligned}$$

where, the number of infected humans H_i^* is

$$H_i^* = \frac{\beta_h \beta_m \theta_m \theta_h \mu_h H - (\theta_h + \mu_h)(\gamma_h + \mu_h)(\theta_m + \mu_m)\mu_h \mu_m H}{\beta_m(\theta_h + \mu_h)(\gamma_h + \mu_h)(\beta_h \theta_m + \mu_h(\theta_m + \mu_m))}$$

3.4.3 Model 3.3

Since $M(t) = M_s(t)+M_e(t)+M_i(t)$, we see from the first three equations of Model 3.3 that mosquito dynamics is governed by

$$\frac{dM}{dt} = \Lambda - \mu_m M \tag{3.8}$$

The solution M of this equation approach the equilibrium as Λ/μ_m $t \to \infty$. Moreover, only when Λ is equal to zero, the equilibrium point would be free of mosquitoes.

To obtain a steady-state among humans for Model 3.3, we consider the solutions to the system:

$$\begin{aligned}
\Lambda - \beta_m \frac{H_i}{H} M_s - \mu_m M_s &= 0 \\
\beta_m \frac{H_i}{H} M_s - (\theta_m + \mu_m) M_e &= 0 \\
\theta_m M_e - \mu_m M_i &= 0 \\
\mu_h H - \beta_h \frac{M_i}{M} H_s - \mu_h H_s &= 0 \\
\beta_h \frac{M_i}{M} H_s - (\theta_h + \mu_h) H_e &= 0 \\
\theta_h H_e - (\gamma_h + \mu_h) H_i &= 0 \\
\gamma_h H_i - \mu_h H_r &= 0
\end{aligned}$$

Human population infested with mosquito but free of dengue: The trivial (with respect to the disease) equilibrium point is given by

$$\begin{aligned}
M_s^* &= M^* = \frac{\Lambda}{\mu_m} \\
M_e^* &= M_i^* = 0 \\
H_s^* &= H \\
H_e^* &= H_i^* = H_r^* = 0
\end{aligned} \tag{3.9}$$

Dengue prevalent in human population: This non-trivial equilibrium point is given by

$$
\begin{aligned}
M_s^* &= \frac{\Lambda H}{(\beta_m H_i^* + \mu_m H)} \\
M_e^* &= \frac{\Lambda H}{(\beta_m H_i^* + \mu_m H)} \cdot \frac{\beta_m}{(\theta_m + \mu_m)} \cdot \frac{H_i^*}{H} \\
M_i^* &= \frac{\Lambda H}{(\beta_m H_i^* + \mu_m H)} \cdot \frac{\beta_m \theta_m}{\mu_m(\theta_m + \mu_m)} \cdot \frac{H_i^*}{H} \\
H_s^* &= \frac{\mu_h H(\theta_m + \mu_m)(\mu_m H + \beta_m H_i^*)}{\beta_h \beta_m \theta_m H_i^* + \mu_h(\theta_m + \mu_m)(\mu_m H + \beta_m H_i^*)} \\
H_e^* &= \frac{(\gamma_h + \mu_h)}{\theta_h} H_i^* \\
H_r^* &= \frac{\gamma_h}{\mu_m} H_i^*
\end{aligned}
$$

where, the number of infected humans H_i^* is calculated by the equation

$$
H_i^* = \frac{\beta_h \beta_m \theta_m \theta_h \mu_h H - (\theta_h + \mu_h)(\gamma_h + \mu_h)(\theta_m + \mu_m)\mu_h \mu_m H}{\beta_m(\theta_h + \mu_h)(\gamma_h + \mu_h)(\beta_h \theta_m + \mu_h(\theta_m + \mu_m))}
$$

3.5 Basic reproductive number, R_0

Models (3.1)–(3.3) have four infected states, notably, exposed mosquitoes M_e, infected mosquitoes M_i, exposed human H_e, and infected human H_i. The infected subsystem associated with these models is given by

$$
\begin{aligned}
\frac{dM_e}{dt} &= \beta_m \frac{H_i}{H} M_s - (\theta_m + \mu_m) M_e \\
\frac{dM_i}{dt} &= \theta_m M_e - \mu_m M_i \\
\frac{dH_e}{dt} &= \beta_h \frac{M_i}{M} H_s - (\theta_h + \mu_h) H_e \\
\frac{dH_i}{dt} &= \theta_h H_e - (\gamma_h + \mu_h) H_i
\end{aligned}
\tag{3.10}
$$

The *human population infested with mosquito but free of dengue* for each model are given by Equations (3.5), (3.7) and (3.9), respectively.

Then, the linearization of System 3.10 around the *infection-free steady state* for all three models can be stated as

$$\dot{\mathbf{x}} = (T + \Sigma)\mathbf{x}$$

where, $\mathbf{x} = [\, M_e \, M_i \, H_e \, H_i \,]^T$, $T = \begin{pmatrix} 0 & 0 & 0 & \beta_m \frac{M_s^*}{H} \\ 0 & 0 & 0 & 0 \\ 0 & \beta_h \frac{H_s^*}{M} & 0 & 0 \\ 0 & 0 & 0 & 0 \end{pmatrix}$ is the transmission matrix,

and $\Sigma = \begin{pmatrix} -(\theta_m + \mu_m) & 0 & 0 & 0 \\ \theta_m & -\mu_m & 0 & 0 \\ 0 & 0 & (\theta_h + \mu_h) & 0 \\ 0 & 0 & \theta_h & -(\gamma_h + \mu_h) \end{pmatrix}$ is the transition matrix.

Hence the NGM matrix $\mathbf{K}$ is four-dimensional, and it is

$$\begin{aligned} \mathbf{K} &= -T\Sigma^{-1} \\ &= \begin{pmatrix} 0 & 0 & 0 & \beta_m \frac{M_s^*}{H} \\ 0 & 0 & 0 & 0 \\ 0 & \beta_h \frac{H_s^*}{M} & 0 & 0 \\ 0 & 0 & 0 & 0 \end{pmatrix} \begin{pmatrix} \frac{1}{(\theta_m+\mu_m)} & 0 & 0 & 0 \\ \frac{\theta_m}{\mu_m(\theta_m+\mu_m)} & \frac{1}{\mu_m} & 0 & 0 \\ 0 & 0 & \frac{1}{(\theta_h+\mu_h)} & 0 \\ 0 & 0 & \frac{\theta_h}{(\theta_h+\mu_h)(\gamma_h+\mu_h)} & \frac{1}{(\gamma_h+\mu_h)} \end{pmatrix} \\ &= \begin{pmatrix} 0 & 0 & \frac{\beta_m \theta_h}{(\theta_h+\mu_h)(\gamma_h+\mu_h)} \frac{M_s^*}{H} & \frac{\beta_m}{(\gamma_h+\mu_h)} \frac{M_s^*}{H} \\ 0 & 0 & 0 & 0 \\ \frac{\beta_h \theta_m}{\mu_m(\theta_m+\mu_m)} \frac{H_s^*}{M} & \frac{\beta_h}{\mu_m} \frac{H_s^*}{M} & 0 & 0 \\ 0 & 0 & 0 & 0 \end{pmatrix} \end{aligned}$$

The eigenvalues of **K** are zero of multiplicity 2, and

$$\pm\sqrt{\frac{\beta_m\beta_h\theta_m\theta_h}{\mu_m(\theta_m+\mu_m)(\theta_h+\mu_h)(\gamma_h+\mu_h)}\frac{H_s^*M_s^*}{HM}}.$$

Therefore,

$$R_0=\sqrt{\frac{\beta_m\beta_h\theta_m\theta_h}{\mu_m(\theta_m+\mu_m)(\theta_h+\mu_h)(\gamma_h+\mu_h)}} \tag{3.11}$$

because in the *infection-free steady state*, $H_s^*=H$ and $M_s^*=M$.

The expression in Equation (3.11) gives us the geometric mean between the number of secondary infections of all sub-populations considered in each model, where the component

$$R_{0_H}=\sqrt{\frac{\beta_h\theta_h}{(\theta_h+\mu_h)(\gamma_h+\mu_h)}} \tag{3.12}$$

gives us information about the number of infected humans in the next generation. Meanwhile, the expression

$$R_{0_M}=\sqrt{\frac{\beta_m\theta_m}{\mu_m(\theta_m+\mu_m)}}$$

gives us information about the number of infected mosquitoes in the next generation.

In this way, according to [62], it is possible that an outbreak may occur when $R_0<1$ but as long as the component of infected human will be greater than one and the presence of certain number of infected mosquitoes.

3.5.1 Local sensitivity analysis of R_0

To investigate the local sensitivity of the basic reproductive number (R_0) for changes in the parameters, we calculated the derivatives with respect to each

one. We observed from the expression in Equation (3.11) that

$$\begin{aligned}
\frac{\partial R_0}{\partial \beta_m} &= \frac{1}{2\beta_m} R_0 \\
\frac{\partial R_0}{\partial \beta_h} &= \frac{1}{2\beta_h} R_0 \\
\frac{\partial R_0}{\partial \theta_m} &= \frac{\mu_m}{2\theta_m(\theta_m + \mu_m)} R_0 \\
\frac{\partial R_0}{\partial \theta_h} &= \frac{\mu_h}{2\theta_h(\theta_h + \mu_h)} R_0 \\
\frac{\partial R_0}{\partial \mu_m} &= -\frac{1}{2(\theta_m + \mu_m)} \left(2 + \frac{\theta_m}{\mu_m}\right) R_0 \\
\frac{\partial R_0}{\partial \gamma_h} &= -\frac{1}{2(\gamma_h + \mu_h)} R_0
\end{aligned}$$

Partial derivatives of parameters such as transmission rate from human to mosquito (β_m), transmission rate from mosquito to human (β_h), transition rate from exposed to infected mosquitoes (θ_m), and transition rate from exposed to infected humans (θ_h) are always positive, i.e. an increase in them increases the value of R_0. Meanwhile, for mortality rate in mosquitoes (μ_m) and the recovery rate in humans (γ_h), partial derivatives are always negative, thus when values of these parameters decrease, the value of R_0 increases.

To determine which parameters have more influence in the occurrence of new dengue cases, we calculated the *elasticity* of R_0 with respect to each parameter θ. The elasticity is given by

$$\varepsilon_\theta^{R_0} = \frac{\partial R_0}{\partial \theta} \frac{\theta}{R_0} \approx \frac{\%\Delta R_0}{\%\Delta \theta}. \tag{3.13}$$

The elasticities give the percentage change in R_0 in response to 1% increase in the parameter θ. When $\varepsilon_\theta^{R_0} > 0$, that means that R_0 increases with θ; when $\varepsilon_\theta^{R_0} < 0$ that means that R_0 decreases when θ increases [60].

For instance, we consider for Itagüí the parameter values as $\beta_m = 0.12$, $\beta_h = 2.5$, $\theta_m = 0.6$, $\theta_h = 1.3$, $\mu_m = 0.22$, and $\gamma_h = 1.75$. For Neiva, we consider the

parameter values as $\beta_m = 0.14$, $\beta_h = 2.5$, $\theta_m = 0.8$, $\theta_h = 1.3$, $\mu_m = 0.4$, and $\gamma_h = 1.7$. The fact that $\varepsilon_{\beta_m}^{R_0} = 0.5$ means that 1% increase in β_m will produce 0.5% increase in R_0. We summarize these results for each municipality in Table 3.3.

Table 3.3 – **Elasticity of R_0 for Neiva and Itagüí.**

Elasticity	Itagüí	Neiva
$\varepsilon_{\beta_m}^{R_0}$	0.5	0.5
$\varepsilon_{\beta_h}^{R_0}$	0.5	0.5
$\varepsilon_{\theta_m}^{R_0}$	0.134	0.167
$\varepsilon_{\theta_h}^{R_0}$	8.8×10^{-5}	4.2×10^{-5}
$\varepsilon_{\mu_m}^{R_0}$	-0.634	-0.667
$\varepsilon_{\gamma_h}^{R_0}$	-0.5	-0.5

It is important to notice that $\varepsilon_{\beta_m}^{R_0}$ and $\varepsilon_{\beta_h}^{R_0}$ always are equal to 0.5, while the other elasticities depend on parameter values. Table 3.4 shows the elasticity ranges for Itagüí and Neiva considering the parameter ranges given in Table 3.1. We compute these ranges using interval arithmetic.

Table 3.4 – **Elasticity ranges of R_0 for Neiva and Itagüí.**

Elasticity	Itagüí	Neiva
$\varepsilon_{\theta_m}^{R_0}$	$[0.0045, 0.1548]$	$[0.0686, 0.5]$
$\varepsilon_{\theta_h}^{R_0}$	$[6.5 \times 10^{-5}, 1.7 \times 10^{-4}]$	$[3.1 \times 10^{-5}, 7.9 \times 10^{-5}]$
$\varepsilon_{\mu_m}^{R_0}$	$[-0.8050, -0.3543]$	$[-0.8682, -0.4189]$
$\varepsilon_{\gamma_h}^{R_0}$	$[-0.5, -0.4998]$	$[-0.5, -0.4999]$

3.6 Structural identifiability analysis

"In many sciences, it is possible to conduct experiments to obtain information and test hypotheses. However, experiments with the spread of infectious diseases in human populations are often impossible, unethical, or expensive." [42]. Therefore, we can not measure all parameters of the models through experimental assays. However, indirect approaches such as parameter estimation methods can help us

to determine the values of these parameters using the available information. To know if it is possible to estimate unique values to model unknown parameters from the available observables (assuming noise-free data and error-free model), we have to conduct a study on structural identifiability analysis. This analysis does not require experimental data. For that reason, this analysis is called *a prior analysis* and can be used to design experimental assays and determine which information should be collected. To set up this problem, we considered the models (3.1)–(3.3) in the following form

$$\dot{\mathbf{x}}(t) = \mathbf{f}(t, \mathbf{x}(t), \boldsymbol{\theta}), \ \mathbf{x}(0) = \mathbf{x}_0 \tag{3.14}$$

where, $\boldsymbol{\theta}$ denotes the parameters of the system, $\mathbf{x}(t)$ is the vector of state variables, and $\mathbf{x}_0$ are the initial values. The cumulative number of dengue cases are given by the output function $\mathbf{h}(\mathbf{x}(t), \boldsymbol{\theta})$. To establish a system that is *structural identifiable*, we introduced the following definitions mentioned in [67].

Definition 3.6.1. A system structure (3.14) is said to be *globally identifiable* if for any two parameter vectors $\boldsymbol{\theta}_1$ and $\boldsymbol{\theta}_2$ in the parameter space, $\mathbf{h}(\mathbf{x}(t), \boldsymbol{\theta}_1) = \mathbf{h}(\mathbf{x}(t), \boldsymbol{\theta}_2)$ holds if and only if $\boldsymbol{\theta}_1 = \boldsymbol{\theta}_2$.

Definition 3.6.2. A system structure (3.14) is said to be *locally identifiable* if for any $\boldsymbol{\theta}$ within an open neighborhood of some point $\boldsymbol{\theta}^*$ in the parameter space, $\mathbf{h}(\mathbf{x}(t), \boldsymbol{\theta}_1) = \mathbf{h}(\mathbf{x}(t), \boldsymbol{\theta}_2)$ holds if and only if $\boldsymbol{\theta}_1 = \boldsymbol{\theta}_2$.

There are several approaches to perform this method [67] like direct methods, implicit function based approaches, and Taylor's generating series. A deeper discussion, comparison, and details of structural identifiability analysis are mentioned in [15]. As per our knowledge, in computational approach, we count with various software tools designed to perform structural identifiability analysis of non-linear models, such as DAISY [8], GenSSI [16], the Identifiability Analysis package in MATHEMATICA [45], COMBOS [66], and STRIKE-GOLDD [106].

In this study, we use the *Identifiability Analysis* package in MATHEMATICA software to test for the local identifiability of the epidemiological models of dengue transmission (3.1)–(3.3). This implementation is based on a probabilistic numerical method of computing the identifiability (Jacobian) matrix's rank where the matrix parameters and initial state variables are specialized to random integers. For more detailed information, refer to [45].

For models (3.1)–(3.3), we evaluated if these are locally identifiable from the number of cumulative dengue cases reported by official entities only. We also fixed the values of human mortality rate, μ_h and the initial condition for infected humans, $H_i(0)$ according to ranges obtained from experimental assays (see Tables 3.1–3.2). Table 3.5 shows the parameters are not locally identifiable for any of the models. For all models, we obtained that the parameters describing the vector's development stages, the recruitment rate in the adult population, and the vector population's initial conditions were not identifiable from the cumulative number of dengue cases in humans. However, the number of non-identifiable parameters assumed to obtain a locally structural identifiable system for models Models 3.1 to 3.3 are five, three and one, respectively. These numbers correspond to the minimal necessary information that grants the identifiability matrix (Jacobian matrix) a full range.

3.7 Discussion and conclusions

This chapter described the three models published in [54] to simulate dengue transmission disease. The main difference among these models is the number of parameters and state variables used to describe the development stages of the vector population.

Similar models have been published earlier to evaluate different control strategies and to simulate outbreaks in different cities [17, 19, 89]. However, the

Table 3.5 – **Non-structurally identifiable parameters and initial conditions for models (3.1)–(3.3).**

	Non-structural identifiable	
	Parameters	**Initial Conditions**
Model (3.1)	δ Per capita oviposition rate C Carrying capacity of the environment γ_e Transition rate from eggs to larvae μ_e Mortality rate in eggs phase γ_l Transition rate from larvae to pupae μ_l Mortality rate in larvae phase γ_p Transition rate from pupae to the adult phase μ_p Mortality rate in pupae phase f Fraction of female mosquitoes hatched from all eggs	$E(0)$ Eggs $L(0)$ Larvae $P(0)$ Pupae $M_s(0)$ Susceptible mosquitoes $M_e(0)$ Exposed mosquitoes $M_i(0)$ Infected mosquitoes
Model (3.2)	ρ Effective per capita oviposition rate C Carrying capacity of the environment γ_m Transition rate from the aquatic phase to the adult phase μ_a Mortality rate in the aquatic phase f Fraction of female mosquitoes hatched from all eggs	$A(0)$ Aquatic phase $M_s(0)$ Susceptible mosquitoes $M_e(0)$ Exposed mosquitoes $M_i(0)$ Infected mosquitoes
Model (3.3)	Λ Recruitment rate	$M_s(0)$ Susceptible mosquitoes $M_e(0)$ Exposed mosquitoes $M_i(0)$ Infected mosquitoes

majority of these studies consider parameter values taken from the literature. Here to simulate the outbreaks in Itagüí and Neiva, we use local parameters relevant to the study area. To do this, we considered (i) results from experimental assays with local mosquito populations for each municipality; (ii) the average transition time from exposed to infected (mosquitoes and humans); (iii) the average recovery time in humans; (iv) official information of new dengue cases

per week; and (v) the size of the human population for each municipality. It is pertinent to note that experimental assays under laboratory conditions did not consider the mortality rate for external factors. In this way, these results do not always correspond to the vector life in the wild. For this reason, we extended the range for mosquito mortality rate to include external causes that increase it.

It is relevant to point out that much research has been done to formulate new models that include different transmission characteristics as multiple serotypes, age groups, migrations, and the influence of climatic factors [30, 102, 64]. However, few studies have evaluated the relationship between the model formulation and the available data to obtain more reliable and accurate conclusions.

For instance, in [103, 104], those authors evaluated the performance and reliability of the fitting data of different models, considering the results of the identifiability analyses. While other studies perform sensitivity analyses on the Basic Reproductive Number, R_0, to determine which parameters are more critical in producing secondary cases [112, 108]. Nonetheless, we found that it is necessary to carry out these analyses together because they are complementary.

An essential expression for outbreak characterization is R_0. This number gives us information about the average number of secondary cases that a single case can produce if introduced into a susceptible population [22]. We found that the same expression gives the Basic Reproductive Number for all models by applying the Next Generation Matrix operator [23]. To determine which parameters influence the production of secondary cases, we calculated the elasticity of R_0 for each parameter. Table 1 showed that the occurrence of new dengue cases was more sensitive to transmission rate from human to mosquito, transmission rate from mosquito to human, the recovery rate in humans, and the mortality rate in mosquitoes. These results coincide with the results shown in [32].

Finally, the locally structural identifiability analysis results showed that the parameters that describe the interactions and transitions between the human

population are locally identifiable from the cumulative number of reported dengue cases. In contrast, the parameters that describe the development stages and sizes of the vector population are not identifiable (see Table 3.5). For these reasons, to obtain locally structural identifiable models, it is required to collect information about the mosquito population. However, collecting this information for long periods can be expensive and unreliable.

In summary, the findings from elasticities and identifiability analysis allow us to conclude that the most suitable model to simulate an outbreak when the only available information is the number of new cases per week is Model 3.3.

In the subsequent chapters, we will only work with Model 3.3. Moreover, we will use the results obtained in this chapter to determine which parameters and initial conditions should be considered uncertain.

Bibliography of the current chapter

[8] Giuseppina Bellu, Maria Pia Saccomani, Stefania Audoly, and Leontina D'Angiò. DAISY: A new software tool to test global identifiability of biological and physiological systems. Computer Methods and Programs in Biomedicine 88.1 (2007), pp. 52–61. DOI: https://doi.org/10.1016/j.cmpb.2007.07.002 (cit. on p. 80).

[15] Oana-Teodora Chis, Julio R Banga, and Eva Balsa-Canto. Structural Identifiability of systems biology models: A critical comparison of methods. PLoS ONE 6.11 (2011), e27755. DOI: https://doi.org/10.1371/journal.pone.0027755 (cit. on p. 80).

[16] Oana Chiş, Julio R. Banga, and Eva Balsa-Canto. GenSSI: A software toolbox for structural identifiability analysis of biological models. Bioinformatics 27.18 (2011), pp. 2610–2611. DOI: https://doi.org/10.1093/bioinformatics/btr431 (cit. on p. 80).

[17] Laurent Coudeville and Geoff P Garnett. Transmission dynamics of the four dengue serotypes in southern Vietnam and the potential impact of vaccination. PloS one 7.12 (2012), e51244 (cit. on pp. 27, 81).

[19] Michel De Lara and Lilian Sofia Sepulveda Salcedo. Viable control of an epidemiological model. Mathematical biosciences 280 (2016), pp. 24–37 (cit. on pp. 26, 81).

[22] O. Diekmann, J. A.P. Heesterbeek, and J. A.J. Metz. On the definition and the computation of the basic reproduction ratio R_0 in models for infectious diseases in heterogeneous populations. Journal of Mathematical Biology 28.4 (1990), pp. 365–382. DOI: https://doi.org/10.1007/BF00178324 (cit. on pp. 25, 83).

[23] O. Diekmann, J.A.P. Heesterbeek, and M.G. Roberts. The construction of next-generation matrices for compartmental epidemic models. Journal of the Royal Society Interface 7.47 (2010), pp. 873–885. DOI: https://doi.org/10.1098/rsif.2009.0386 (cit. on pp. 25, 83).

[28] Lourdes Esteva and Cristobal Vargas. A model for dengue disease with variable human population. Journal of Mathematical Biology 38.3 (1999), pp. 220–240. DOI: https://doi.org/10.1007/s002850050147 (cit. on pp. 27, 59).

[29] Lourdes Esteva and Cristobal Vargas. Analysis of a dengue disease transmission model. Mathematical Biosciences 150.2 (1998), pp. 131–151. DOI: https://doi.org/10.1016/S0025-5564(98)10003-2 (cit. on pp. 27, 62).

[30] Lourdes Esteva and Cristobal Vargas. Coexistence of different serotypes of dengue virus. Journal of Mathematical Biology 46.1 (2003), pp. 31–47 (cit. on pp. 27, 83).

[32] Lourdes Esteva and Hyun Mo Yang. Assessing the effects of temperature and dengue virus load on dengue transmission. Journal of Biological Systems 23.04 (2015), p. 1550027. DOI: https://doi.org/10.1142/S0218339015500278 (cit. on pp. 27, 83).

[42] Herbert W Hethcote. The basic epidemiology models: models, expressions for R_0, parameter estimation, and applications. In: Mathematical understanding of infectious disease dynamics. World Scientific, 2009, pp. 1–61. DOI: https://doi.org/10.1142/9789812834836_0001 (cit. on pp. 18, 45, 79).

[45] Johan Karlsson, Milena Anguelova, and Mats Jirstrand. An Efficient Method for Structural Identifiability Analysis of Large Dynamic Systems. 16th IFAC Symposium on System Identification. IFAC Proceedings Volumes 45.16 (2012), pp. 941–946. DOI: https://doi.org/10.3182/20120711-3-BE-2027.00381 (cit. on pp. 80, 81).

[53] Diana Paola Lizarralde-Bejarano, Sair Arboleda-Sánchez, and María Eugenia Puerta-Yepes. Understanding epidemics from mathematical models: Details of the 2010 dengue epidemic in Bello (Antioquia, Colombia). Applied Mathematical Modelling 43 (2017), pp. 566–578. DOI: https://doi.org/10.1016/j.apm.2016.11.022 (cit. on p. 66).

[54] Diana Paola Lizarralde-Bejarano, Daniel Rojas-Díaz, Sair Arboleda-Sánchez, and María Eugenia Puerta-Yepes. Sensitivity, uncertainty and identifiability analyses to define a dengue transmission model with real data of an endemic municipality of Colombia. PLoS ONE 15.3 (2020), e0229668. DOI: https://doi.org/10.1371/journal.pone.0229668 (cit. on pp. 58, 81, 131, 162).

[60] Maia Martcheva. Ch. 6: Fitting Models to Data in: An Introduction to Mathematical Epidemiology. Springer US, 2015, pp. 123–148. DOI: https://doi.org/10.1007/978-1-4899-7612-3_6 (cit. on p. 78).

[62] E Massad, FAB Coutinho, MN Burattini, and M Amaku. Estimation of R_0 from the initial phase of an outbreak of a vector-borne infection. Tropical medicine & international health 15.1 (2010), pp. 120–126 (cit. on p. 77).

[64] Emanuele Massaro, Daniel Kondor, and Carlo Ratti. Assessing the interplay between human mobility and mosquito borne diseases in urban environments. Scientific Reports 9.1 (Nov. 2019). DOI: 10.1038/s41598-019-53127-z (cit. on p. 83).

[66] Nicolette Meshkat, Christine Er-zhen Kuo, and Joseph DiStefano. On finding and using identifiable parameter combinations in nonlinear dynamic systems biology models and COMBOS: A novel web implementation. PLoS ONE 9.10 (2014), e110261. DOI: https://doi.org/10.1371/journal.pone.0110261 (cit. on p. 80).

[67] Hongyu Miao, Xiaohua Xia, Alan S. Perelson, and Hulin Wu. On identifiability of nonlinear ODE models and applications in viral dynamics. SIAM review 53.1 (2011), pp. 3–39. DOI: https://doi.org/10.1137/090757009 (cit. on p. 80).

[79] World Health Organization et al. Dengue: Guías para el diagnóstico, tratamiento, prevención y control: nueva edición. Tech. rep. Ginebra: Organización Mundial de la Salud, May 2009 (cit. on pp. 26, 66).

[89] Suani Tavares Rubim de Pinho, Claudia P Ferreira, Lourdes Esteva, FR Barreto, VC Morato e Silva, and MGL Teixeira. Modelling the dynamics of dengue real epidemics. Philosophical Transactions of the Royal Society A: Mathematical, Physical and Engineering Sciences 368.1933 (2010), pp. 5679–5693 (cit. on pp. 27, 81).

[102] Khoa T. D. Thai et al. Age-Specificity of Clinical Dengue during Primary and Secondary Infections. PLoS Neglected Tropical Diseases 5.6 (June 2011). Ed. by Benedito A. Lopes da Fonseca, e1180. DOI: 10.1371/journal.pntd.0001180 (cit. on p. 83).

[103] Necibe Tuncer, Hayriye Gulbudak, Vincent L Cannataro, and Maia Martcheva. Structural and practical identifiability issues of immuno-epidemiological vector-host models with application to rift valley fever. Bulletin of mathematical biology 78.9 (2016), pp. 1796–1827 (cit. on p. 83).

[104] Necibe Tuncer, Maia Marctheva, Brian LaBarre, and Sabrina Payoute. Structural and practical identifiability analysis of Zika epidemiological models. Bulletin of mathematical biology 80.8 (2018), pp. 2209–2241 (cit. on p. 83).

[106] Alejandro F. Villaverde, Antonio Barreiro, and Antonis Papachristodoulou. Structural Identifiability of Dynamic Systems Biology Models. PLoS Computational Biology 12.10 (2016), pp. 1–22. DOI: https://doi.org/10.1371/journal.pcbi.1005153 (cit. on p. 80).

[108] Liping Wang, Hongyong Zhao, Sergio Muniz Oliva, and Huaiping Zhu. Modeling the transmission and control of Zika in Brazil. Scientific Reports 7.1 (Aug. 2017). DOI: 10.1038/s41598-017-07264-y (cit. on p. 83).

[112] Kenta Yashima and Akira Sasaki. Spotting Epidemic Keystones by R_0 Sensitivity Analysis: High-Risk Stations in the Tokyo Metropolitan Area. PLOS ONE 11.9 (Sept. 2016). Ed. by Hiroshi Nishiura, e0162406. DOI: 10.1371/journal.pone.0162406 (cit. on p. 83).

Chapter 4

Forward problem: Interval differential equations

Outline of the current chapter

4.1 Abstract

This chapter introduces a strategy first to select the uncertain quantities (parameters and initial conditions) and second to find guaranteed enclosures on the solutions of ODEs. To illustrate the performance of this approach, we consider Model 3.3 and include the uncertainty in the parameters and the initial conditions through interval analysis. The selection process of the uncertain quantities (parameters and initial conditions) was carried out based on the results of (i) the sensitivity analysis of R_0, (ii) the structural identifiability analysis of the model, (iii) the characteristics of the available information about mosquito population, and (iii) the incidence data of dengue in two municipalities in Colombia, Itagüí and Neiva, during the outbreaks in 2016. Then, to find guaranteed enclosures on such a system's solutions, we use numerical methods in the framework on interval analysis. These methods compute the solutions using self-verified integrators. Specifically, we use a method where the solution is expressed as an Interval Taylor Serie (ITS), where its coefficients are given by Taylor models that can depend on simultaneously the parameters and the initial conditions.

The experiments demonstrated the importance of including interval-valued uncertainty in parameters as the mortality rate in mosquito and the transmission rates since these parameters cannot be measured accurately. Also, it was possible to consider scenarios in which the vector populations were more extensive and get solutions when the number of reported cases is higher. Obtaining robust and verified solutions in these scenarios are relevant for decision-making and applying more efficient control measures.

4.2 Problem statement

Our focus here is on non-linear ODE models which are formulated as Initial Value Problems (IVPs) as

$$\dot{x}(t) = f(x, \theta), \qquad x(t_0) = x_0, \tag{4.1}$$

where, $t \in [t_0, t_k]$, $t_k > t_0$, $\theta \in \Theta$ is the m-dimensional vector of parameters, x is the n-dimensional vector of state variables, and x_0 is the n-dimensional vector of initial conditions. Furthermore, Θ and X_0 are interval vectors that represent the enclosures of the uncertainties of parameters and initial conditions, respectively.

Usually, an analytical solution does not exist for Equation (4.1), so we have to use numerical methods to obtain the model trajectories. The purpose here is to obtain mathematically and computationally guaranteed enclosures for the vector of state variables x at all times, i.e. from t_0 to t_m, and compare these enclosures with the behaviour of real data. To do this, we will use the software VSPODE (Validating Solver for Parametric ODEs), which can produce guaranteed enclosures on models when initial states and parameters are given by intervals. Moreover, VSPODE has been applied to obtain rigorous enclosures for some psychology models, ecology models, and epidemiological models [26, 27, 25]. For more discussion on different methodologies proposed to solve Equation (4.1) and the main drawbacks caused due to the overestimation caused by the dependency problem and wrapping effect that arise and strategies to solve them, refer to [72, 55]. To illustrate the performance of this methodology, we considered Model 3.3 and the reported dengue cases for Itagüí and Neiva (see Figures 3.4 and 3.5).

4.3 Taylor models

Most often, the verified methods (interval methods) result useless to deal with practical problems. This is because of the overestimation caused by the dependency problem and the wrapping effect. One way to handle these drawbacks is through the application of the Taylor model methods developed by Berz and his co-workers since the 1990s, which combined interval arithmetic with symbolic computations [74]. To apply these methods, we have to consider Taylor expansions and an enclosure for the remainder.

Formally, let a function $f : D \subset \mathbb{R}^s \to \mathbb{R}$ that is $(n+1)$ times continuously partially differentiable. A *Taylor model* for f is given by $T = (P, e) = P + e$ where, P denotes the n-th order Taylor polynomial of f around the expansion point $x_0 \in D$ and e is a small bounding set for the remainder of this approximation:

$$f(x) - P(x - x_0) \in e, \ \forall x \in D \text{ where } x_0 \in D. \tag{4.2}$$

For two Taylor models, $T_1 = (P_1, e_1)$ and $T_2 = (P_2, e_2)$ of order n, it is possible to define addition and multiplication as follows

$$\begin{aligned} T_1 + T_2 &= (P_1 + P_2, e_1 + e_2) \\ T_1 \cdot T_2 &= P_1 \cdot P_2 + P_1 \cdot e_2 + P_2 \cdot e_1 + e_1 \cdot e_2 \ \text{ is a polynomial of order } 2n \\ &= (P_{1.2}, e_{1.2}) \ \text{ is a polynomial of order } n \end{aligned}$$

where, $P_{1.2}$ contains all terms of order n or less, and $e_{1.2}$ contains the higher order terms. A comparison between traditional enclosure methods for IVPs for ODEs and Taylor models is presented in [74] with a simple example to illustrate how the application and calculation of the Taylor models to solve ODEs.

4.4 Solution procedure

In this study, similar to [25] and [52], we consider systems of ordinary differential equations given by the following formulation

$$\dot{x}(t) = f(x, \theta), \qquad x(t_0) = x_0, \tag{4.3}$$

where, $t \in [t_0, t_k]$, $t_k > t_0$, and $\theta \in \Theta$ is the m-dimensional vector of parameters. The variables x and x_0 are n-dimensional vectors of state variables and initial conditions, respectively. In addition, Θ and X_0 are interval vectors that represent the enclosures of the uncertainties of parameters and initial conditions, respectively. We also assumed that $f : \mathbb{R}^n \times \mathbb{R}^p \to \mathbb{R}^n$ is $k-1$ times continuously differentiable with respect to x and $q+1$ times continuously differentiable with respect to θ.

To solve Equation (4.3), we applied the method proposed in [52] which the authors implemented in the VSPODE software (Validated solutions of initial value problems for parametric ODEs [52]. Briefly, the method is as follows;

First, consider a sequence of values $t_0 < t_1 < \cdots < t_m$ with step size $h_j = t_{j+1} - t_j$ at the $(j+1)$-th integration step, $j = 0, 1, \ldots, m-1$. A solution to the IVP

$$\dot{x}(t) = f(x, \theta), \qquad x(t_j) = x_j$$

is given by

$$x(t; t_j, X_j, \Theta) = \{x(t; t_j, x_j, \theta) | x_j \in X_j, \theta \in \Theta\}.$$

In algorithms to solve Equation (4.3), each integration step is divided into two stages. The first stage consists of validating the existence and uniqueness of the solution, while the second stage consists of computing a tighter enclosure.

4.4.1 First stage

The goal in the first stage is to find a step size $h_j = t_{j+1} - t_j > 0$ and an a priori enclosure $\tilde{X}_j$ of the solution such that a unique solution $x(t; t_j, x_j, \theta)$ is guaranteed to exist for all $t \in [t_j, t_{j+1}]$, all $x_j \in X_j$ and all $\theta \in \Theta$. For this purpose, the algorithm uses Interval Taylor Series (ITS) with respect to time. The uniqueness of the solution $x(t; t_j, x_j, \theta)$ is proved by using the Picard-Lindelöf operator and the Banach fixed-point theorem [72]. To compute the enclosure $\tilde{X}_j$, VSPODE uses high-order enclosure methods based on using many terms in the Taylor series. In this way, it is possible to determine $h_j = t_{j+1} - t_j$ and $\tilde{X}_j$ such that

$$\tilde{X}_j = \sum_{i=0}^{k-1} [0, h_j]^i F^{[i]}(X_j, \Theta) + [0, h_j]^k F^{[k]}(\tilde{X}_j^0, \Theta) \subseteq \tilde{X}_j^0, \tag{4.4}$$

where, $(X_i)_j = F^{[i]}(X_j, \Theta)$ are the interval extensions of the Taylor coefficients[1] for $x_j \in X_j$ and $\theta \in \Theta$.The main advantage of considering more terms in the Taylor series is that it is possible to consider larger step sizes, unlike first-order enclosure methods (constant enclosure methods).

4.4.2 Second stage

The goal in the second stage is to compute a tighter enclosure X_{j+1} such that $X_{j+1} \subseteq \tilde{X}_j$. In VSPODE, this is done by using ITS to compute a Taylor model $T_{f^{[i]}} = f^{[i]}(T_{x_j}, T_\theta)$, which depends on the initial conditions (x_0) and parameters (θ). For the Taylor model computations, the interval initial states and parameters are represented by the Taylor models

$$x_{0_i} \in T_{x_{0_i}} = m(X_{0_i}) + (x_0 - m(X_{0_i})) + [0, 0], \ i = 1, \ldots, n.$$

$$\theta_i \in T_{\theta_i} = m(\Theta_i) + (\theta_i - m(\Theta_i)) + [0, 0], \ i = 1, \ldots, p.$$

[1] The j-th Taylor coefficient evaluated at t_i is denoted by $(x_i)_j = \frac{x^{(j)}(t_i)}{j!}$

It is then possible to determine Taylor models $T_{f^{[i]}}$ of the ITS coefficients $f^{[i]}(x_j, \theta)$ by using remainder differential algebra (RDA) [58] to compute $T_{f^{[i]}} = f^{[i]}(T_{x_j}, T_\theta)$. To reduce the overestimation produced due to interval dependency and the continuous growth of the remainder in each integration step, we used Taylor models $T_{f^{[i]}}$ and the mean value theorem to compute the enclosure for each coefficient $f^{[i]}(x_j, \theta)$ for the ITS of x_{i+j}. Thus, we obtained the Taylor model $T_{x_{j+1}}$ for x_{j+1} in terms of the uncertain quantities θ and x_0. Finally, to control the wrapping effect, the state enclosures are propagated using a new type of Taylor model. This new Taylor model consists of a polynomial and a remainder bound represented by an n-dimensional parallelepiped.

4.5 Numerical Simulations

To illustrate the performance of VSPODE, we considered the model given by Model 3.3. In the formulation of this model, we included nine parameters, seven state variables, and their respective initial conditions (see Tables 3.1 and 3.2 for a description). Additionally, the vector function is a polynomial function in the model parameters and a rational function in the state variables. In this way, the function satisfies the condition of continuous differentiability for the state variables and model parameters necessary to apply the VSPODE algorithm.

We perform simulations for Itagüí and Neiva considering uncertainty in some parameters and initial conditions according to results obtained from local sensitivity analysis of R_0 and the locally structurally identifiability analysis of Model 3.3. We applied VSPODE, with its default ITS (Interval Taylor Series) order, $k = 17$ and a default Taylor model order $q = 5$, to determine a verified enclosure of all possible solutions for Model 3.3 under several scenarios for each municipality. The interval integration was defined for each municipality

according to the duration of the outbreak. For Itagüí, the interval of integration was from $t = 0$ to $t = 60$ epidemiological weeks, while, for Neiva it was from $t = 0$ to $t = 30$ epidemiological weeks. We considered the following scenarios for our study.

4.5.1 Scenario 1: Considering uncertainty in one parameter at a time

Here, we considered uncertainty in transmission rates from human to mosquito and from mosquito to human (β_m and β_h respectively), the mortality rate in mosquitoes (μ_m), the recovery rate in humans (γ_h) and recruitment rate in mosquitoes (Λ). The first four parameters were included according to the results obtained from local sensitivity analysis of R_0 (see Table 3.3). The recruitment rate (Λ) was included since it was the only parameter that is not locally structurally identifiable (see Table 3.5).

For Itagüí, we fixed the initial condition and the parameters values as $M_s(0) = 1800000$, $M_e(0) = 50$, $M_i(0) = 40$, $H_s(0) = 223000$, $H_e(0) = 21$, $H_i(0) = 10$, $H_r(0) = 25005$, $H = 248036$, $\mu_h = 0.00023$, $\theta_m = 0.6$, and $\theta_h = 1.3$. We also fixed the initial condition and the parameters values for Neiva as $M_s(0) = 3000000$, $M_e(0) = 100$, $M_i(0) = 50$, $H_s(0) = 315952$, $H_e(0) = 27$, $H_i(0) = 16$, $H_r(0) = 8471$, $H = 324466$, $\mu_h = 0.00011$, $\theta_m = 0.8$, and $\theta_h = 1.3$. Figures 4.1–4.4 show the guaranteed enclosures for all the possible trajectories of infected humans for Itagüí and Neiva, respectively.

Tables 4.1–4.2 show the interval enclosures and their widths at different times t (in epidemiological weeks), calculated with VSPODE for Itagüí and Neiva, respectively.

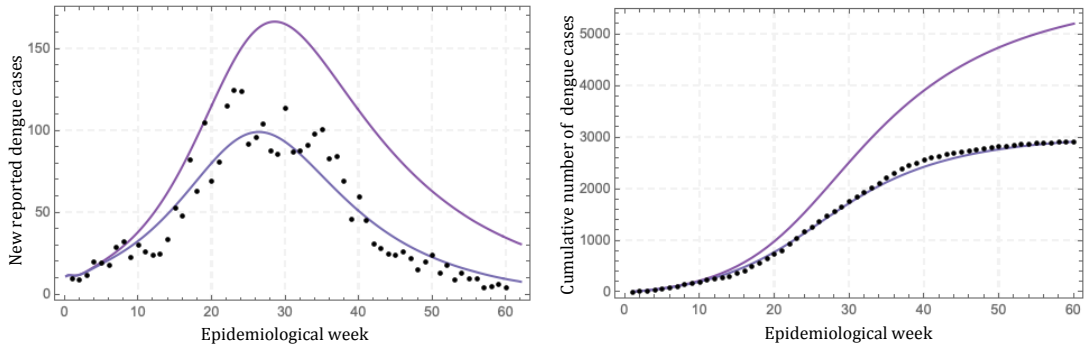

(a) Considering uncertainty in $\beta_m \in [0.12, 0.15]$

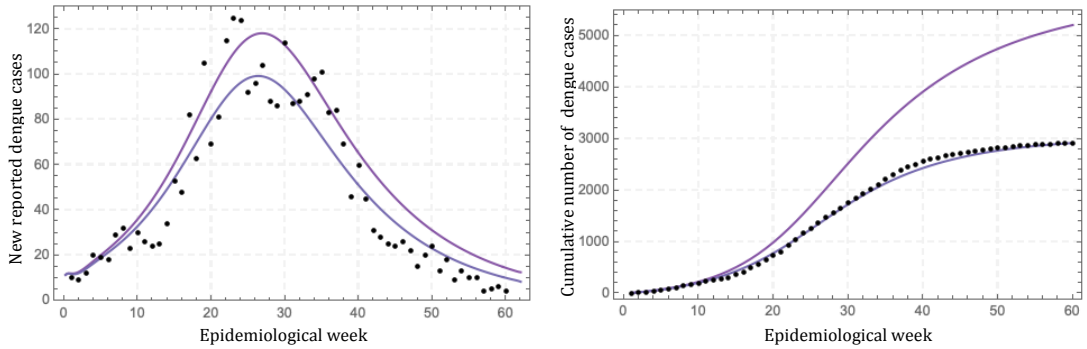

(b) Considering uncertainty in $\beta_h \in [2.5, 2.65]$

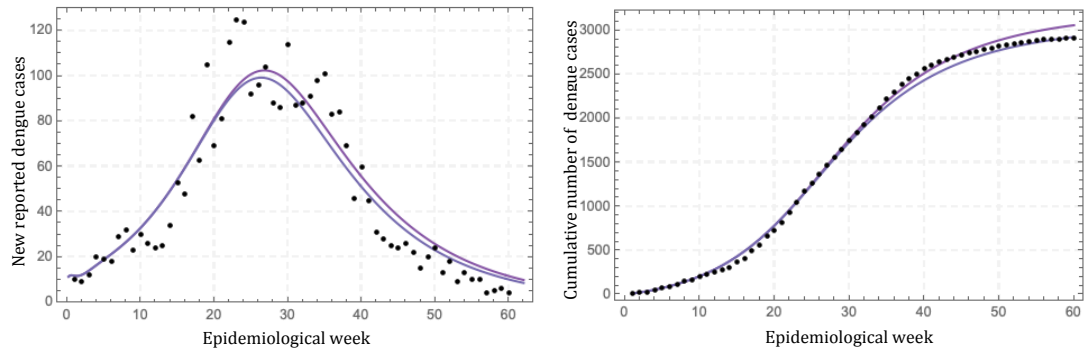

(c) Considering uncertainty in $\mu_m \in [0.217, 0.22]$

Figure 4.1 – **Enclosures for the scenario 1 for Itagüí.** Enclosures computed using VSPODE to solve the system in Model 3.3 for the number of new dengue cases per week (figures on the left) and for the cumulative number of dengue cases (figures on the right). Parameter values used to obtain these enclosures: **(a)** $\Lambda = 2000$, $\gamma_h = 1.75$, $\mu_m = 0.22$, $\beta_h = 2.5$, and $\beta_m \in [0.12, 0.15]$. **(b)** $\Lambda = 2000$, $\gamma_h = 1.75$, $\mu_m = 0.22$, $\beta_m = 0.12$, and $\beta_h \in [2.5, 2.65]$. **(c)** $\Lambda = 2000$, $\gamma_h = 1.75$, $\beta_m = 0.12$, $\beta_h = 2.5$, and $\mu_m \in [0.217, 0.22]$.

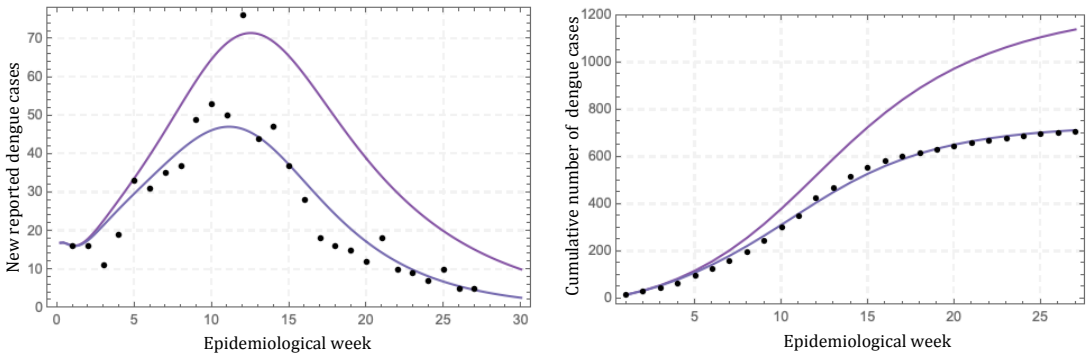

(a) Considering uncertainty in $\beta_m \in [0.14, 0.2]$

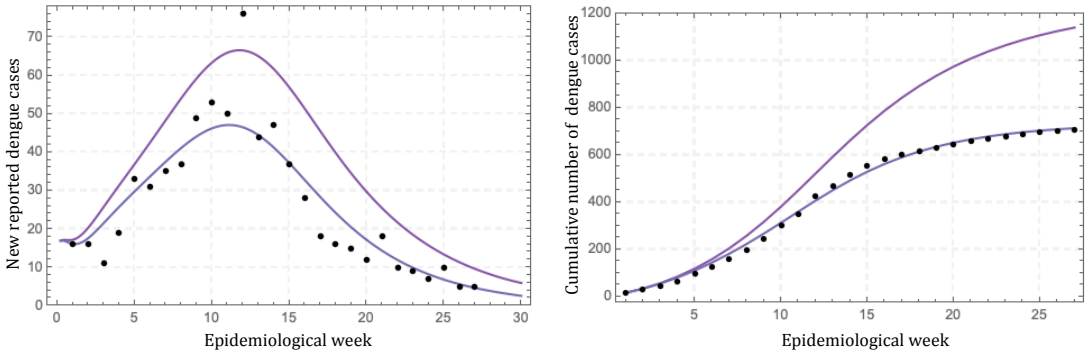

(b) Considering uncertainty in $\beta_h \in [2.5, 3.0]$

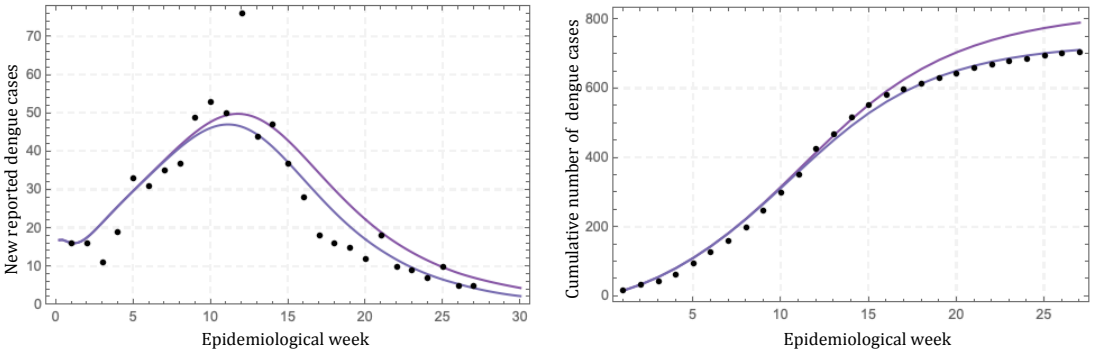

(c) Considering uncertainty in $\mu_m \in [0.38, 0.4]$

Figure 4.2 – **Enclosures for the scenario 1 for Neiva.** We show the number of new dengue cases per week (figures on the left) and the cumulative number of dengue cases (figures on the right). Parameter values used to obtain these enclosures: **(a)** $\Lambda = 15000$, $\gamma_h = 1.7$, $\mu_m = 0.4$, $\beta_h = 2.5$, and $\beta_m \in [0.14, 0.2]$. **(b)** $\Lambda = 15000$, $\gamma_h = 1.7$, $\mu_m = 0.4$, $\beta_m = 0.14$, and $\beta_h \in [2.5, 3.0]$. **(c)** $\Lambda = 15000$, $\gamma_h = 1.7$, $\beta_h = 2.5$, $\beta_m = 0.14$, and $\mu_m \in [0.38, 0.4]$.

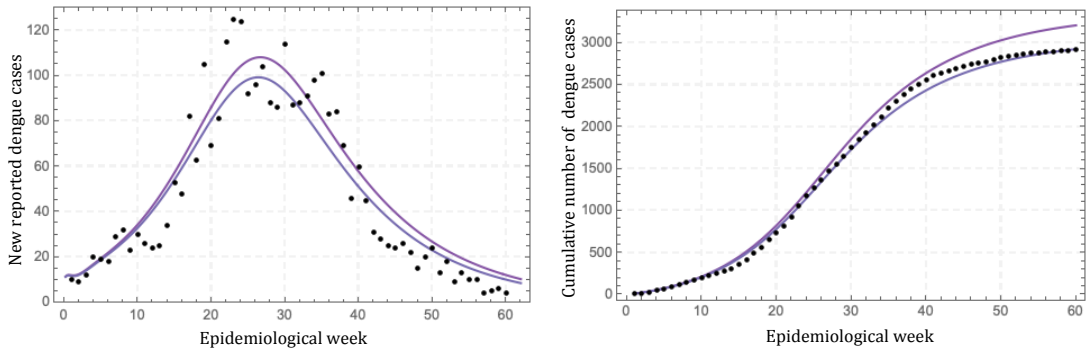

(a) Considering uncertainty in $\gamma_h \in [1.7, 1.75]$

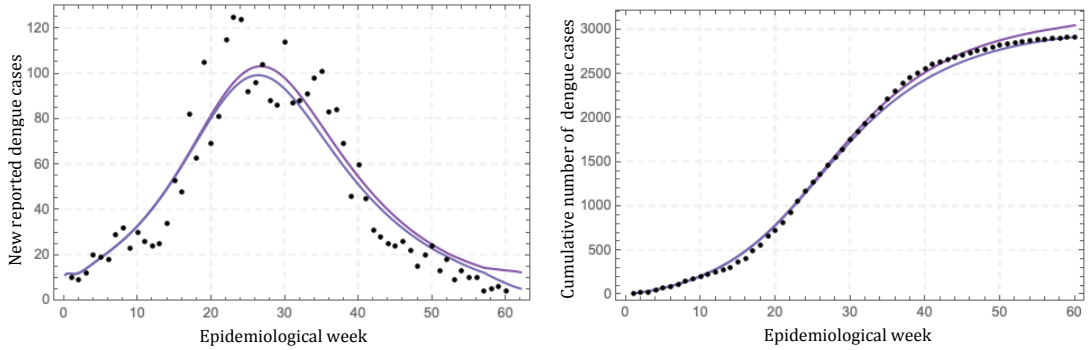

(b) Considering uncertainty in $\Lambda \in [1850, 2000]$

Figure 4.3 – **Enclosures for the scenario 1 for Itagüí.** We show the number of new dengue cases per week (figures on the left) and the cumulative number of dengue cases (figures on the right). Parameter values used to obtain these enclosures: **(a)** $\mu_m = 0.22$, $\beta_m = 0.12$, $\beta_h = 2.5$, $\Lambda = 2000$, and $\gamma_h \in [1.7, 1.75]$. **(b)** $\mu_m = 0.22$, $\beta_m = 0.12$, $\beta_h = 2.5$, $\gamma_h = 1.75$, and $\Lambda \in [1850, 2000]$.

4.5.2 Scenario 2: Considering uncertainty in several parameters at the same time.

In this scenario we obtained verified computational and mathematical enclosures when (a) uncertain values are assumed for β_m and β_h, (b) uncertain values are assumed for β_m, β_h, and μ_m, and (c) uncertain values are assumed for β_m, β_h, μ_m, and γ_h.

For Itagüí, we fixed the initial condition and the parameters values as $M_s(0) = 1800000$, $M_e(0) = 50$, $M_i(0) = 40$, $H_s(0) = 223000$, $H_e(0) = 21$, $H_i(0) = 10$, $H_r(0) = 25005$, $H = 248036$, $\mu_h = 0.00023$, $\theta_m = 0.6$, $\theta_h = 1.3$, and $\Lambda = 2000$. For Neiva,

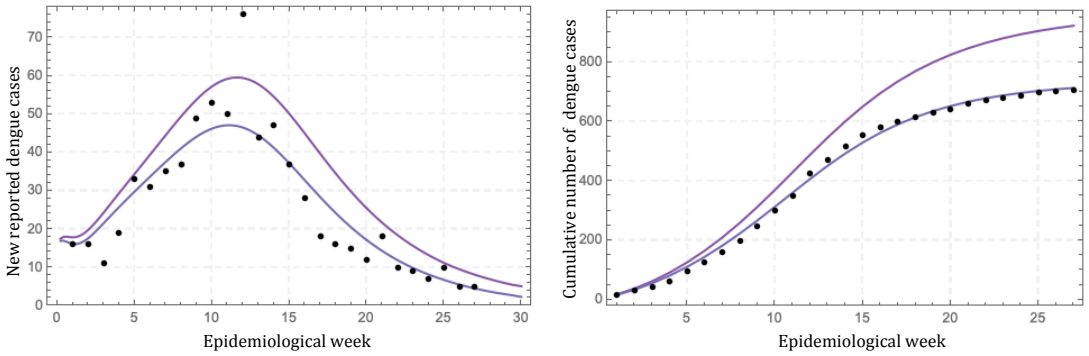

(a) Considering uncertainty in $\gamma_h \in [1.5, 1.7]$

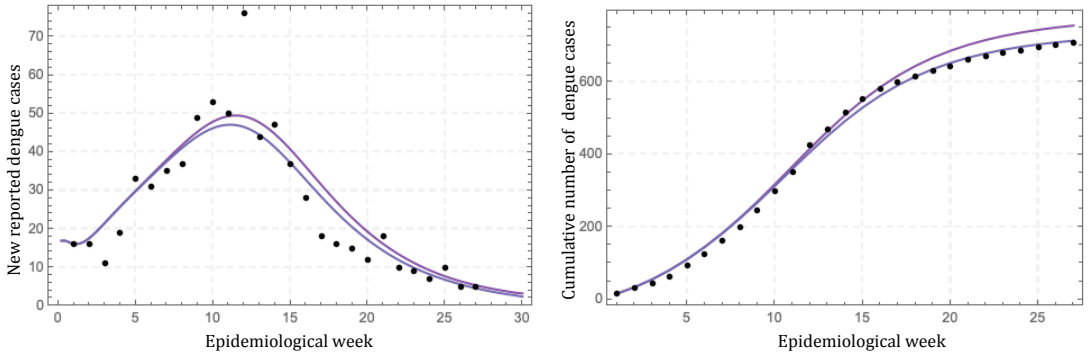

(b) Considering uncertainty in $\Lambda \in [13000, 15000]$

Figure 4.4 – **Enclosures for the scenario 1 for Neiva.** We show the number of new dengue cases per week (figures on the left) and the cumulative number of dengue cases (figures on the right). Parameter values used to obtain these enclosures: **(a)** $\mu_m = 0.4$, $\beta_h = 2.5$, $\beta_m = 0.14$, $\Lambda = 15000$, and $\gamma_h \in [1.5, 1.7]$. **(b)** $\mu_m = 0.4$, $\beta_h = 2.5$, $\beta_m = 0.14$, $\gamma_h = 1.7$, and $\Lambda \in [13000, 15000]$.

we fixed the initial condition and the parameters values as $M_s(0) = 3000000$, $M_e(0) = 100$, $M_i(0) = 50$, $H_s(0) = 315952$, $H_e(0) = 27$, $H_i(0) = 16$, $H_r(0) = 8471$, $H = 324466$, $\mu_h = 0.00011$, $\theta_m = 0.8$, $\theta_h = 1.3$, and $\Lambda = 15000$. Figures 4.5–4.6 show mathematically and computationally guaranteed upper and lower bounds for the possible trajectories of infected humans for Itagüí and Neiva, respectively.

Tables 4.3–4.4 summarize the values at some times for these enclosures.

Table 4.1 – **Scenario 1 Itagüí:** Upper bound, lower bound, and width at different times. In grey colour, we show the point when the enclosure start to blow up.

Uncertain values		**Epidemiological weeks** t						
		1	10	20	30	40	50	60
β_m	Sup	11.761	38.548	115.888	165.067	112.207	62.855	34.315
	Inf	11.749	32.979	80.647	93.126	50.953	22.914	9.966
	Width	0.012	5.569	35.241	71.941	61.254	39.941	24.348
β_h	Sup	11.991	36.057	92.789	112.843	65.175	31.018	14.447
	Inf	11.7492	32.9785	80.6475	93.1356	50.9797	22.9754	10.0339
	Width	0.2414	3.079	12.142	19.707	14.195	8.043	4.414
μ_m	Sup	11.749	32.994	81.409	97.631	55.520	25.73	11.595
	Inf	11.749	32.979	80.648	93.135	50.980	22.980	10.098
	Width	0.0	0.016	0.762	4.496	4.540	2.750	1.497
γ_h	Sup	12.032	34.452	86.341	102.432	57.705	26.778	12.113
	Inf	11.749	32.979	80.648	93.136	50.980	22.981	10.098
	Width	0.283	1.473	5.693	9.296	6.725	3.797	2.014
Λ	Sup	11.749	33.046	81.980	97.931	54.384	24.651	13.281
	Inf	11.749	32.979	80.648	93.136	50.980	22.879	7.598
	Width	0.0	0.067	1.332	4.795	3.404	1.772	5.683

Table 4.2 – **Scenario 1 Neiva:** Upper bound, lower bound, and width at different times.

Uncertain values		**Epidemiological weeks** t						
		1	5	10	15	20	25	30
β_m	Sup	16.174	33.859	64.821	65.392	38.764	19.893	9.984
	Inf	16.122	29.811	46.241	37.155	17.144	6.774	2.604
	Width	0.051	4.048	18.581	28.236	21.620	13.120	7.380
β_h	Sup	17.187	36.948	63.395	56.895	29.674	13.339	5.917
	Inf	16.122	29.811	46.241	37.157	17.150	6.783	2.561
	Width	1.064	7.138	17.155	19.739	12.524	6.556	3.356
μ_m	Sup	16.123	29.874	47.833	42.820	22.232	9.789	4.380
	Inf	16.122	29.811	46.239	37.125	17.040	6.564	2.249
	Width	0.001	0.064	1.594	5.695	5.191	3.225	2.131
γ_h	Sup	17.839	34.433	57.253	50.074	25.434	11.158	5.073
	Inf	16.122	29.810	46.238	37.149	17.128	6.716	2.273
	Width	1.717	4.623	11.016	12.926	8.306	4.441	2.800
Λ	Sup	16.124	29.979	47.927	40.654	19.219	7.663	3.209
	Inf	16.122	29.810	46.241	37.157	17.148	6.760	2.365
	Width	0.002	0.169	1.686	3.497	2.071	0.903	0.844

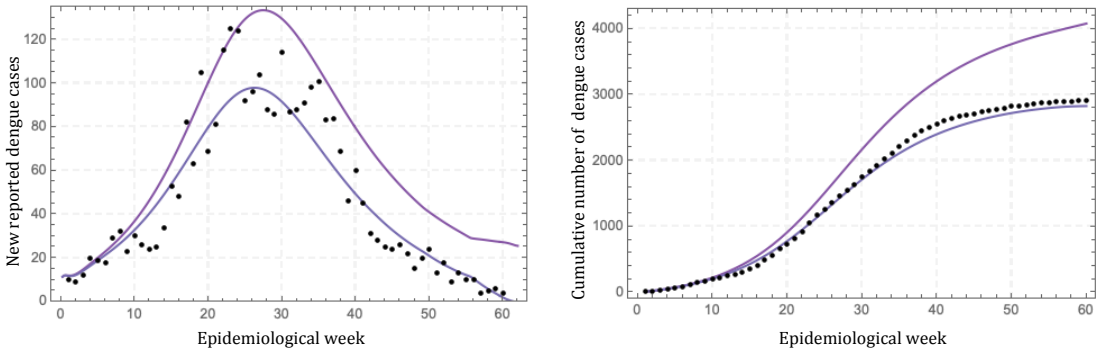

(a) Considering uncertainty in $\beta_m \in [0.12, 0.13]$ and $\beta_h \in [2.5, 2.6]$

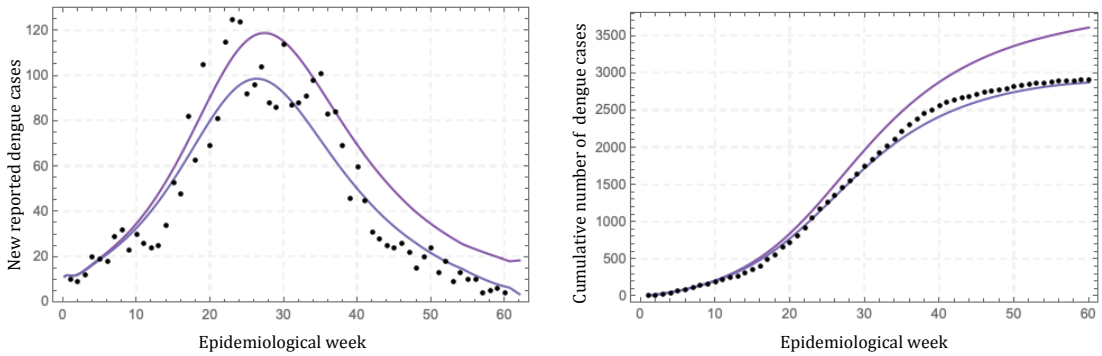

(b) Considering uncertainty in $\beta_m \in [0.12, 0.125], \beta_h \in [2.5, 2.55],$ and $\mu_m \in [0.217, 0.22]$

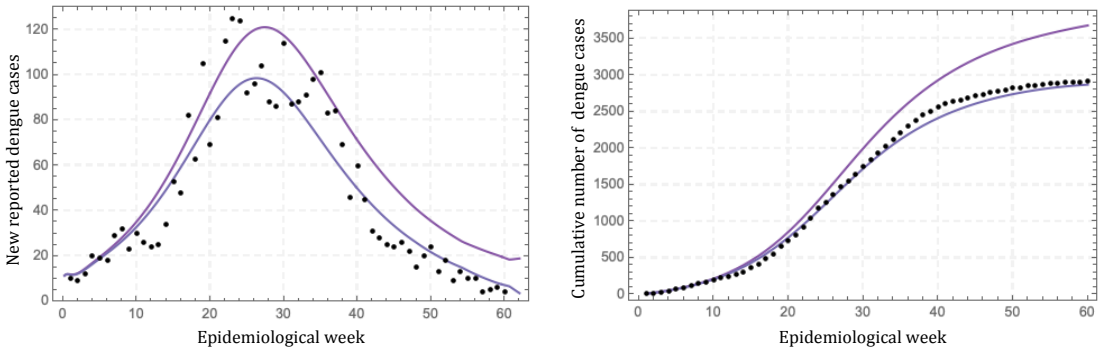

(c) Considering uncertainty in $\beta_m \in [0.12, 0.125], \beta_h \in [2.5, 2.55], \mu_m \in [0.217, 0.22],$ and $\gamma_h \in [1.74, 1.75]$

Figure 4.5 – **Enclosures for the scenario 2 for Itagüí.** We show the number of new dengue cases per week (figures on the left) and the cumulative number of dengue cases (figures on the right). Parameter values used to obtain these enclosures: **(a)** $\gamma_h = 1.75$, $\mu_m = 0.22$, $\beta_m \in [0.12, 0.13]$, and $\beta_h \in [2.5, 2.6]$. **(b)** $\gamma_h = 1.75$, $\beta_m \in [0.12, 0.125]$, $\beta_h \in [2.5, 2.55]$, and $\mu_m \in [0.217, 0.22]$. **(c)** $\gamma_h = 1.75$, $\beta_m \in [0.12, 0.125]$, $\beta_h \in [2.5, 2.55]$, $\mu_m \in [0.217, 0.22]$, and $\gamma_h \in [1.74, 1.75]$.

4.5.3 Scenario 3: Considering uncertainty in initial conditions only.

In this scenario we considered uncertainty in (a) the initial mosquito population ($M_s(0), M_e(0)$ and $M_i(0)$), (b) initial human population ($H_s(0), H_e(0), H_i(0)$

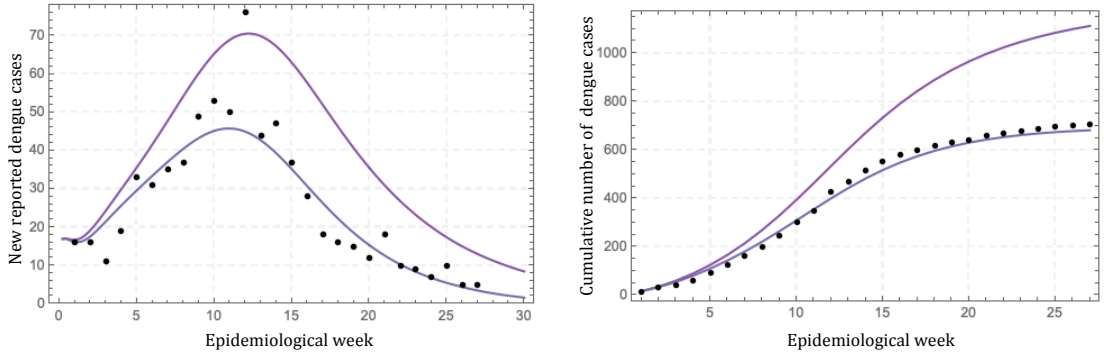

(a) Considering uncertainty in $\beta_m \in [0.14, 0.17]$ and $\beta_h \in [2.5, 2.75]$

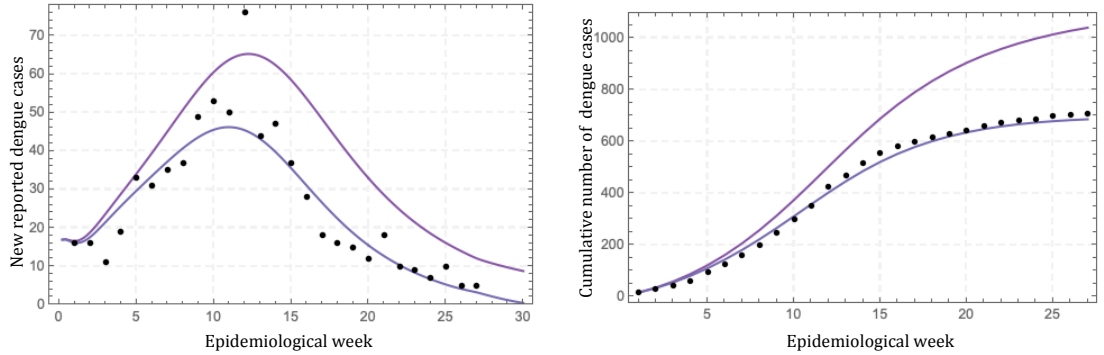

(b) Considering uncertainty in $\beta_m \in [0.14, 0.16], \beta_h \in [2.5, 2.7]$, and $\mu_m \in [0.39, 0.4]$

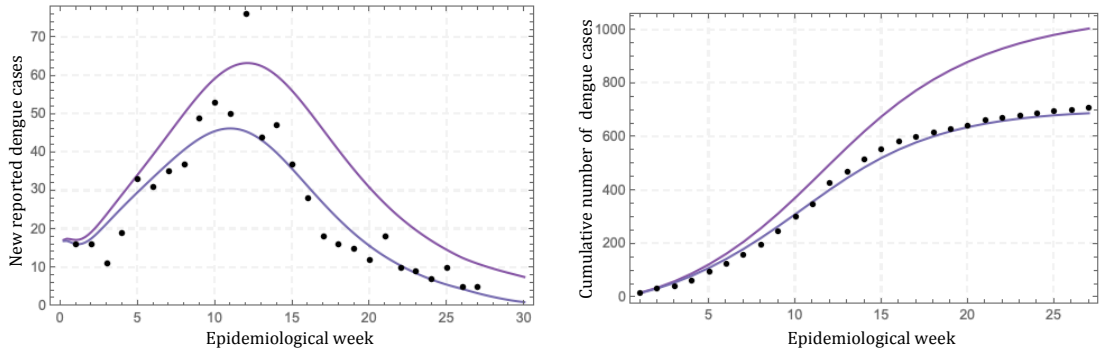

(c) Considering uncertainty in $\beta_m \in [0.14, 0.16], \beta_h \in [2.5, 2.7], \mu_m \in [0.39, 0.4]$, and $\gamma_h \in [1.6, 1.7]$

Figure 4.6 – **Enclosures for the scenario 2 for Neiva.** We show the number of new dengue cases per week (figures on the left) and the cumulative number of dengue cases (figures on the right). Parameter values used to obtain these enclosures: **(a)** $\gamma_h = 1.7$, $\mu_m = 0.4$, $\beta_m \in [0.14, 0.17]$, and $\beta_h \in [2.5, 2.75]$. **(b)** $\gamma_h = 1.7$, $\beta_m \in [0.14, 0.16]$, $\beta_h \in [2.5, 2.7]$, and $\mu_m \in [0.39, 0.4]$. **(c)** $\beta_m \in [0.14, 0.16]$, $\beta_h \in [2.5, 2.7]$, $\mu_m \in [0.39, 0.4]$, and $\gamma_h \in [1.6, 1.7]$.

and $H_r(0)$), and (c) all initial conditions of Model 3.3. These scenarios make sense because it is not possible to determine exactly which is the number of

Table 4.3 – **Scenario 2 Itagüí:** Upper bound, lower bound, and width at different times. In grey colour, we show the point when the enclosure start to blow up.

Uncertain values		**Epidemiological weeks** t						
		1	10	20	30	40	50	60
β_m, β_h	Sup	11.914	36.972	100.601	129.509	79.466	40.931	27.182
	Inf	11.749	32.901	79.978	91.469	49.227	20.929	1.846
	Width	0.165	4.071	20.623	38.040	30.239	20.002	25.336
β_m, β_h, μ_m	Sup	11.832	34.937	90.925	115.121	69.343	34.570	18.846
	Inf	11.749	32.959	80.444	92.350	49.972	21.687	6.991
	Width	0.083	1.978	10.481	22.771	19.371	12.883	11.855
$\beta_m, \beta_h, \mu_m, \gamma_h$	Sup	11.888	35.244	92.181	117.345	71.051	35.451	19.166
	Inf	11.749	32.948	80.361	92.109	49.753	21.674	7.144
	Width	0.139	2.296	11.820	25.236	21.298	13.777	12.022

Table 4.4 – **Scenario 2 Neiva:** Upper bound, lower bound, and width at different times. In grey colour, we show the point when the enclosure start to blow up.

Uncertain values		**Epidemiological weeks** t						
		1	5	10	15	20	25	30
β_m, β_h	Sup	16.683	35.665	65.361	62.949	35.481	17.324	8.442
	Inf	16.121	29.642	45.166	35.128	15.290	5.442	1.588
	Width	0.562	6.023	20.196	27.821	20.192	11.881	6.854
β_m, β_h, μ_m	Sup	16.567	34.159	60.618	58.464	32.888	16.055	8.746
	Inf	16.122	29.720	45.569	35.489	15.408	5.235	0.434
	Width	0.445	4.439	15.049	22.975	17.480	10.820	8.313
$\beta_m, \beta_h, \mu_m, \gamma_h$	Sup	17.176	34.286	59.366	55.984	30.771	14.565	7.516
	Inf	16.119	29.698	45.586	35.629	15.581	5.498	0.963
	Width	1.057	4.588	13.781	20.355	15.190	9.067	6.553

susceptible, exposed, and infected mosquitoes in a specific region. Additionally, these initial conditions are not locally structurally identifiable (see Table 3.5). On the other hand, according to the World Health Organization (WHO), the number of reported dengue cases is not 100% reliable or accurate because of under-reporting concerns, which can affect up to 75% of the total number of cases occurring wherever Dengue transmission is present [9].

For Itagüí, we fixed the parameters values as $H = 248036$, $\mu_h = 0.00023$, $\theta_m = 0.6$, $\theta_h = 1.3$, $\Lambda = 2000$, $\gamma_h = 1.75$, $\mu_m = 0.22$, $\beta_m = 0.12$, and $\beta_h = 2.5$. For Neiva, we fixed the parameters values: $H = 324466$, $\mu_h = 0.00011$, $\theta_m = 0.8$, $\theta_h = 1.3$, $\Lambda = 15000$, $\gamma_h = 1.7$, $\mu_m = 0.4$, $\beta_h = 2.5$, and $\beta_m = 0.14$.

Figures 4.7 and 4.8 show mathematically and computationally guaranteed upper and lower bounds on the possible trajectories of infected humans for Itagüí and Neiva, respectively.

Tables 4.5–4.6 show the interval enclosures and their widths at different times t (in epidemiological weeks), calculated with VSPODE for Itagüí and Neiva, respectively.

Table 4.5 – **Scenario 3 Itagüí:** Upper bound, lower bound, and width at different times.

Uncertain values		**Epidemiological weeks** t						
		1	10	20	30	40	50	60
Mosquito initial conditions	Sup	13.652	45.921	112.037	129.164	71.357	32.909	15.351
	Inf	11.244	29.458	73.881	89.996	49.399	21.384	8.411
	Width	2.408	16.463	38.156	39.168	21.958	11.525	6.940
Human initial conditions	Sup	35.308	49.040	125.575	151.516	86.668	41.208	23.689
	Inf	11.745	32.472	78.516	89.978	48.351	21.071	4.317
	Width	23.563	16.568	47.059	61.538	38.317	20.137	19.372
All initial conditions	Sup	20.759	47.320	121.232	146.477	83.930	39.592	18.213
	Inf	11.596	31.624	76.988	89.637	48.535	21.589	9.325
	Width	9.163	15.696	44.244	56.840	35.395	18.003	8.888

Table 4.6 – **Scenario 3 Neiva:** Upper bound, lower bound, and width at different times.

Uncertain values		**Epidemiological weeks** t						
		1	5	10	15	20	25	30
Mosquito initial conditions	Sup	20.406	47.292	73.043	58.646	27.042	10.690	4.125
	Inf	15.036	24.960	40.620	35.347	16.876	6.718	2.598
	Width	5.370	22.332	32.423	23.299	10.167	3.971	1.527
Human initial conditions	Sup	49.036	44.165	70.251	57.261	26.852	10.803	4.244
	Inf	16.118	29.626	45.794	36.658	16.846	6.635	2.551
	Width	32.918	14.538	24.457	20.604	10.005	4.168	1.693
All initial conditions	Sup	53.435	62.252	98.763	81.077	38.464	15.589	6.171
	Inf	14.960	24.416	39.385	34.003	15.743	6.079	2.269
	Width	38.476	37.836	59.378	47.075	22.721	9.510	3.902

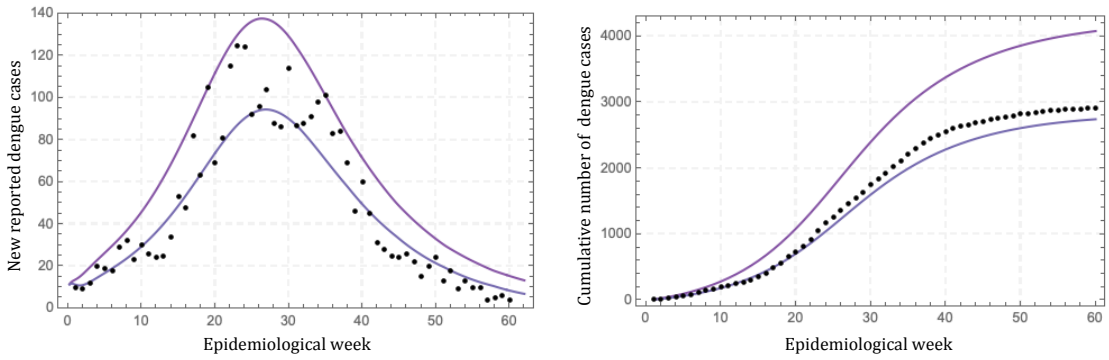

(a) Considering uncertainty in mosquito initial conditions

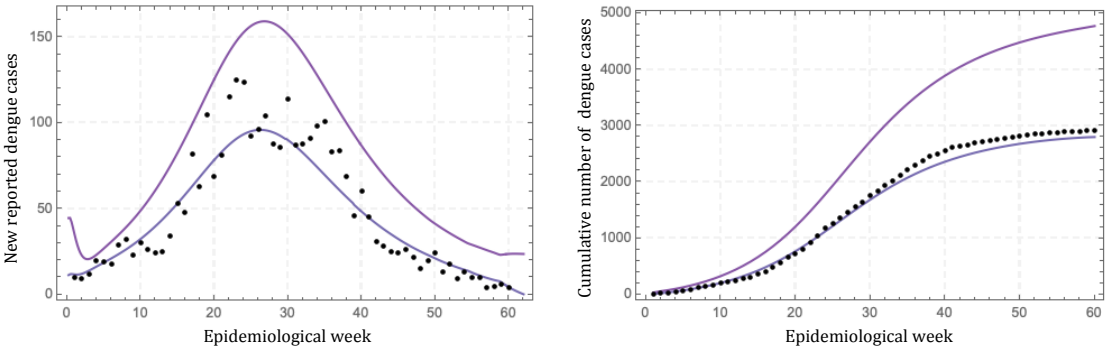

(b) Considering uncertainty in human initial conditions

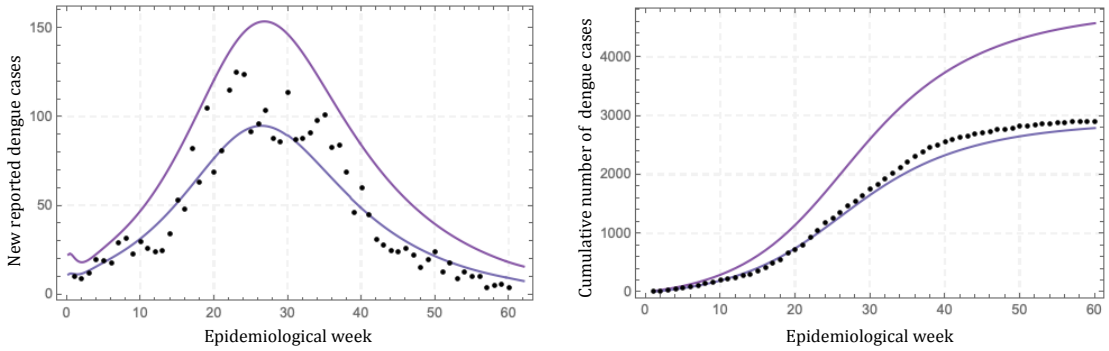

(c) Considering uncertainty in all initial conditions

Figure 4.7 – **Enclosures for the scenario 3 for Itagüí.** We show the number of new dengue cases per week (figures on the left) and the cumulative number of dengue cases (figures on the right). (a) $M_s(0) \in [1800000, 2000000]$, $M_e(0) \in [50, 70]$, $M_i(0) \in [40, 60]$, $H_s(0) = 223000$, $H_e(0) = 21$, $H_i(0) = 10$, and $H_r(0) = 25005$. (b) $M_s(0) = 1800000$, $M_e(0) = 50$, $M_i(0) = 40$, $H_s(0) \in [223000, 235634]$, $H_e(0) \in [21, 84]$, $H_i(0) \in [10, 40]$, and $H_r(0) \in [12340, 25005]$. (c) $M_s(0) \in [1800000, 1850000]$, $M_e(0) \in [50, 60]$, $M_i(0) \in [40, 50]$, $H_s(0) \in [223000, 235634]$, $H_e(0) \in [21, 42]$, $H_i(0) \in [10, 20]$, and $H_r(0) \in [12340, 25005]$.

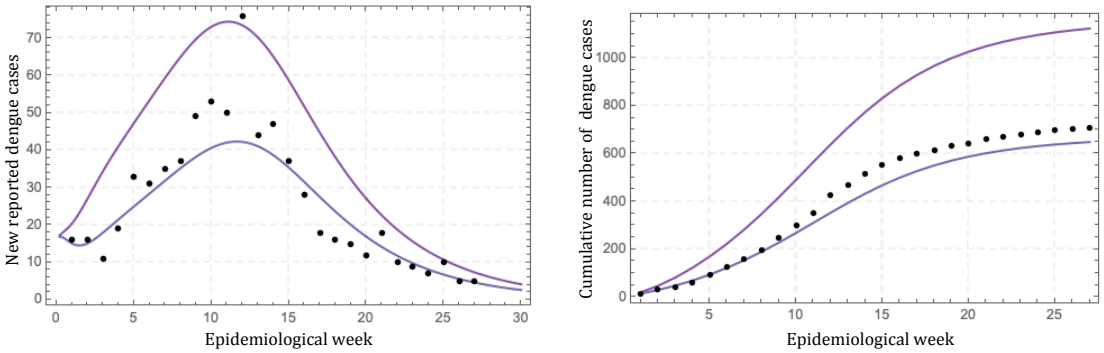

(a) Considering uncertainty in mosquito initial conditions

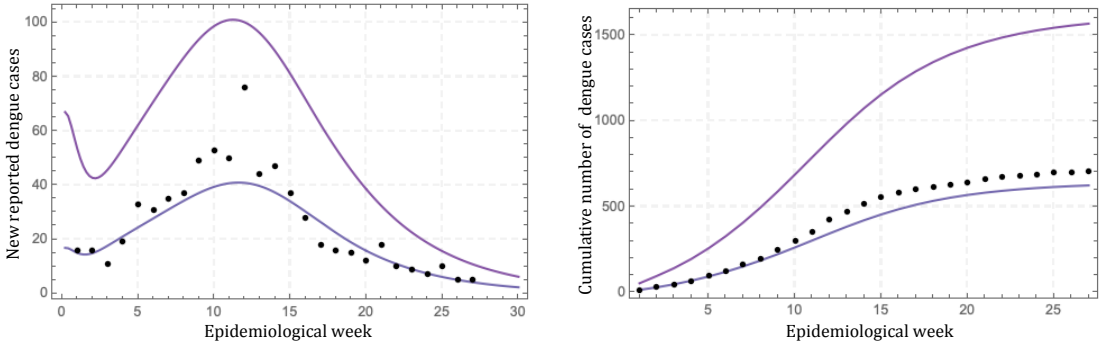

(b) Considering uncertainty in human initial conditions

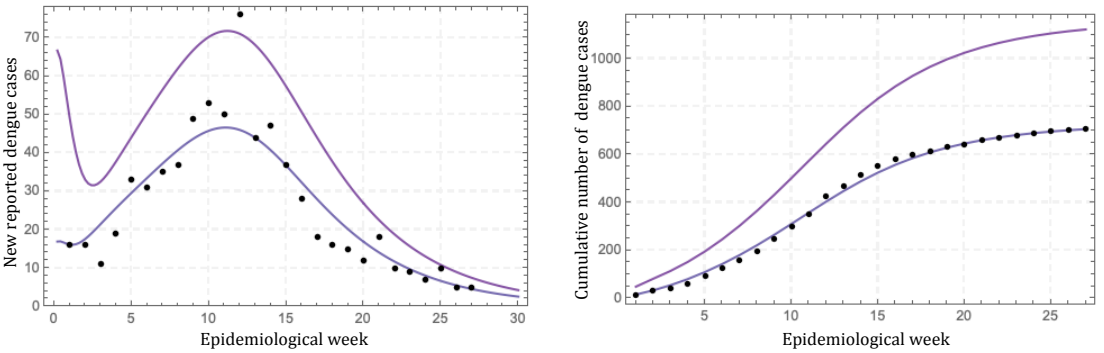

(c) Considering uncertainty in all initial conditions

Figure 4.8 – **Enclosures for the scenario 3 for Neiva.** We show the number of new dengue cases per week (figures on the left) and the cumulative number of dengue cases (figures on the right). Initial conditions used to obtain these enclosures: (a) $M_s(0) \in [3000000, 3500000]$, $M_e(0) \in [100, 150]$, $M_i(0) \in [50, 100]$, $H_s(0) = 315952$, $H_e(0) = 27$, $H_i(0) = 16$, and $H_r(0) = 8471$. (b) $M_s(0) = 3000000$, $M_e(0) = 100$, $M_i(0) = 50$, $H_s(0) \in [315952, 324294]$, $H_e(0) \in [27, 108]$, $H_i(0) \in [16, 64]$, and $H_r(0) \in [0, 8471]$. (c) $M_s(0) \in [3000000, 3500000]$, $M_e(0) \in [100, 150]$, $M_i(0) \in [50, 100]$, $H_s(0) \in [315952, 324294]$, $H_e(0) \in [27, 108]$, $H_i(0) \in [16, 64]$, and $H_r(0) \in [0, 8471]$.

4.5.4 Scenario 4: Considering uncertainty in parameters and initial conditions at the same time.

In this scenario, we included uncertainty in transition rate from exposed to infected mosquito (θ_m) and exposed and infected human initial conditions ($H_e(0)$ and $H_i(0)$, respectively). VSPODE breaks down at the second integration step for Itagüí when $H_e(0) \in [21, 61]$ and $H_i(0) \in [10, 30]$, and for Neiva at $t = 18$ when $H_e(0) \in [27, 77]$ and $H_i(0) \in [16, 46]$ due to rapid growth of the enclosure. Thus, to obtain guaranteed enclosures, we split the intervals of $H_e(0)$ and $H_i(0)$ into 10 equal-sized sub-boxes for both municipalities, and then used VSPODE to determine the solution for each sub-box. The final solution enclosure is then the union of all the enclosures resulting from each sub-box. However, with the VSPODE specifications that we mention above, the solutions for Itagüí always blow up in some integration point. For that reason, we considered (only for Itagüí and this scenario) ITS (Interval Taylor Series) order $k = 12$ and a default Taylor model order $q = 9$.

For Itagüí, we fixed the parameters and initial condition values as follows $H = 248036$, $\mu_h = 0.00023$, $\theta_h = 1.3$, $\Lambda = 2000$, $\gamma_h = 1.75$, $\mu_m = 0.22$, $\beta_m = 0.12$, $\beta_h = 2.5$, $M_s(0) = 1800000$, $M_e(0) = 50$, $M_i(0) = 40$, $H_s(0) = 223000$, and $H_r(0) = 25005$. Similarly, for Neiva, we fixed the parameters values as mentioned below $H = 324466$, $\mu_h = 0.00011$, $\theta_m = 0.8$, $\theta_h = 1.3$, $\Lambda = 15000$, $\gamma_h = 1.7$, $\mu_m = 0.4$, $\beta_h = 2.5$, $\beta_m = 0.14$, $M_s(0) = 3000000$, $M_e(0) = 100$, $M_i(0) = 50$ $H_s(0) = 315952$, and $H_r(0) = 8471$.

Figures 4.9 and 4.10 show mathematically and computationally guaranteed upper and lower bounds on the possible trajectories of infected humans for Itagüí and Neiva, respectively.

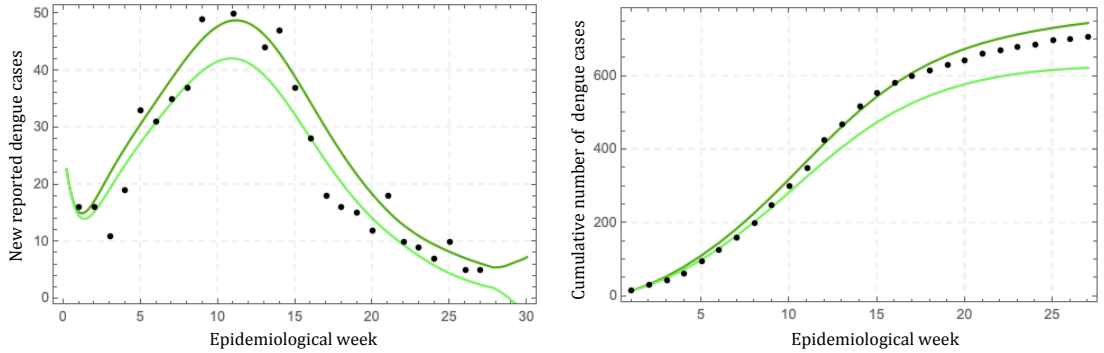

(a) Considering uncertainty in $\theta_m \in [0.58, 0.88]$

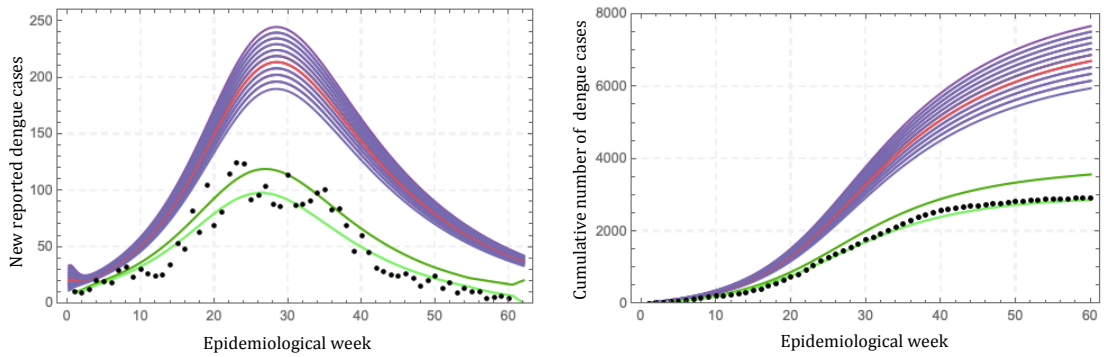

(b) Considering uncertainty in $\theta_m \in [0.58, 0.88]$, $H_e(0) \in [21, 61]$, and $H_i(0) \in [10, 30]$

Figure 4.9 – **Enclosures for the scenario 4 for Itagüí.** We show the number of new dengue cases per week (figures on the left) and the cumulative number of dengue cases (figures on the right). In (a) we consider $H_e(0) = 21$, $H_i(0) = 10$ and uncertainty in $\theta_m \in [0.58, 0.88]$. In (b) we consider uncertainty in $\theta_m \in [0.58, 0.88]$, $H_e(0) \in [21, 61]$, and $H_i(0) \in [10, 30]$. The curves shown in this figure are upper and lower bounds, obtained by dividing into sub-intervals of four and two width $[21, 61]$ and $[10, 30]$ respectively, to guarantee verified solutions.

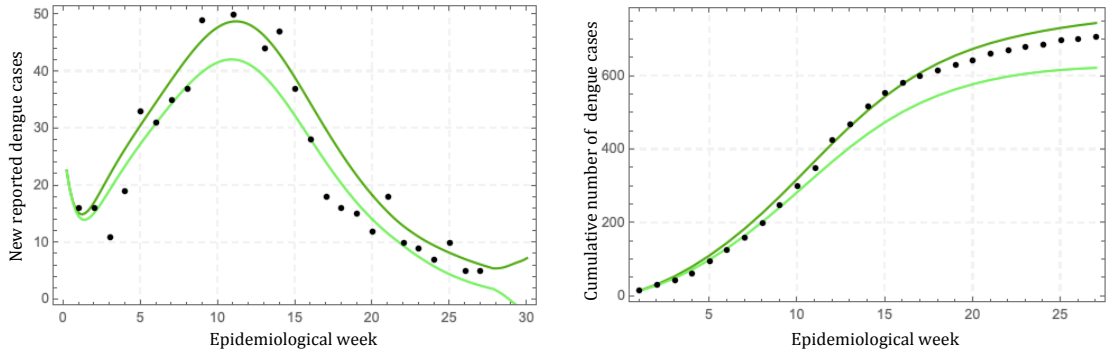

(a) Considering uncertainty in $\theta_m \in [0.58, 0.88]$

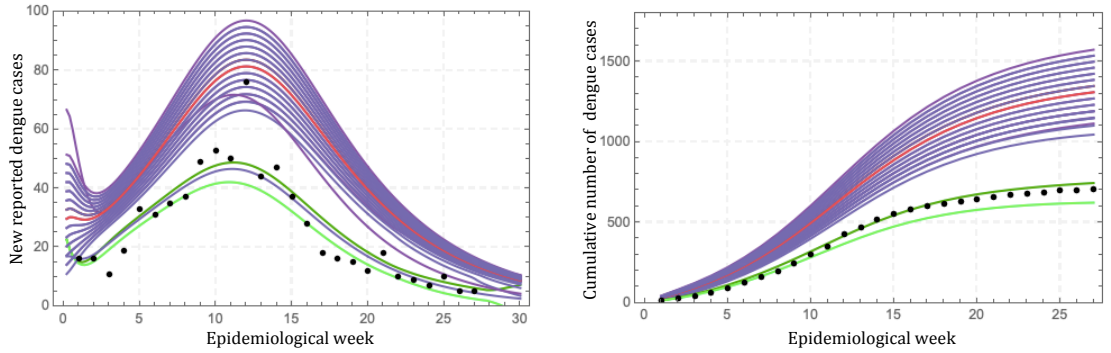

(b) Considering uncertainty in $\theta_m \in [0.58, 0.88], H_e(0) \in [32, 82],$ and $H_i(0) \in [16, 49]$

Figure 4.10 – **Enclosures for the scenario 4 for Neiva.** We show the number of new dengue cases per week (figures on the left) and the cumulative number of dengue cases (figures on the right). In **(a)** we consider $He(0) = 21$, $Hi(0) = 10$ and uncertainty in $\theta_m \in [0.58, 0.88]$. In **(b)** we consider uncertainty in $\theta_m \in [0.58, 0.88]$, $H_e(0) \in [32, 82]$, and $H_i(0) \in [16, 49]$. The curves shown in these figures are upper and lower bounds, obtained by dividing into sub-intervals of three ($[32, 82]$) and five ($[16, 49]$) width respectively, to guarantee verified solutions.

4.6 Discussion and conclusions

This chapter presented a strategy to include uncertainty in models based on ODEs by applying interval arithmetic, structural identifiability analysis, and local sensitivity analysis (see Chapters 1 and 3). Moreover, we consider the available information, knowledge, and understanding of the phenomenon under study. To the best of our knowledge, this is the first study in which a strategy to select the uncertain quantities (parameters and initial conditions) based on the results of structural identifiability analysis and local sensitivity analysis is introduced.

Previous studies in mathematical epidemiology have incorporated uncertainty via fuzzy and stochastic approaches, and to a lesser extent, through the application of interval analysis [6, 7, 12, 25]. Nevertheless, few studies have assessed the relation between the available data and the model formulation to decide which is the best option to include the uncertainty [41, 113]. This study represented uncertain quantities (parameters or initial values) of a dengue transmission model by intervals, since the available information is not always accurate. It might not be sufficient either to determine the probability distribution function or the membership function that parameters follow.

For Model 3.3, it was possible to obtain the trajectories using ITS, where its coefficients are given by Taylor models, since its vector field is sufficiently continuously differentiable concerning the state variables and the parameters. Nonetheless, it was not possible to consider uncertainty in a larger set of parameters and initial conditions simultaneously due to overestimation caused by the dependency problem, the wrapping effect, and the curse of dimensionality [72]. For these reasons, it was necessary to examine alternative strategies to select the uncertain quantities that should be considered. Here, we regarded the results of locally structural identifiability analysis, local sensitivity analysis, the available

information, and the knowledge of the study phenomenon to accomplish it. In this way, we can reduce the problem's dimension and successfully apply interval methods to find guaranteed bounds for model solutions.

From the biological point of view, it is relevant to consider uncertainty in parameters measured under laboratory conditions, since these results do not always correspond to the vector's life in the wild. Additionally, the local structurally identifiability analysis results suggest that considering uncertainty in the initial conditions of mosquito population through interval arithmetic is an excellent way to determine how an outbreak would be in the presence of larger populations (see Figures 4.7 and 4.8). This result is significant since, at present, the only way to mitigate dengue outbreaks efficiently is by controlling the vector population [92]. Finally, we consider as uncertain values the human initial conditions, as according to [9], the number of reported new dengue cases per week does not correspond to the total number of cases that occurred in a period. Figures 4.7 and 4.8 show that the human initial conditions have more impact on the number of dengue cases per week than mosquito initial conditions. These results make sense, since there exist cities with large mosquito population where the number of dengue cases is low and some cities with a significant number of dengue cases where the presence of mosquitoes is not significant [88]. This relation can be explained by vector capacity of the vector [14].

These findings highlight the potential usefulness of verified methods in mathematical epidemiology as an alternative to manage uncertainty in actual phenomenon modeling.

Bibliography of the current chapter

[6] L. C. Barros, R. C. Bassanezi, R. Z. G. Oliveira, and M. B. F. Leite. A disease evolution model with uncertain parameters. In: Proceedings Joint 9th IFSA World Congress and 20th NAFIPS International Conference (Cat. No. 01TH8569). Vol. 3. IEEE. 2001, pp. 1626–1630. DOI: https://doi.org/10.1109/NAFIPS.2001.943794 (cit. on pp. 46, 47, 110).

[7] L.C.DE Barros, M.B.Ferreira Leite, and R.C Bassanezi. The SI epidemiological models with a fuzzy transmission parameter. Computers & Mathematics with Applications 45.10 (2003), pp. 1619–1628. DOI: https://doi.org/10.1016/S0898-1221(03)00141-X (cit. on pp. 46, 110).

[9] Samir Bhatt et al. The global distribution and burden of dengue. Nature 496.7446 (2013), pp. 504–507. DOI: https://doi.org/10.1038/nature12060 (cit. on pp. 103, 111).

[12] Tom Britton and David Lindenstrand. Epidemic modelling: Aspects where stochasticity matters. Mathematical Biosciences 222.2 (2009), pp. 109–116. DOI: https://doi.org/10.1016/j.mbs.2009.10.001 (cit. on pp. 46, 47, 110).

[14] Alexandra Catano-Lopez, Daniel Rojas-Diaz, Henry Laniado, Sair Arboleda-Sánchez, María Eugenia Puerta-Yepes, and Diana Paola Lizarralde-Bejarano. An alternative model to explain the vectorial capacity using as example *Aedes aegypti* case in dengue transmission. Heliyon 5.10 (2019), e02577. DOI: https://doi.org/10.1016/j.heliyon.2019.e02577 (cit. on p. 111).

[25] Joshua Enszer and Mark Stadtherr. Verified Solution Method for Population Epidemiology Models with Uncertainty. International Journal of Applied Mathematics and Computer Science 19.3 (2009), pp. 501–512. DOI: https://doi.org/10.2478/v10006-009-0040-4 (cit. on pp. 46, 90, 92, 110, 168).

[26] Joshua A Enszer and Mark A Stadtherr. Verified Solution and Propagation of Uncertainty in Physiological Models. Reliable Computing 15.3 (2011), pp. 168–178 (cit. on pp. 90, 168).

[27] Joshua A. Enszer, D. Andrei Măces, and Mark A. Stadtherr. Probability bounds analysis for nonlinear population ecology models. Mathematical Biosciences 267 (2015), pp. 97–108. DOI: https://doi.org/10.1016/j.mbs.2015.06.012 (cit. on pp. 90, 168).

[41] J.C. Helton, J.D. Johnson, and W.L. Oberkampf. An exploration of alternative approaches to the representation of uncertainty in model predictions. Reliability Engineering $&$ System Safety 85.1 (2004), pp. 39–71. DOI: https://doi.org/10.1016/j.ress.2004.03.025 (cit. on p. 110).

[52] Youdong Lin and Mark A. Stadtherr. Validated solutions of initial value problems for parametric ODEs. Applied Numerical Mathematics 57.10 (2007), pp. 1145–1162. DOI: https://doi.org/10.1016/j.apnum.2006.10.006 (cit. on pp. 4, 6, 11, 92, 117, 118, 143).

[55] Rudolf J Lohner. On the ubiquity of the wrapping effect in the computation of error bounds. In: Perspectives on enclosure methods. Springer, 2001, pp. 201–216 (cit. on pp. 6, 36, 37, 90).

[58] Kyoko Makino and Martin Berz. Remainder differential algebras and their applications. Computational Differentiation: Techniques, Applications and Tools (1996). Ed. by Martin Berz, Christian Bischof, George Corliss, and Andreas Griewank, pp. 63–74 (cit. on p. 94).

[72] Nedialko S Nedialkov, Kenneth R Jackson, and George F Corliss. Validated solutions of initial value problems for ordinary differential equations. Applied Mathematics and Computation 105.1 (1999), pp. 21–68 (cit. on pp. 6, 35, 90, 93, 110, 143).

[74] Markus Neher, Kenneth R Jackson, and Nedialko S Nedialkov. On Taylor model based integration of ODEs. SIAM Journal on Numerical Analysis 45.1 (2007), pp. 236–262 (cit. on pp. 6, 91).

[88] Víctor Hugo Peña-García, Omar Triana-Chávez, Ana María Mejía-Jaramillo, Francisco J Díaz, Andrés Gómez-Palacio, and Sair Arboleda-Sánchez. Infection Rates by Dengue Virus in Mosquitoes and the Influence of Temperature May Be Related to Different Endemicity Patterns in Three Colombian Cities. International Journal of Environmental Research and Public Health 13.7 (2016), p. 734. DOI: https://doi.org/10.3390/ijerph13070734 (cit. on pp. 28, 111).

[92] Irfan A. Rather et al. Prevention and Control Strategies to Counter Dengue Virus Infection. Frontiers in Cellular and Infection Microbiology 7 (2017), p. 336. DOI: https://doi.org/10.3389/fcimb.2017.00336 (cit. on p. 111).

[113] H.-J. Zimmermann. An application-oriented view of modeling uncertainty. European Journal of Operational Research 122.2 (2000), pp. 190–198. DOI: https://doi.org/10.1016/S0377-2217(99)00228-3 (cit. on pp. 45, 110).

Chapter 5

Parameter estimation considering interval uncertainty

Outline of the current chapter

5.1 Abstract

The goal of this chapter is to solve a parameter estimation problem considering uncertain data. To achieve this goal, we propose the algorithm PISA (Parameter Interval Search Algorithm) to settle which interval parameters produce the best fit to actual data. PISA exploits the relation between the value of R_{0_H} and the behavior of the reported dengue cases to drop regions with biological inconsistency. The algorithm's effectiveness is demonstrated by estimating the most sensitive parameters of R_0 for Itagüí and Neiva.

On the other hand, we introduce two key concepts, weak and strong compatibility, between the output of the model and the given interval data. In particular, we formulate these notions when the model is an ODEs, and real closed intervals give the variables' values. These concepts help us understand the meaning of the model fit to interval data. To exemplify this point, we add noise in the data follows a uniform distribution to evaluate how much uncertainty can explain a fixed estimation.

The results showed that PISA was able to fit the data for both municipalities. Moreover, we found that the transmission rate values from mosquito to human (β_h) and the mortality rate in mosquitoes (μ_m) were higher for Neiva than for Itagüí. Finally, applying the compatibility measure, we found that the uncertain initial conditions of the model can explain an increase in the number of reported dengue cases for Itagüí and Neiva with the same parameter values.

5.2 Problem statement

In this chapter, we wanted to develop a method for analyzing data that is inaccurate and with interval uncertainties. Unfortunately, as far as we know, it is not possible to find analytic expressions for the solution of nonlinear ODEs as given in Model 3.3, so we investigated using numerical methods. Moreover, for this kind of model, the vector of parameters and the vector of initial conditions are unknown. In summary, the goal of this chapter was to determine these unknowns parameters from some measurements (observations) of some variables X_i in Equation (4.1) that can or cannot be precise.

The problem of determining the parameter values of a dynamic model from experimental results is commonly known as *parameter estimation problem*, and is present in many applications that involve the modeling of real phenomena.

One of the strategies to solve this problem is through the formulation of an optimization problem Equation (5.1) which frequently is nonlinear and non-convex.

$$\begin{aligned} \min_{\theta \in \Theta} \ & \phi(Y_i(t_j, \theta), X_{ij}) \\ \text{s.t. } & \dot{y} = f(t, y(t), \theta) \\ & y(t_0, \theta) = y_0(\theta) \\ & g(y(t_i), \theta) \leq 0, \\ & t \in [t_0, t_f] \end{aligned} \tag{5.1}$$

where, θ is a p-dimensional parameter vector, $Y_{ij} = Y_i(t_j, \theta)$ is the solution of the ODEs, X_{ij} is the experimental data for the variable i at the time t_j, the solution of the ODEs, ϕ is the objective function that measures the error between the model and the data, and g is a constraint.

Here, we want to solve Equation (5.1) when the decision variable is the

parameter vector $\theta = (\beta_m, \beta_h, \mu_m, \gamma_h) \in R$, where, R is given by the cartesian product of the parameter's range of each municipality (see Table 3.1). The idea at this point is discarding portions of $\mathcal{R}$ that are inconsistent with Model 3.3 and data. To do this, we follow a sequential approach where the optimization problem in Equation (5.1) is divided into two modules, the ODEs integration and the optimization modules. The integration module's goal is to obtain the numerical solution for the ODEs with decision variable values given by the optimization module. In this study, we obtain these numerical solutions from the VSPODE software [52]. It is important to mention that the solution is completely rigorous since it is based on its solver's numerical solution. The optimization module's objective is to compare the objective function values between boxes to determine each iteration's optimum. These optimal boxes will then be divided to obtain enclosures as narrow as determined by the modeler.

Then, when the data is inaccurate, that is, when each measurement represents an entire set of possible values rather than a single point, the concept of "fit a model to the data" must be rethought [96]. For this purpose, we define the concept of "*compatibility and strong compatibility*" between interval-data and a vector formed by uncertain initial conditions or uncertain parameters of the given model. Following the theory of interval linear equations, we call the set of compatible vectors with data the "*united solution set*", while the set of strong compatibility vectors with the data is called "*tolerable solution set*".

5.3 Parameter estimation

To fit the nonlinear ODEs formulated in Model 3.3 to our data described in Section Section 3.3, we express the parameter estimation problem in Equation (5.1). We refer to these interval vectors of parameter values as *boxes*. To solve this optimization problem, we propose a search algorithm in this section.

The search space, R, for this task is considerably large. According to the results from elasticity ranges of R_0 (see Table 3.4), for Model 3.3, we need to consider uncertainty on four parameters, β_m, β_h, μ_m, and γ_h. Therefore, the size of such a space of boxes makes our fitting problem impractical for any brute-force algorithm, as we must solve its corresponding ODEs for each parameter combination. This is also expensive as we require verified solutions. We request for such solutions to the verified-numerical software VSPODE, introduced in [52].

According to specific rules, referred as *filters* in Section 5.4.3, the proposed algorithm explores a graph by expanding the most promising nodes. This approach follows similar ideas of a *best-first search* algorithm. However, our node-expansion happens for a node-set. Usually, one only expands the most promising node. This choice design relies on the fact that our optimization problem often exhibits multiple optima.

To find the promising nodes, we perform a *depth-first search* on the *grid* of the defined parent box. This search discards boxes of the parameter domain inconsistent with the given data by using the constraints defined. Consequently, we get promising boxes, on which we compute the objective function value described in Section 5.4.1. This finishes the grid exploration. At this stage of the algorithm, we could stop and determine the optimum found. Otherwise, using the same strategy on every promising box, we could iterate the algorithm to get new optima, and consequently a global solution. As part of the algorithm's input, one sets the number of times the algorithm iterates.

We pointed out that as the algorithm recurses, its recursive sub-calls are independent, as they have no shared values. This observation suggests one can execute each sub-call in parallel, improving the run time execution. Further, each algorithm's component is precisely described.

5.4 Algorithm's description

5.4.1 Objective function

For our parameter estimation problem, we consider the l_1-norm Equation (1.12) as the objective function ϕ. This function ϕ measures the error between the data and the output model. We chose the l_1-norm since it is less sensitive to outliers [4].

5.4.2 Initial region

As part of the algorithm's input, we must provide an *initial* box. We refer to such box as Z. This box corresponds to the root in the graph in which the algorithm explores. To establish Z, we start with a box named R, based on ranges given in the Table 3.1 for the uncertain parameter intervals.

We perform a preliminary search to discard *non-informative* boxes in R. To do so, we divide R into smaller boxes, precisely, 625 boxes of equal size. We solve the optimization problem, Equation (5.1) using a local-search algorithm on each of these boxes. In our setting, we perform such a search by using the Mathematica built-in method FindFit, initialized with the midpoint of each box. With a refinement of these 625 estimations, we find for each parameter an interval, namely B_{β_m}, B_{β_h}, B_{μ_m}, and B_{γ_h}. The initial box Z is as follows

$$Z = B_{\beta_m} \times B_{\beta_h} \times B_{\mu_m} \times B_{\gamma_h}. \tag{5.2}$$

5.4.3 Filters

A *filter* is a function that decides whether we must consider a box or not for graph exploration.

- F1. We consider the constraint $R^2_{0_H} \geq 1$ (see Equation (3.12)), since we want

to simulate two outbreaks of dengue transmission. Therefore, the average number of infected humans must be greater than one. In this way, it is possible to eliminate boxes that do not make biological sense in our case study. Thus, we avoid undesirable computations with VSPODE.

- F2. To formulate this filter, we consider in which directions the objective function value increase or decrease. To do this, we examine how the behavior of β_m, β_h, μ_m, and γ_h make the trajectory of infected humans grow. We obtain for our case study, the following set of vectors Dir.

$$\mathsf{Dir} = \{(1,0,0,0),(0,1,0,0),(0,0,-1,0),(0,0,0,-1)\}.$$

The first two vectors in Dir indicate we move in the direction in which β_m and β_h increase. While the other vectors indicate, we move in the direction in which μ_m and γ_h decrease.

Let b be the filter's input. We discard certain boxes based on the objective function value of their neighbors. The NeighborBoxes function gives such neighbors using Dir, as it is illustrated by Figure 5.1(a). If $\phi(b)$ is the objective value function on b, and b' is one of its neighbor in the direction $d \in \mathsf{Dir}$, we compute $\phi(b')$. If $\phi(b') > \phi(b)$, we discard all boxes that one can find in the current grid following direction d.

$$\mathsf{NeighborBoxes}(b) = \{b' \,|\, b' = b + \omega_\theta d_\theta, \text{ for all } d \in \mathsf{Dir}\} \tag{5.3}$$

where, ω_θ corresponds to the width of the coordinate θ of b. We summarize this procedure in Algorithm 1.

- F3. This filter is always the last criterion we apply to discard boxes. To avoid discarding boxes where one could find a good estimation in later iterations, we admit an error level η for the optimal value found, where,

Algorithm 1 : F2: Discarding boxes by ϕ monotonicity

```
   Input : b, Dir, φ, R, θ ∈ {β_m, β_h, μ_m, γ_h}
1  if φ(b_θ) > φ(b) then
2      Color(b_θ) ← PURPLE
3      for d_θ ∈ Dir do
4          b'_θ ← b_θ + d_θ
5          while b'_θ ⊆ R do
6              if Color(b'_θ) = WHITE then
7                  Color(b'_θ) ← PURPLE
```

$0 \leq \eta \leq 1$. This η value represents the error percentage the modeler accepts. Let ϕ^* be the optimum value for the current iteration. The filter F3 accepts boxes Z_i only if $\phi(Z_i) < (1+\eta)\phi^*$.

We summarize the general procedure in Algorithm 2.

Example 5.4.1. Consider Model 3.3 and the cumulative number of dengue cases for Neiva (see Section 3.3). To explain how Algorithm 2 works, we consider two uncertain parameters, β_m and β_h. The resulting region Z after the preliminary search is $Z = [0.054, 0.21] \times [2.23, 3.23]$ which is the initial box and the root in the graph. In the first algorithm's iteration, we split β_m and β_h in 5 and 4 subintervals, respectively. In total, we split Z into 20 sub-boxes. In this way, it is possible to compute verified enclosures for the trajectories using VSPODE.

Moreover, we define the directions set as $\mathsf{Dir} = \{(1,0),(0,1)\}$ indicating that we move towards increase in β_m and β_h. Thus, for example, the $\mathsf{NeighborBoxes}(Z_1) = \{Z_2, Z_5\}$ (see Figure 5.1(a)). For subsequent iterations, we only split each region into three sub-boxes according to their maximum width. For instance, in the first iteration $w(\beta_m) = 0.156$ and $w(\beta_h) = 1$, so we split the coordinate β_h into three parts (see Figure 5.1(c)). In total, we performed 16 algorithm's iterations. We summarized these results in Table 5.1, while Figure 5.3 shows the enclosures obtained for the cumulative number of infected humans. The values used for the other parameters and initial conditions are as follows $H = 324466$, $\mu_h = 0.00011$,

Algorithm 2 : Parameter interval search algorithm (PISA)

Input : Region R (split by boxes), objective function ϕ, tolerance error η, a positive number n, and global variable ArgMin
Output : Parameter estimation assignment ArgMin

$Z^{(1)} \leftarrow \{R\}$
for $k = 1$ *to* n **do**
  $Z^{(k+1)} \leftarrow \emptyset$
  for $R \in Z^{(k)}$ **do**
    $W_{\mathsf{F1}} \leftarrow \emptyset$
    for $b \in R$ **do**
      update graph with entry b
      if $\min(R_H(b)) \geq 1$ **then**
        $W_{\mathsf{F1}} \leftarrow W_{\mathsf{F1}} \cup \{b\}$
    $\mathcal{G} \leftarrow \emptyset$
    for $b \in W_{\mathsf{F1}}$ **do**
      if $\mathsf{Color}(b) = \mathsf{WHITE}$ **then**
        $B \leftarrow$ **Explore**$(R, \phi, \eta, W_{F1}, b, \mathsf{ArgMin})$
        $\mathcal{G} \leftarrow \mathcal{G} \cup B$
    $\phi^* \leftarrow \min\{\phi(b) \mid b \in \mathcal{G}\}$
    for $Z \in \mathcal{G}$ **do**
      if $\phi(b) \leq \phi^*$ **then**
        $\mathsf{ArgMin} \leftarrow b$
      if $\phi(b) \leq (1+\eta) \cdot \phi^*$ **then**
        $\mathsf{Color}(b) \leftarrow \mathsf{GREEN}$
      else
        $\mathcal{G} \leftarrow \mathcal{G} \setminus \{b\}$
    for $b \in \mathcal{G}$ **do**
      $Z^{(k+1)} \leftarrow Z^{(k+1)} \cup \{\mathsf{Split}(b)\}$
return ArgMin

$\mu_m = 0.45$, $\theta_m = 0.8$, $\theta_h = 1.3$, $\gamma_h = 1.7$, $\Lambda = 24000$, $M_s(0) = 3500000$, $M_e(0) = 80$, $M_i(0) = 25$, $H_s(0) = 315952$, $H_e(0) = 27$, $H_i(0) = H_c(0) = 16$, and $H_r(0) = 8471$.

Remark. It is important to note that this algorithm allows us to find clusters of regions with reasonable solutions. For instance, when we run iteration nine, we found three candidate regions for searching solutions. In this case, it is up to the modeller to decide the uncertainty he wants to admit in the final parameters to accept the answer, considering that the solutions found are mathematically

Algorithm 3 : Explore

Input : R, ϕ, η, W_{F1}, b, ArgMin
Output : $\mathcal{G} = \{b \subseteq R \mid b$ satisfied the filter F3$\}$

```
1  G ← ArgMin
2  W_F3 ← b
3  if Color(b) = WHITE and b ∈ W_F1 then
4      Color(b) ← GRAY
5      Y_b ← VSPODE(b)
6      for b' ∈ NeighborBoxes(b) do
7          Y_b ← VSPODE(b)
8          if φ(b') ≤ φ(b) then
9              ArgMin ← b'
10             φ* ← φ(b')
11             W_F3 ← W_F3 ∪ {b'}
12             Explore(R, φ, η, W_F1, b', ArgMin)
13         else
14             Apply F2(b)
15 for b ∈ W_F3 do
16     if φ(b) ≤ (1 + η) · φ* then
17         G ← G ∪ {b}
18 return G
```

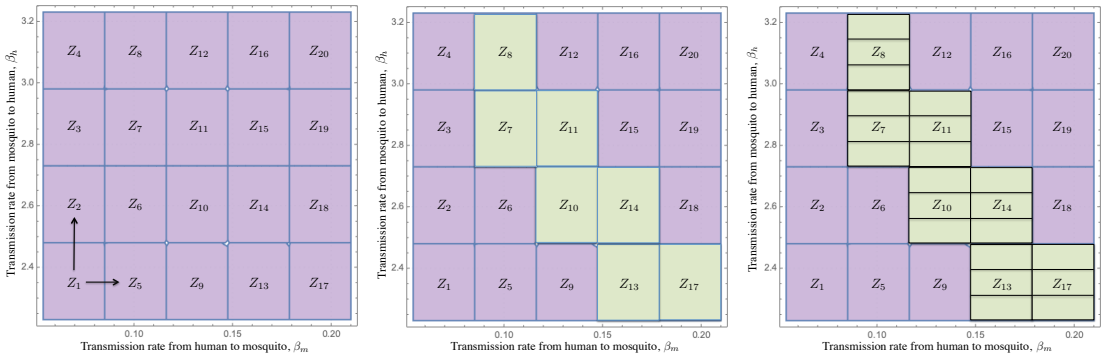

(a) (b) (c)

Figure 5.1 – Figure 5.1(a) shows the initial region split into 20 sub-boxes and the directions to explore. Figure 5.1(b) shows in green the boxes that satisfied all the three filters in the first iteration, and in purple, the boxes discarded. Figure 5.1(c) shows how the green boxes are split in the second iteration.

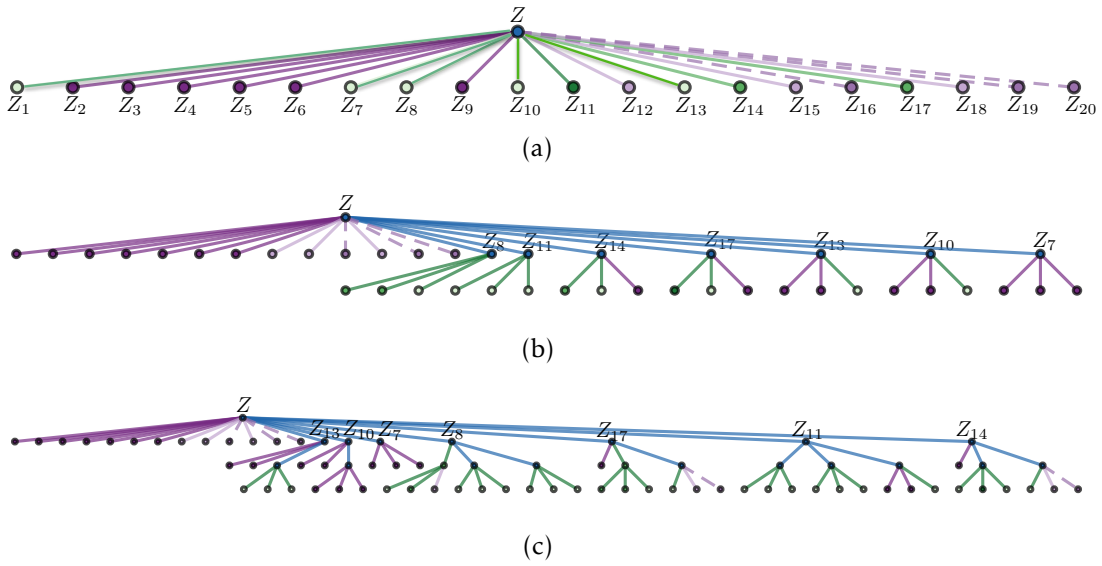

Figure 5.2 – The figure shows the first, second, and third iteration of the algorithm's graph for Model 3.3 when we consider uncertainty in two parameters, β_m and β_h. The green edges correspond to the boxes that the algorithm will split in the following iteration. The purple edges correspond to the boxes discarded by the algorithm in the current iteration.

verified.

5.4.4 Compatibility between parameters, initial conditions, and interval data

According to [96], intuitively, we can understand the compatibility between parameters and data as passaging a curve through all the corridors of uncertainty data for the output variable.

The idea here is to evaluate how much uncertainty in the data can explain the interval solutions found using the VSPODE when including uncertainty first in the parameters and then in the initial conditions. For this, we introduced the definitions and results needed to establish compatibility between parameters and uncertain data. These are mainly taken from [96], where were formulated in the context of solving the data fitting problem for a linear function under

Table 5.1 – Table shows the best-fitted parameter enclosures results in each iteration for Model 3.3 considering as uncertain parameters, β_m and β_h.

Iter	Obf. function value	Parameter vector	
		β_m	β_h
1	2387.5855	[0.116399, 0.147600]	[2.729999, 2.980000]
2	1532.6969	[0.178800, 0.210000]	[2.230000, 2.313333]
3	1286.0055	[0.178800, 0.210000]	[2.257778, 2.285555]
4	734.2488	[0.189200, 0.199600]	[2.257778, 2.285555]
5	614.0078	[0.189199, 0.199600]	[2.276296, 2.285555]
6	424.7480	[0.192667, 0.196133]	[2.276296, 2.28555]
7	388.1020	[0.192667, 0.196133]	[2.282469, 2.28555]
8	324.3913	[0.194978, 0.196133]	[2.276296, 2.279382]
9	315.4371	[0.194978, 0.196133]	[2.276296, 2.27325]
10	294.2311	[0.195363, 0.195748]	[2.276296, 2.277325]
11	291.2613	[0.195363, 0.195748]	[2.276296, 2.276639]
12	284.2207	[0.195491, 0.19562]	[2.276296, 2.276639]
13	283.1019	[0.195363, 0.195491]	[2.276525, 2.276639]
14	280.7129	[0.195448, 0.195491]	[2.276525, 2.276639]
15	280.3869	[0.195448, 0.195491]	[2.276525, 2.276563]
16	279.5394	[0.195448, 0.195462]	[2.276525, 2.276563]

interval data uncertainty. We adapt them according to our case study.

Below are some variables we used to introduce new definitions.

- Let $Z = (Y_0, \Theta) \in \mathbb{IR}^p$ be a $p-$dimensional vector, where its first m coordinates correspond to the interval initial conditions and its last $p - m$ coordinates correspond to interval parameters of the model in Equation (4.1), respectively.

- The vector $X_i = (X_{i_1}, X_{i_2}, \ldots, X_{i_k})$ is the interval experimental data regarding Equation (4.1), where n is the number of variables, $1 \leq i \leq n$, and the number of measurements at different times is denoted by k.

- The vector $Y_i = (Y_{i_1}, Y_{i_2}, \ldots, Y_{i_k})$ is the enclosure of the system solution in Equation (4.1) for the variable i at the time t_k.

Definition 5.4.1. The vector Z is *compatible* with an interval experimental data $X_{i_1}, X_{i_2}, \ldots, X_{i_k}$, if for each measurement k, there are representatives $x_{i_1} \in$

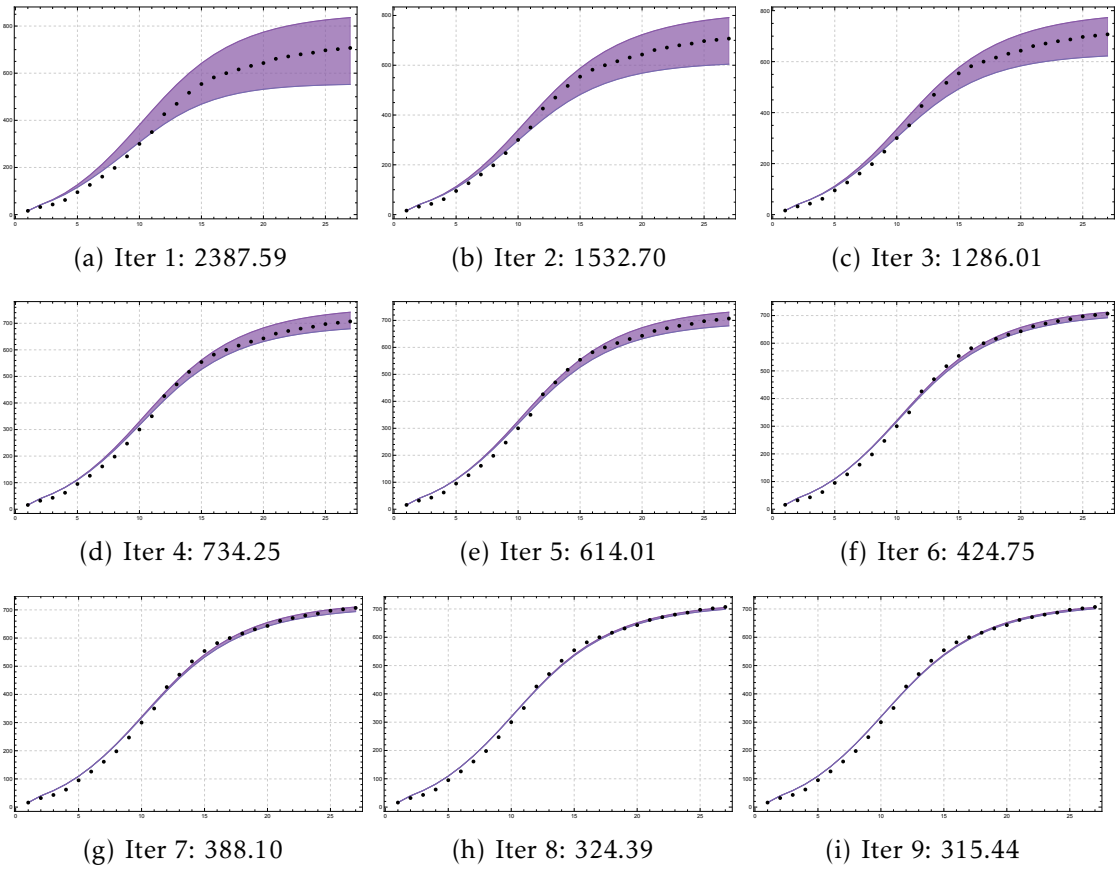

(a) Iter 1: 2387.59 (b) Iter 2: 1532.70 (c) Iter 3: 1286.01

(d) Iter 4: 734.25 (e) Iter 5: 614.01 (f) Iter 6: 424.75

(g) Iter 7: 388.10 (h) Iter 8: 324.39 (i) Iter 9: 315.44

Figure 5.3 – The figure shows how the enclosures obtained solving the system Model 3.3 for the cumulative number of infected humans are reduced in each iteration.

$X_{i_1},\ldots,x_{i_k} \in X_{i_k}$ such that $x_{i_1} \in Y_{i_1},\ldots,x_{i_k} \in Y_{i_k}$.

This set of vectors is called *the united solution set* of Equation (4.1).

$$E_{unit}(\mathbf{X},\mathbf{Y}) = \{Z \in \mathbb{IR}^p \,|\, \text{there exist } \mathbf{x} \in \mathbf{X} \text{ such that } \mathbf{x} \in \mathbf{Y}\}$$

where, $\mathbf{X}$ and $\mathbf{Y}$ are interval matrices, and $\mathbf{x}$ is a real matrix. All these matrices have the same dimension, $k \times n$.

Definition 5.4.2. The vector Z is *strongly compatible* with the interval experimental data $X_{i_1}, X_{i_2},\ldots,X_{i_k}$ if for each measurement k, and for any representatives $x_{i_1} \in X_{i_1},\ldots,x_{i_k} \in X_{i_k}$ there holds that $x_{i_1} \in Y_{i_1},\ldots,x_{i_k} \in Y_{i_k}$.

The set composed of Z vectors that satisfies the previous definition is called *the tolerable solution set* of the Eq. (4.1).

$$E_{tol}(\mathbf{X},\mathbf{Y}) = \{Z \in \mathbb{IR}^p \,|\, \text{for any } \mathbf{x} \in \mathbf{X},\ \mathbf{x} \in \mathbf{Y}\} \tag{5.4}$$

From Definition 5.4.1 and Definition 5.4.2, it follows that the *tolerable solution set* is always a subset of the *united solution set*, i.e. if there is *strong compatibility* between the vector of parameters, the vector of initial conditions and the data, then the usual *compatibility* takes place naturally.

$$E_{tol}(\mathbf{X},\mathbf{Y}) \subseteq E_{unit}(\mathbf{X},\mathbf{Y}).$$

Example 5.4.2. Consider the *sir* model normalized, i.e. $0 \leq s \leq 1$, $0 \leq i \leq 1$, and $0 \leq r \leq 1$:

$$\begin{aligned}
\dot{s} &= \mu - \beta si - \mu s \\
\dot{i} &= \beta si - (\mu + \gamma) i \\
\dot{r} &= \gamma i - \mu r
\end{aligned}$$

where, μ, β, and γ represent the mortality rate, the transmission probability and the recovery rate, respectively. Also the population is constant, $s + i + r = 1$. We can reduce this system to the first two equations

$$\begin{aligned}
\dot{s} &= \mu - \beta si - \mu s \\
\dot{i} &= \beta si - (\mu + \gamma) i.
\end{aligned} \tag{5.5}$$

To illustrate the definition of *compatibility* and *strong compatibility* with the system Equation (5.5), we consider just one uncertain parameter, the transmission probability β. The mortality rate and the recovery rate are given by $\mu = 0.5$ and $\gamma = 0.1$, respectively. The initial conditions are $s(0) = 0.97$ and $i(0) = 0.03$.

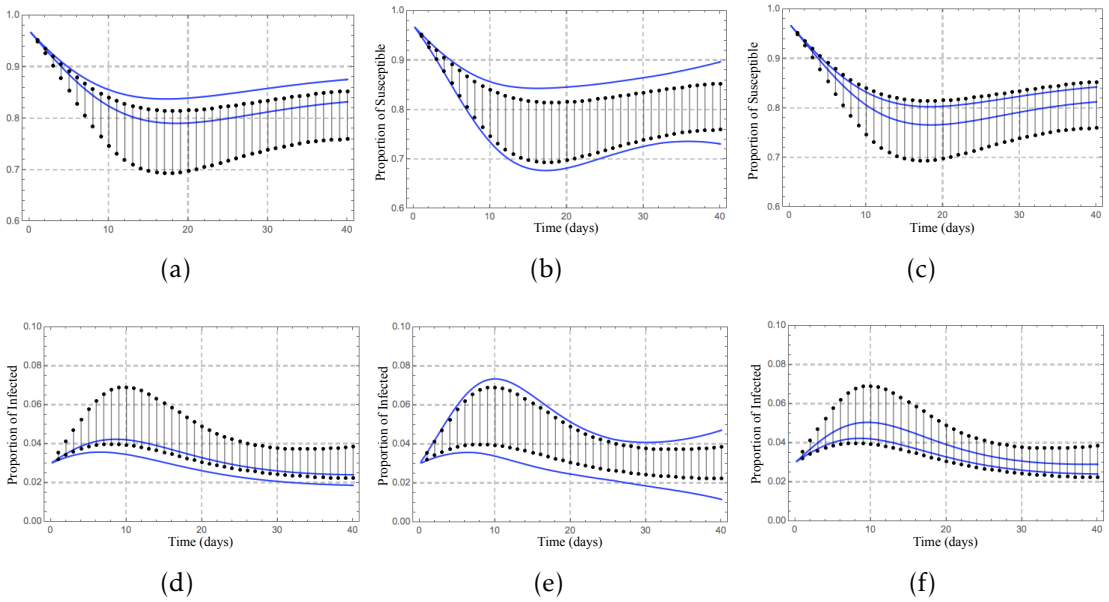

Figure 5.4 – in Figures 5.4(a) and 5.4(d) we consider $\beta = [\,0.68, 0.72\,]$. These figures show that just one part of the interval data belongs to the enclosure obtained to solve Equation (5.5). For Figures 5.4(b) and 5.4(e) we consider $\beta = [\,0.71\,, 0.74\,]$. These figures show the enclosure obtained to solve Equation (5.5) is a subset of the interval data for each measure. Finally, for Figures 5.4(c) and 5.4(f) we consider $\beta = [\,0.68\,, 0.81\,]$. These figures show how the interval data is a subset of the enclosure obtained to solve Equation (5.5) for each measure and each variable. In this way, Figures 5.4(a), 5.4(b), 5.4(d) and 5.4(e) show *compatibility* between the vector of parameters and initial conditions of Equation (5.5) and interval measurement data. Meanwhile, Figures 5.4(c) and 5.4(f) show *strongly compatibility* between parameters and initial conditions, and interval data.

Another case that may arise is when the interval data and the enclosure obtained to solve Equation (4.1) do not have any common point. In this case, we say that the interval data and the vector of parameters and initial conditions are *incompatible*.

To settle the compatibility type between the vector of parameters and initial conditions and the interval data, we introduce a *quantitative measure of compatibility*. For this, let's consider a vector Z. To know if Z belongs to the *tolerable solution set* we have to check that $X_{i_1} \subseteq Y_{i_1}, X_{i_2} \subseteq Y_{i_2}, \ldots, X_{i_k} \subseteq Y_{i_k}$ for each variable i. Doing so, we consider $X_{i_j} = [\underline{X_{i_j}}, \overline{X_{i_j}}]$ and $Y_{i_j} = [\underline{Y_{i_j}}, \overline{Y_{i_j}}]$, where $j = 1, \ldots k$. We say X_{i_j} is subset of Y_{i_j} if and only if

$$\min_{1\leq i\leq n} \min_{1\leq j\leq k} \{(\underline{X_{i_j}} - \underline{Y_{i_j}}), (\overline{Y_{i_j}} - \overline{X_{i_j}})\} \geq 0 \tag{5.6}$$

or equivalently if

$$\min_{1\leq i\leq n} \min_{1\leq j\leq k} \{rad\, Y_{i_j} - rad\, X_{i_j} - |mid\, X_{i_j} - mid\, Y_{i_j}|\} \geq 0 \tag{5.7}$$

where, $X = [\underline{X}, \overline{X}] = mid\, X + [-rad\, X, rad\, X]$.

Now, we can state the following result as

Theorem 5.4.1. *Let* $\mathbf{X}$ *and* $\mathbf{Y}$ *be* $n \times k$ *interval matrices, where* n *corresponds to the number of variables of the system Equation* (4.1) *and* k *corresponds to the number of measurements for each variable. The expression*

$$Tol(Z, \boldsymbol{X}, \boldsymbol{Y}) = \min_{1\leq i\leq n} \min_{1\leq j\leq k} \{rad\, Y_{i_j} - rad\, X_{i_j} - |mid\, X_{i_j} - mid\, Y_{i_j}|\} \tag{5.8}$$

determines the mapping $Tol : \mathbb{IR}^p \times \mathbb{IR}^{n\times k} \times \mathbb{IR}^{n\times k} \to \mathbb{R}$ *such that the membership of a point* $Z \in \mathbb{IR}^p$ *in the tolerable solution set,* $E_{tol}(\mathbf{X}, \mathbf{Y})$ *of the system given by Equa-*

tion (4.1) *is equivalent to non-negativity of the mapping Tol in the point* Z*, i. e.*

$$Z \in E_{tol}(\boldsymbol{X}, \boldsymbol{Y}) \iff Tol(Z, \boldsymbol{X}, \boldsymbol{Y}) \geq 0.$$

We call the function given in Equation (5.8), compatibility measure.

Example 5.4.3. Let's consider again the model given by Equation (5.5) and Example 5.4.2. We have two variables; the proportion of susceptible, s and the proportion of infected, i. Additionally, we have forty measures for each variable.

- For Figures 5.4(a) and 5.4(d) the value of Equation (5.7) is given by:

$$\min_{1 \leq i \leq 2} \{-0.0974893, -0.0243558\} = -0.0974893 \leq 0$$

- For Figures 5.4(b) and 5.4(e) the value of Equation (5.7) is given by:

$$\min_{1 \leq i \leq 2} \{-0.0733967, -0.0186444\} = -0.0733967 \leq 0$$

- For Figures 5.4(c) and 5.4(f) the value of Equation (5.7) is given by:

$$\min_{1 \leq i \leq 2} \{0.000414505, 0.000336667\} = 0.000336667 \geq 0$$

These values correspond to the minimum when we consider the interval-data and the enclosure for the proportion of susceptible and for the proportion of infected, respectively.

From the compatibility measure values in these three scenarios we conclude that the only vector Z of initial conditions and parameters which belongs to E_{tol} correspond to Figures 5.4(c) and 5.4(f).

5.5 Results of model fitting and parameter estimation

We fitted Model 3.3 to the cumulative reported dengue cases for each municipality. For this, as in [54], we added a new state variable, $H_c = \theta_h H_e$ that describes the number of cumulative dengue cases without considering the recovered. We decided to proceed in this way as the available information regarding the new number of reported dengue cases is gathered per week. Hence, it was also not possible to knew the average recovery period was for each population beforehand. Thus, we did not know how many infected humans were for a given time.

In addition, in the `Filter-3`, we define $\eta = 0.5$, i.e. we accept an error level up to 50% in the optimal value found in each iteration.

5.5.1 Itagüí

The resulting region from the local method for Itagüí was

$$\begin{aligned} Z &= B_{\beta_m} \times B_{\beta_h} \times B_{\mu_m} \times B_{\gamma_h} \\ &= [0.05, 0.25] \times [1.3, 2.3] \times [0.16, 0.26] \times [1.45, 1.75] \end{aligned} \tag{5.9}$$

where, $w(B_{\beta_m}) = 0.2$, $w(B_{\beta_h}) = 1$, $w(B_{\mu_m}) = 0.1$, and $w(B_{\gamma_h}) = 0.3$. To compute mathematically and computationally guaranteed upper and lower bounds for the trajectories of cumulative infected humans, we split $B_{\beta_m}, B_{\beta_h}, B_{\mu_m}$, and B_{γ_h} in $40, 20, 40$, and 30 subintervals. So, in total we split Z in 960000 sub-boxes. The values used for the other parameters and initial conditions for Itagüí were $H = 248036$, $\mu_h = 0.00023$, $\theta_m = 0.6$, $\theta_h = 1.3$, $\Lambda = 2500$, $M_s(0) = 1800000$, $M_e(0) = 50$, $M_i(0) = 20$, $H_s(0) = 223000$, $H_e(0) = 21$, $H_i(0) = H_c(0) = 10$, and $H_r(0) = 25005$.

Table 5.2 – Best fitted results for each iteration from Algorithm 2 for Itagüí considering uncertainty in β_m, β_h, μ_m, and γ_h.

Iter	Obj. function value	Parameter vector			
		β_m	β_h	μ_m	γ_h
1	10213.7	[0.1350, 0.1400]	[2.0500, 2.1000]	[0.2150, 0.2175]	[1.7400, 1.7500]
2	7748.63	[0.1750, 0.1800]	[1.7666, 1.7834]	[0.2250, 0.2275]	[1.7000, 1.7100]
3	6873.96	[0.1750, 0.1800]	[1.7722, 1.7778]	[0.2250, 0.2275]	[1.7000, 1.7100]
4	6505.94	[0.1750, 0.1800]	[1.7722, 1.7778]	[0.2250, 0.2275]	[1.7033, 1.7067]
5	6210.98	[0.1750, 0.1800]	[1.7759, 1.7778]	[0.2250, 0.2275]	[1.7066, 1.7100]
6	4400.80	[0.1766, 0.1784]	[1.7759, 1.7778]	[0.2250, 0.2275]	[1.7066, 1.7100]
7	4282.48	[0.1766, 0.1784]	[1.7759, 1.7778]	[0.2250, 0.2275]	[1.7077, 1.7089]
8	3445.23	[0.1766, 0.1784]	[1.7759, 1.7778]	[0.2258, 0.2267]	[1.7077, 1.7089]
9	3351.44	[0.1766, 0.1784]	[1.7771, 1.7778]	[0.2258, 0.2267]	[1.7077, 1.7089]
10	2757.75	[0.1772, 0.1778]	[1.7771, 1.7778]	[0.2258, 0.2267]	[1.7077, 1.7089]
11	2718.50	[0.1772, 0.1778]	[1.7771, 1.7778]	[0.2258, 0.2267]	[1.7077, 1.7082]
12	2441.93	[0.1772, 0.1778]	[1.7771, 1.7778]	[0.2261, 0.2264]	[1.7077, 1.7082]
13	2411.34	[0.1772, 0.1778]	[1.7773, 1.7776]	[0.2261, 0.2264]	[1.7077, 1.7082]
14	2214.38	[0.1774, 0.1776]	[1.7773, 1.7776]	[0.2261, 0.2264]	[1.7077, 1.7082]
15	2201.27	[0.1774, 0.1776]	[1.7773, 1.7776]	[0.2261, 0.2264]	[1.7077, 1.7079]
16	2109.08	[0.1774, 0.1776]	[1.7773, 1.7776]	[0.2262, 0.2263]	[1.7077, 1.7079]
17	2098.68	[0.1774, 0.1776]	[1.7775, 1.7776]	[0.2262, 0.2263]	[1.7077, 1.7079]
18	2032.76	[0.1774, 0.1775]	[1.7775, 1.7776]	[0.2262, 0.2263]	[1.7077, 1.7079]
19	2028.53	[0.1774, 0.1775]	[1.7775, 1.7776]	[0.2262, 0.2263]	[1.7078, 1.7079]

Table 5.2 shows the best-fitted parameter enclosures results in each iteration for Itagüí. In total, we performed 24 iterations for Itagüí. However, from iteration 20 to 24, the width of each interval of each parameter decreases slightly. For this reason, we define the stopped criterion considering the width of each interval as smaller or equal to 0.0001.

5.5.2 Neiva

The resulting region from the local method for Neiva was

$$\begin{aligned} Z &= B_{\beta_m} \times B_{\beta_h} \times B_{\mu_m} \times B_{\gamma_h} \\ &= [0.054, 0.21] \times [2.23, 3.23] \times [0.37, 0.45] \times [1.05, 1.75] \end{aligned} \tag{5.10}$$

where, $w(B_{\beta_m}) = 0.156$, $w(B_{\beta_h}) = 1$, $w(B_{\mu_m}) = 0.08$, and $w(B_{\gamma_h}) = 0.7$. To compute mathematically and computationally guaranteed upper and lower bounds for the trajectories of cumulative infected humans, we had to split $B_{\beta_m}, B_{\beta_h}, B_{\mu_m}$, and

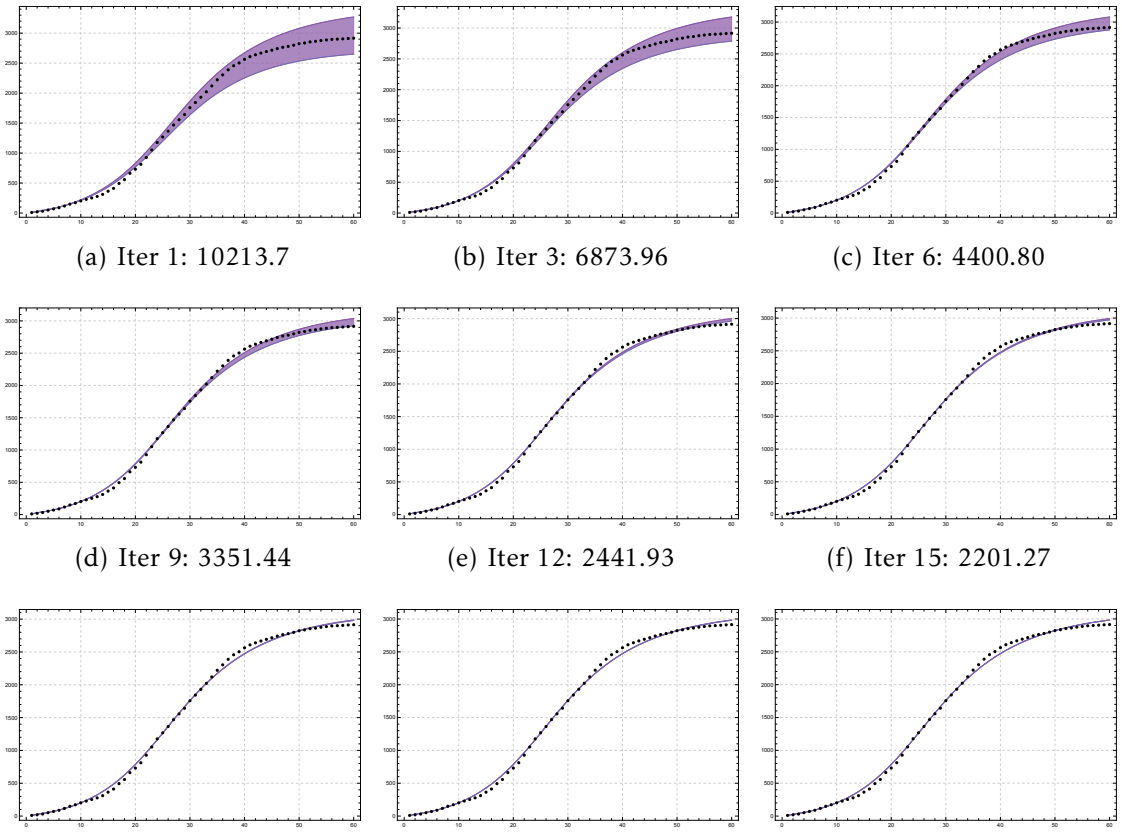

(a) Iter 1: 10213.7 (b) Iter 3: 6873.96 (c) Iter 6: 4400.80

(d) Iter 9: 3351.44 (e) Iter 12: 2441.93 (f) Iter 15: 2201.27

(g) Iter 18: 2032.76 (h) Iter 21: 1994.40 (i) Iter 24: 1960.77

Figure 5.5 – The horizontal axis corresponds to the number of epidemiological weeks, while the vertical axis corresponds to the cumulative number of dengue cases. The Figure shows the enclosures obtained to solve Model 3.3 for Itagüí in various iterations. We see how the enclosure's width decreases by reducing the width of the interval parameter.

B_{γ_h} in 8, 5, 8, and 7 subintervals. Thus, we split Z in 2240 sub-boxes. The values used for the other parameters and initial conditions for Neiva were as follows $H = 324466$, $\mu_h = 0.00011$, $\theta_m = 0.8$, $\theta_h = 1.3$, $\Lambda = 24000$, $M_s(0) = 3500000$, $M_e(0) = 80$, $M_i(0) = 25$, $H_s(0) = 315952$, $H_e(0) = 27$, $H_i(0) = H_c(0) = 16$, and $H_r(0) = 8471$.

Table 5.3 shows the best-fitted parameter enclosures results in each iteration for Neiva. In total, we performed 25 iterations for Neiva. We define the stopped criterion considering the width of each interval as smaller or equal to 0.0002.

Table 5.3 – Best fitted results for each iteration from Algorithm 2 for Neiva considering uncertainty in β_m, β_h, μ_m, and γ_h.

Iter	**Obj. function value**	**Parameter vector**			
		β_m	β_h	μ_m	γ_h
1	2267.9390	[0.1515, 0.1710]	[2.4300, 2.6300]	[0.4400, 0.4500]	[1.6500, 1.7500]
2	1663.6236	[0.1515, 0.1710]	[2.4966, 2.5634]	[0.4400, 0.4500]	[1.6500, 1.7500]
3	1453.3555	[0.1515, 0.1710]	[2.4966, 2.5634]	[0.4400, 0.4500]	[1.6833, 1.7167]
4	1273.7758	[0.1515, 0.1710]	[2.5411, 2.5634]	[0.4400, 0.4500]	[1.7167, 1.7500]
5	1209.2094	[0.1515, 0.1710]	[2.5411, 2.5634]	[0.4400, 0.4500]	[1.7277, 1.7389]
6	1150.2161	[0.1515, 0.1710]	[2.5337, 2.5412]	[0.4400, 0.4500]	[1.7055, 1.7167]
7	739.1561	[0.1580, 0.1645]	[2.5262, 2.5338]	[0.4400, 0.4500]	[1.6944, 1.7056]
8	718.7904	[0.1580, 0.1645]	[2.5262, 2.5338]	[0.4400, 0.4500]	[1.6981, 1.7019]
9	606.0115	[0.1580, 0.1645]	[2.5262, 2.5338]	[0.4433, 0.4467]	[1.6981, 1.7019]
10	587.9288	[0.1580, 0.1645]	[2.5287, 2.5313]	[0.4433, 0.4467]	[1.6981, 1.7019]
11	453.9854	[0.1601, 0.1624]	[2.5287, 2.5313]	[0.4433, 0.4467]	[1.6981, 1.7019]
12	446.8474	[0.1601, 0.1624]	[2.5287, 2.5313]	[0.4433, 0.4467]	[1.6981, 1.6994]
13	409.9975	[0.1601, 0.1624]	[2.5287, 2.5313]	[0.4444, 0.4456]	[1.6981, 1.6994]
14	403.9465	[0.1601, 0.1624]	[2.5304, 2.5313]	[0.4444, 0.4456]	[1.6981, 1.6994]
15	359.4694	[0.1608, 0.1617]	[2.5304, 2.5313]	[0.4444, 0.4456]	[1.6981, 1.6994]
16	357.3291	[0.1608, 0.1617]	[2.5304, 2.5313]	[0.4444, 0.4456]	[1.6985, 1.6990]
17	345.0918	[0.1608, 0.1617]	[2.5304, 2.5313]	[0.4448, 0.4452]	[1.6985, 1.6990]
18	343.1475	[0.1608, 0.1617]	[2.5306, 2.5310]	[0.4448, 0.4452]	[1.6985, 1.6990]
19	328.3344	[0.1611, 0.1614]	[2.5306, 2.5310]	[0.4448, 0.4452]	[1.6985, 1.6990]
20	327.6251	[0.1611, 0.1614]	[2.5306, 2.5310]	[0.4448, 0.4452]	[1.6986, 1.6989]
21	323.4286	[0.1611, 0.1614]	[2.5306, 2.5310]	[0.4448, 0.4450]	[1.6988, 1.6990]
22	322.7318	[0.1611, 0.1614]	[2.5306, 2.5308]	[0.4448, 0.4450]	[1.6988, 1.6990]
23	317.7128	[0.1611, 0.1613]	[2.5306, 2.5308]	[0.4448, 0.4450]	[1.6986, 1.6989]
24	317.4508	[0.1611, 0.1613]	[2.5306, 2.5308]	[0.4448, 0.4450]	[1.6986, 1.6988]
25	316.0426	[0.1611, 0.1613]	[2.5306, 2.5308]	[0.4448, 0.4449]	[1.6987, 1.6989]

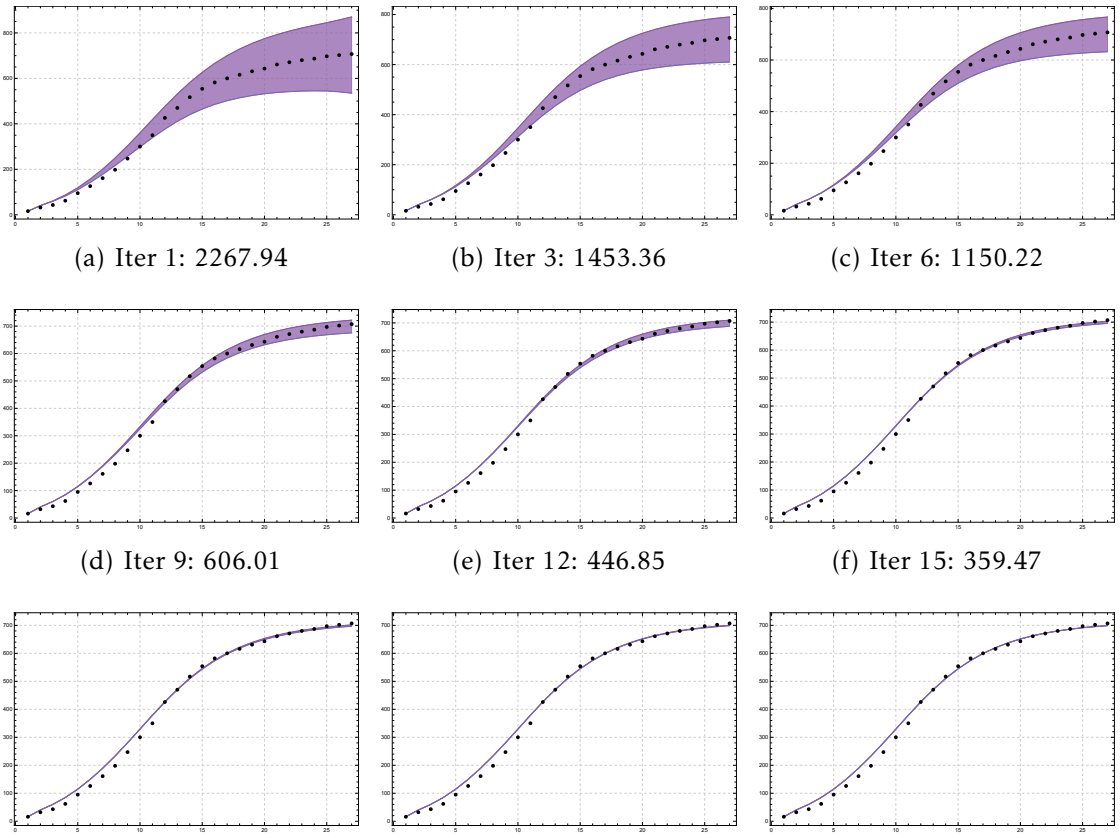

(a) Iter 1: 2267.94 (b) Iter 3: 1453.36 (c) Iter 6: 1150.22

(d) Iter 9: 606.01 (e) Iter 12: 446.85 (f) Iter 15: 359.47

(g) Iter 18: 343.15 (h) Iter 21: 323.43 (i) Iter 24: 317.04

Figure 5.6 – The horizontal axis corresponds to the number of epidemiological weeks, while the vertical axis corresponds to the cumulative number of dengue cases. The Figure shows the enclosures obtained to solve Model 3.3 for Neiva in various iterations. We see how the enclosure's width decreases by reducing the width of the interval parameter.

5.6 Results of compatibility

As we mentioned before, for Model 3.3 we have measurements for one of the variables, H_c. Hence, we calculate the compatibility measure given by Equation (5.8) between the vector Z and the interval data only in two scenarios. First, considering $Z = [\beta_m, \beta_h, \mu_m, \gamma_h]$; and second, considering Z as the vector of initial conditions.

To add noise to the data, we assume that the error follows a uniform distribution $\epsilon = \mathcal{U}[a, b]$. Then we generate synthetic data to evaluate how much the parameter estimation can explain a different number of dengue cases. We consider this a validated scenario since the number of reported cases is not 100% accurate.

5.6.1 Itagüí

For Itagüí, the errors considered were $\epsilon_i = \mathcal{U}[-4, 4i]$, with $i = 1, \ldots, 8$, since the minimum number of reported dengue cases in one epidemiological week during the outbreak that occurred in 2016 was four (see Figure 5.7).

When $Z = [\beta_m, \beta_h, \mu_m, \gamma_h]$, where $\beta_m = [0.1774, 0.1824]$, $\beta_h = [1.7775, 1.8275]$, $\mu_m = [0.2233, 0.2263]$, and $\gamma_h = [1.6979, 1.7079]$. The values used for the other parameters and initial conditions are: $H = 248036$, $\mu_h = 0.00023$, $\theta_m = 0.6$, $\theta_h = 1.3$, $\Lambda = 2500$, $M_s(0) = 1800000$, $M_e(0) = 50$, $M_i(0) = 20$, $H_s(0) = 223000$, $H_e(0) = 21$, $H_i(0) = H_c(0) = 10$, and $H_r(0) = 25005$. Figure 5.8 shows that with our Z, it is possible to explain up to an increase of between 25% and 30% in the number of dengue cases reported in each epidemiological week. This is reflected in the fact that by increasing the number of cases by adding noise in the data, the resulting interval-data is almost contained in the computed enclosure. Additionally, as this enclosure is mathematically and computationally verified, it allowed us to evaluate uncertainty in parameters that have the primary role in

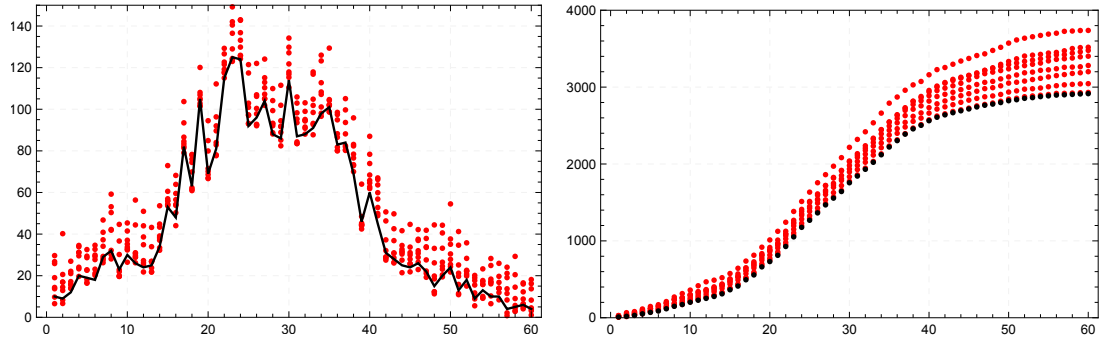

(a) (b)

Figure 5.7 – **Noise in the reported dengue cases for Itagüí.** The horizontal axis corresponds to the number of epidemiological weeks, while the vertical axis corresponds to the cumulative number of dengue cases. The black line in Figure 5.7(a) represents the number of reported dengue cases by the official entities per epidemiological week, while the red points represent eight different noise levels following a uniform distribution $\mathcal{U}[-4, 4i]$, where $i = 1, \ldots, 8$. Figure 5.7(b) shows the cumulative number of dengue cases per epidemiological week. The black line corresponds to the reported by official entities, while each line of red points corresponds to each noise level.

producing new outbreaks.

On the other hand, when $Z = [M_{s_0}, M_{e_0}, M_{i_0}, H_{s_0}, H_{e_0}, H_{i_0}, H_{r_0}, H_{c_0}]$, where $M_{s_0} = [1800000, 1850000]$, $M_{e_0} = [50, 60]$, $M_{i_0} = [40, 50]$, $H_{s_0} = [223000, 235634]$, $H_{e_0} = [21, 42]$, $H_{i_0} = [10, 20]$, $H_{r_0} = [12340, 25005]$, and $H_{c_0} = [10, 20]$. The values used for the other parameters and initial conditions are: $H = 248036$, $\mu_h = 0.00023$, $\theta_m = 0.6$, $\theta_h = 1.3$, $\Lambda = 2500$, $\beta_m = 0.1775$, $\beta_h = 1.7776$, $\mu_m = 0.2262$, and $\gamma_h = 1.7078$. Figure 5.9 shows that when Z is established as above, it is possible to explain an increase of between 35% and 40% in the number of dengue cases reported per epidemiological week. This suggests that considering uncertainty in initial conditions through interval arithmetic is a good way to determine how an outbreak would be in the presence of larger populations.

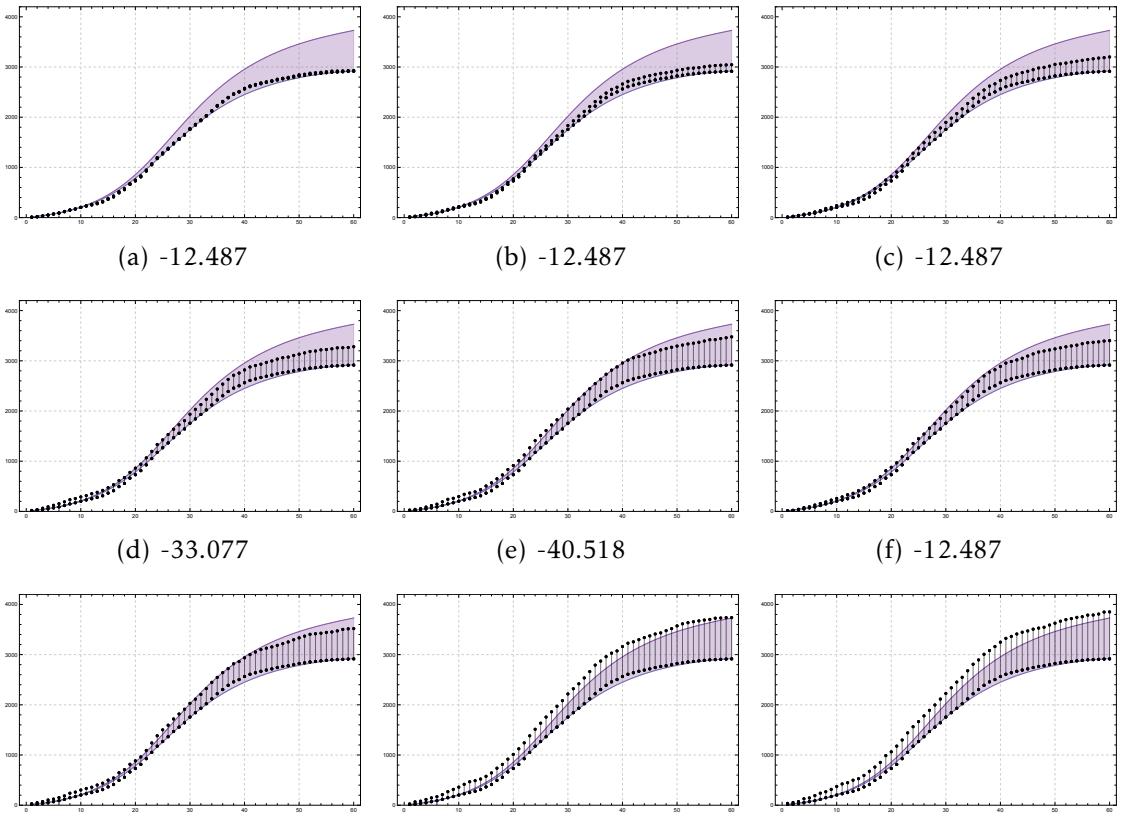

(a) -12.487 (b) -12.487 (c) -12.487

(d) -33.077 (e) -40.518 (f) -12.487

(g) -38.728 (h) -88.069 (i) -95.447

Figure 5.8 – The horizontal axis corresponds to the number of epidemiological weeks, while the vertical axis corresponds to the cumulative number of dengue cases. The figure shows different noise levels adding to data and the enclosure obtained to solve Model 3.3 for Itagüí considering $Z = (\beta_m, \beta_h, \mu_m, \gamma_h)$. These noise levels follow a uniform distribution $\mathcal{U}[-4, 4i]$, where $i = 1, \ldots, 9$. The values below each figure were calculated using the strong compatibility measure given by Equation (5.8).

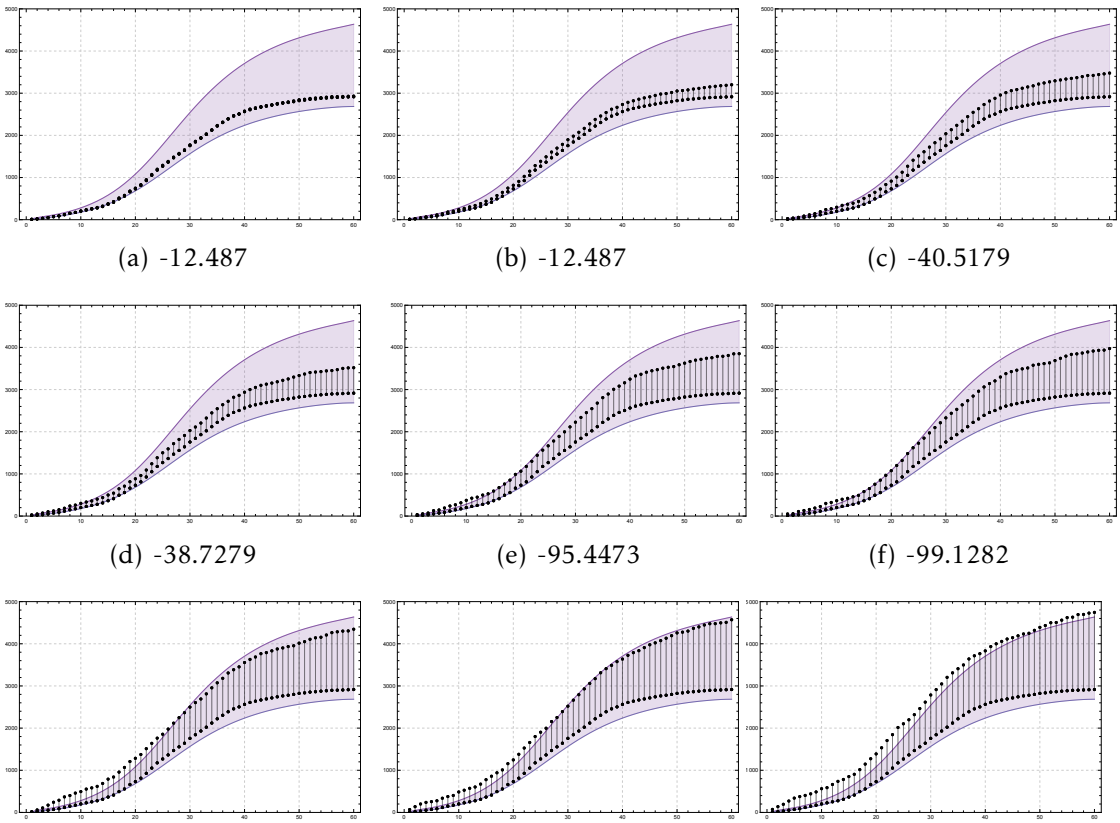

(a) -12.487 (b) -12.487 (c) -40.5179

(d) -38.7279 (e) -95.4473 (f) -99.1282

(g) -243.972 (h) -205.029 (i) -387.562

Figure 5.9 – The horizontal axis corresponds to the number of epidemiological weeks, while the vertical axis corresponds to the cumulative number of dengue cases. The figure shows different noise levels adding to data and the enclosure obtained to solve Model 3.3 for Itagüí considering Z as the vector of initial conditions. These noise levels follow a uniform distribution $\mathcal{U}[-4, 4(2i+1)]$, where $i = 0, \ldots, 8$. The values below each figure were calculated using the compatibility measure given by Equation (5.8).

5.6.2 Neiva

For Neiva, the errors considered were $\epsilon_i = \mathcal{U}[-5, 5i]$, with $i = 1, \ldots, 8$, since the minimum number of reported dengue cases in one epidemiological week during the outbreak that occurred in 2016 was five (see Figure 5.10). When

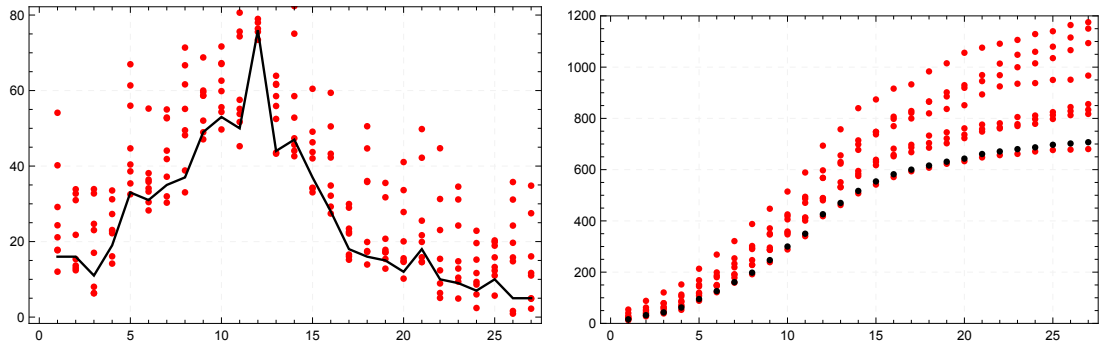

(a) (b)

Figure 5.10 – **Noise in the reported dengue cases for Neiva.** The horizontal axis corresponds to the number of epidemiological weeks, while the vertical axis corresponds to the cumulative number of dengue cases. The black line in Figure 5.10(a) represents the number of reported dengue cases by the official entities per epidemiological week, while the red points represent eight different noise levels following a uniform distribution $\mathcal{U}[-5, i]$, where $i = 5, 10, \ldots, 40$. Figure 5.10(b) shows the cumulative number of dengue cases per epidemiological week. The black line corresponds to the reported by official entities, while each line of red points corresponds to each noise level.

$Z = [\beta_m, \beta_h, \mu_m, \gamma_h]$, where $\beta_m = [0.16, 0.18]$, $\beta_h = [2.53, 2.63]$, $\mu_m = [0.44, 0.45]$, $\gamma_h = [1.6, 1.7]$. The values used for the other parameters and initial conditions for Neiva are: $H = 324466$, $\mu_h = 0.00011$, $\theta_m = 0.8$, $\theta_h = 1.3$, $\Lambda = 24000$, $M_s(0) = 3500000$, $M_e(0) = 80$, $M_i(0) = 25$, $H_s(0) = 315952$, $H_e(0) = 27$, $H_i(0) = H_c(0) = 16$, and $H_r(0) = 8471$. Figure 5.11 shows that when Z is established as above, the interval-data obtained after adding some noise levels is almost included in the computed enclosure. The noise-level that satisfied this condition allows us to

explain an increase of between 25% and 30% in the number of dengue cases reported per epidemiological week.

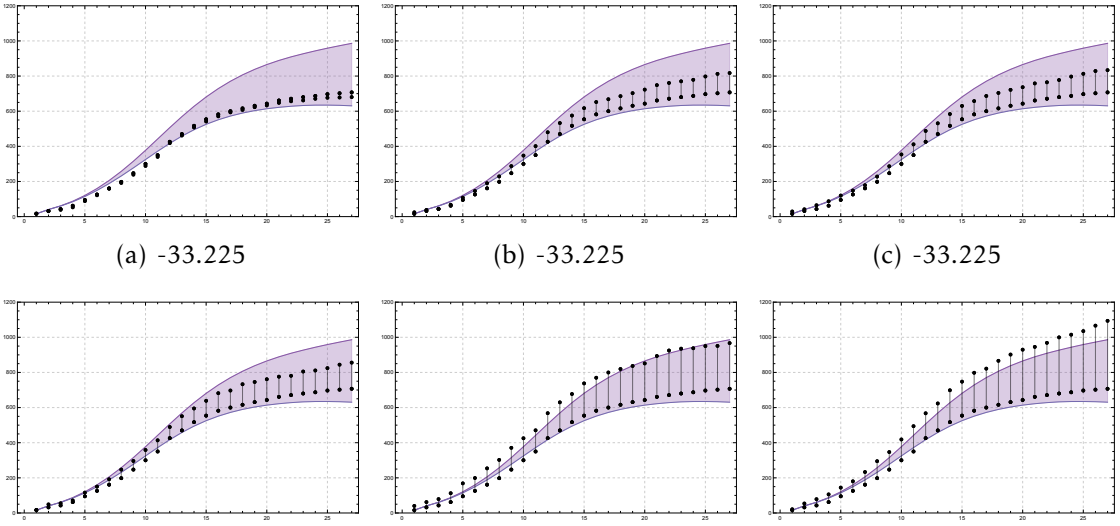

(a) -33.225 (b) -33.225 (c) -33.225

(d) -33.225 (e) -61.446 (f) -107.576

Figure 5.11 – The horizontal axis corresponds to the number of epidemiological weeks, while the vertical axis corresponds to the cumulative number of dengue cases. The figure shows different noise levels adding to data and the enclosure obtained to solve Model 3.3 for Neiva considering $Z = (\beta_m, \beta_h, \mu_m, \gamma_h)$. These noise levels follow a uniform distribution $\mathcal{U}[-5, 5i]$, where $i = 1, \ldots, 6$. The values below each figure were calculated using the compatibility measure given by Equation (5.8).

On the other hand, when $Z = [M_{s_0}, M_{e_0}, M_{i_0}, H_{s_0}, H_{e_0}, H_{i_0}, H_{r_0}, H_{c_0}]$, where $M_{s_0} = [3500000, 4000000]$, $M_{e_0} = [80, 160]$, $M_{i_0} = [25, 50]$, $H_{s_0} = [315952, 324380]$, $H_{e_0} = [27, 54]$, $H_{i_0} = [16, 32]$, $H_{r_0} = [0, 8471]$, and $H_{c_0} = [16, 32]$. The values used for the other parameters are: $H = 324466$, $\mu_h = 0.00011$, $\theta_m = 0.8$, $\theta_h = 1.3$, $\Lambda = 24000$, $\beta_m = 0.18$, $\beta_h = 2.63$, $\mu_m = 0.45$, and $\gamma_h = 1.7$. Figure 5.9 shows that when Z is set as above, it is possible to explain an increase of between 40% and 45% in the number of reported dengue cases per epidemiological week in Neiva. This suggests that considering uncertainty in initial conditions through interval arithmetic is an effective way to evaluate how an outbreak would be in

the presence of larger populations.

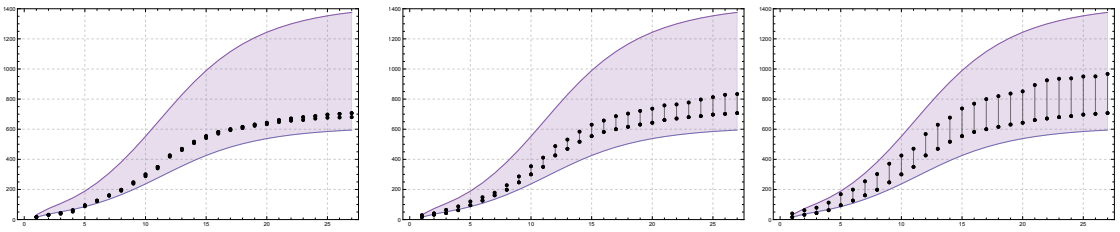

(a) -8.3764 (b) -8.3764 (c) -8.3764

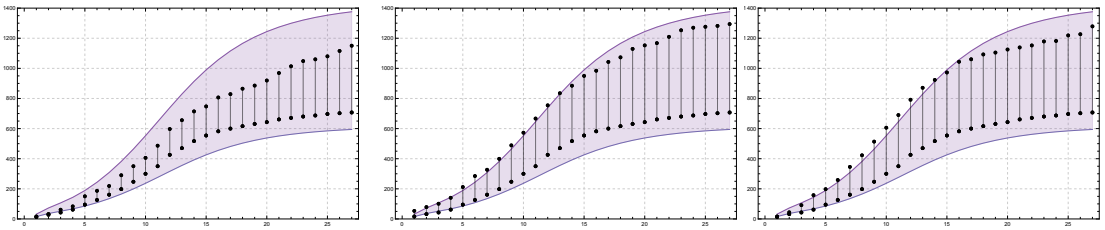

(d) -8.3764 (e) -41.2519 (f) -53.321

Figure 5.12 – The horizontal axis corresponds to the number of epidemiological weeks, while the vertical axis corresponds to the cumulative number of dengue cases. The figure shows different noise levels adding to data and the enclosure obtained to solve Model 3.3 for Neiva considering Z as the vector of initial conditions. These noise levels follow a uniform distribution $\mathcal{U}[-5, 5(2i+1)]$, where $i = 0, \ldots, 5$. The values below each figure were calculated using the compatibility measure given by Equation (5.8).

5.7 Discussion and conclusions

This chapter introduced the algorithm PISA (Parameter Interval Search Algorithm) to solve the guaranteed parameter estimation problem given by Equation (5.1) when the model parameters are real closed intervals. Additionally, to consider uncertainty in the number of reported dengue cases, we provided an original method to determine the compatibility or the strong compatibility between the data and the vector of uncertain quantities.

Previous studies have resolved the guaranteed parameter estimation prob-

lem mainly through two strategies: bounded-error and optimal estimation. In bounded error estimation, the purpose is to find all the parameter vectors compatible with the data, which satisfied an error established by the modeler. In optimal estimation, the purpose is to find all the parameter vectors that minimize a cost function that measures the error between the data and the model output [47].

In this thesis, we focused on optimal estimation. In this direction, the most widely used scheme of interval-based global optimization methods is the branch–and–bound (B&B) technique [75]. Usually these algorithms assume that it is possible to construct and then evaluate an inclusion function of the cost function and its gradient [39]. This strategy is easy to follow when a closed-form expression for the model output is available. However, for our case study, such a closed form does not exist; this makes particularly challenging to obtain those inclusion functions. Under this condition, previous studies have exploited the features of the dynamical system. For instance, in [107], those authors propose a strategy for cooperative dynamical models, while in [47] applied the Müller theorem to bound the solutions for more general dynamical systems. Others proposed to extend the state-space model by considering the first-order sensitivity equations [51]. Then, to obtain the enclosure for the gradient, one has to use one of the guaranteed ODE solvers provided by Interval Analysis, e.g., AWA, COSY, VNODE, or VSPODE [52, 72]. However, increasing the dimensionality of the state-variables space is not recommendable since the guaranteed solvers' performance depends heavily on the number of variables [71].

Model 3.3 is not cooperative, and considering the sensitivity equations duplicate the state variable space dimension for one uncertain parameter. So, we took advantage of our dynamic system's mathematical and epidemiological features. The definition of filters, directions, and elimination criterion reflected the understanding of the case study. We implemented the algorithm in MATHEMATICA

software, and it was necessary to construct a connection between the VSPODE, which is in C++, and MATHEMATICA to make it simpler to use.

The interval parameters estimated by PISA produce for both Itagüí and Neiva an R_0 value less than one. As we show in the next chapter, for this R_0 value, there is only an equilibrium point for the model, the diseases-free point, which is globally asymptotic stable. Nevertheless, the diseases-free point may emerge in three situations: (i) when $R_{0_M} < 1$ and $R_{0_H} < 1$; (ii) when $R_{0_M} > 1$ and $R_{0_H} < 1$; and (iii) when $R_{0_M} < 1$ and $R_{0_H} > 1$, since R_0 is a geometric mean between the secondary infections in humans and mosquitoes. However, as the reported dengue cases in humans exhibit an exponential behavior in the early weeks, we assume that $R_{0_H} \geq 1$. In this way, to discard non-informative regions, we computed the value of R_{0_H}. Moreover, since we cannot calculate the gradient of our system as a monotonicity criterion to explore the parameter space, we considered the direction in which the most sensitive parameters increase the R_0 values (see Algorithm 1).

Finally, the stability of the disease-free point ensures us that admitted uncertainty in the initial conditions does not change the asymptotic behavior of the model solutions. In this way, we were able to estimate robust solutions for Model 3.3 that simulated dengue transmission disease in different regions of Colombia.

Bibliography of the current chapter

[4] Richard C Aster, Brian Borchers, and Clifford H Thurber. Parameter estimation and inverse problems. Elsevier, 2018 (cit. on pp. 7, 119).

[39] Eldon Hansen and G William Walster. Global optimization using interval analysis: revised and expanded. Vol. 264. CRC Press, 2003 (cit. on pp. 7, 143).

[47] Michel Kieffer and Eric Walter. Guaranteed estimation of the parameters of nonlinear continuous-time models: Contributions of interval analysis. International Journal of Adaptive Control and Signal Processing 25.3 (2011), pp. 191–207 (cit. on pp. 8, 143).

[51] Youdong Lin and Mark A. Stadtherr. Deterministic Global Optimization for Parameter Estimation of Dynamic Systems. Industrial & Engineering Chemistry Research 45.25 (Dec. 2006), pp. 8438–8448. DOI: 10.1021/ie0513907 (cit. on p. 143).

[52] Youdong Lin and Mark A. Stadtherr. Validated solutions of initial value problems for parametric ODEs. Applied Numerical Mathematics 57.10 (2007), pp. 1145–1162. DOI: https://doi.org/10.1016/j.apnum.2006.10.006 (cit. on pp. 4, 6, 11, 92, 117, 118, 143).

[54] Diana Paola Lizarralde-Bejarano, Daniel Rojas-Díaz, Sair Arboleda-Sánchez, and María Eugenia Puerta-Yepes. Sensitivity, uncertainty and identifiability analyses to define a dengue transmission model with real data of an endemic municipality of Colombia. PLoS ONE 15.3 (2020), e0229668. DOI: https://doi.org/10.1371/journal.pone.0229668 (cit. on pp. 58, 81, 131, 162).

[71] Nedialko S Nedialkov. Interval tools for ODEs and DAEs. In: 12th GAMM-IMACS International Symposium on Scientific Computing, Computer Arithmetic and Validated Numerics (SCAN 2006). IEEE. 2006, pp. 4–4 (cit. on pp. 143, 169).

[72] Nedialko S Nedialkov, Kenneth R Jackson, and George F Corliss. Validated solutions of initial value problems for ordinary differential equations. Applied Mathematics and Computation 105.1 (1999), pp. 21–68 (cit. on pp. 6, 35, 90, 93, 110, 143).

[75] Arnold Neumaier. Complete search in continuous global optimization and constraint satisfaction. Acta Numerica 13 (May 2004), pp. 271–369. DOI: 10.1017/s0962492904000194 (cit. on p. 143).

[96] Sergey P Shary. Weak and strong compatibility in data fitting problems under interval uncertainty. Advances in data science and adaptive analysis 12.1 (2020), p. 2050002 (cit. on pp. 117, 124).

[107] Éric Walter and Michel Kieffer. Guaranteed nonlinear parameter estimation in knowledge-based models. Journal of Computational and Applied Mathematics 199.2 (Feb. 2007), pp. 277–285. DOI: 10.1016/j.cam.2005.07.039 (cit. on p. 143).

Chapter 6

Stability analysis

Outline of the current chapter

6.1 Abstract

This chapter presents the necessary theory and a methodology to construct polynomial Lyapunov functions. It is known the existence of these kinds of functions for exponentially stable systems on bounded regions. The local and global stability of equilibrium points will be shown by proving that two matrices are positive definite.

To illustrate how this approach works, we consider Model 3.3, which has two equilibrium states, the disease-free point and the endemic point. The presence and stability conditions of each of these depend on the R_0 value. In this research, it is relevant to perform the stability analysis of each point to establish the uncertainty levels that may be included in parameters and initial conditions. Thus, the local, global, and asymptotic behavior of the model solutions do not change.

Additionally, to explicitly consider the dependence among the Lyapunov functions' coefficients and the model parameter values, we computed these functions for Itagüí and Neiva. To do so, first we considering values in the interval parameters estimated with PISA (see Chapter 5). Second, we examine the estimated region considering the R_0 values. This analysis allows us to conclude that for Itagüí and Neiva exists a unique equilibrium point in the estimated region, the disease-free point. Moreover, the Lyapunov function proved the global stability of this point in such a region.

6.2 Problem statement

The vector field of the epidemiological model given by Model 3.3 is polynomial up to degree two or rational functions when populations change with time. Moreover, the R_0 value gives us information about which equilibrium point is present, the diseases-free point, or the endemic point.

We want to prove the stability of these points by constructing a Lyapunov function (see Theorem 1.5.1). We will also evaluate the behavior of this function for the interval parameters, which allows us to simulate the outbreaks in 2016 for Itagüí and Neiva.

However, there is no clear strategy for constructing such functions. In this direction, several authors have proposed different strategies considering the

aspects of the system. For instance, in mathematical epidemiology, the most traditional Lyapunov functions are the common quadratic and Volterra-type functions

- $\mathcal{V}(x_1, x_2, \cdots, x_n) = \sum_{i=1}^{n} c_i (x_i - x_i^*)^2$
- $\mathcal{V}(x_1, x_2, \cdots, x_n) = c \left[\sum_{i=1}^{n} (x_i - x_i^*) \right]^2$
- $\mathcal{V}(x_1, x_2, \cdots, x_n) = \sum_{i=1}^{n} c_i (x_i - x_i^* - x_i^* \ln \frac{x_i}{x_i^*})$.

The quadratic functions are used to prove the disease-free point's global stability while the Volterra-type functions are used to prove the global stability of the endemic point [37, 36, 105, 48]. Meanwhile, in [97] the authors use a method based on graph theory to construct Lyapunov functions to prove the global stability of the endemic point. Nevertheless, one of the biggest obstacles to construct these functions is to find the coefficients c_i in a systematic way. For instance, to avoid calculating these coefficients in [50] the matrix theory of Volterra-Lyapunov is applied to carry out the stability analysis of models of order three and four.

On the other hand, over the past decades, different techniques to construct systematically and efficiently polynomial Lyapunov functions for certain kinds of systems in the convex optimization framework have been proposed [34]. From these approaches, it is natural to examine what conditions must satisfy the ODEs to guarantee the existence of a polynomial Lyapunov function. In this direction, in [85], the author proves the existence of a polynomial Lyapunov function for bounded and exponentially stable systems. From this result, we can reduce the search space of Lyapunov functions to polynomial functions.

Next, we had to figure out a criterion to determine if a polynomial function is non-negative. This is a NP-Hard problem even for four-degree polynomials [83]. However, to make this problem treatable, in [84], the author proposes to search

polynomial Lyapunov functions that can be decomposed as a sum of squares. Here, we follow the above mentioned strategy.

6.3 Materials and methods

We considered a polynomial system of differential equations $\dot{x} = f(x)$ where the equilibrium point is $x^* = 0$. If $x^* \neq 0$, we define the transformation $y = x - x^*$ and work with the system $\dot{y} = g(y) = f(y + x^*)$, which has equilibrium point at the origin.

6.3.1 Framework to construct polynomial Lyapunov function

The main result of [85] guarantees the existence of Lyapunov polynomial functions for polynomial systems that are exponentially stable on bounded regions. In particular, for polynomial systems, the exponentially stable vector field in each equilibrium point is satisfied if it is $n+2$-times continuously differentiable. We first proved that Model 3.3 is exponentially stable. To do this, we proved that the linearization of this model around each equilibrium point is a Hurwitz matrix[1].

Now, we can begin the search of a polynomial Lyapunov function for Model 3.3. For these functions, the conditions of the Lyapunov's theorem are reduced to prove if a polynomial is non-negative. This is an NP-Hard problem even for polynomials of degree four [83]. However, to make this problem computationally tractable, the author in [84] proposes to look for Lyapunov functions that can be decomposed as a sum of squares.

This approach is followed here. To do this, we introduce the definitions and results needed, mainly from [83, 84].

Definition 6.3.1. A multivariate polynomial $p(x) := p(x_1, \ldots, x_n)$ is a sum of

[1] A matrix A is *Hurwitz* if all its eigenvalues have real part smaller than zero, $Re(\lambda) < 0$.

squares, if there exist polynomials $q_1(x),\ldots,q_m(x)$ such that

$$p(x) = \sum_{i=1}^{m} q_i^2(x) \tag{6.1}$$

Theorem 6.3.1. *[83, 84] A multivariate polynomial $p(x)$ in n variables, and of degree $2d$ is a sum of squares if and only if there exists a positive semi-definite matrix Q such that*

$$p(x) = z^T Q z, \quad with, \quad z = [1, x_1, x_2, \ldots, x_n, x_1 x_2, \ldots, x_n^d] \tag{6.2}$$

where z is the vector of monomials of degree up to d.

The search of the matrix Q can be seen as a semi-definite program without objective function, i.e. a feasible problem that must satisfy the conditions given by the previous theorem.

In summary, to construct a polynomial Lyapunov function as a sum of squares, we follow the below mentioned steps

1. We define the even degree of the polynomial Lyapunov function ($2d$).

2. We propose a vector of monomials z, of degree up to d. This z depends on the state variables of the model.

3. We express the Lyapunov function and its orbital derivative as quadratic forms, $\mathcal{V}(x) = z^T P z$ and $\dot{\mathcal{V}}(x) = -w^T Q w$, respectively. To verify that $\mathcal{V}$ is a Lyapunov function, we have to prove that P and Q are definite positive matrices.

To check that P and Q are definite positive matrices, we apply the *Sylvester's criterion*[2], consider the biological region defined for each municipality (see Table 3.1), and the R_0^2 value.

[2] A real-symmetric matrix Q is positive definite if and only if all the leading principal minors of Q are positive.

6.4 Results

To analyze the local and global stability of Model 3.3, we first reduce the number of equations and parameters, and normalize the populations of mosquitoes and humans

$$m_s = \frac{\mu_m}{\Lambda} Ms, \quad m_e = \frac{\mu_m}{\Lambda} Me, \quad m_i = \frac{\mu_m}{\Lambda} Mi, \quad h_s = \frac{H_s}{H}, \quad h_i = \frac{H_i}{H}, \quad \text{and } h_r = \frac{H_r}{H}$$

Moreover, we consider that $m_s = 1 - m_e - m_i$, i.e. the mosquito population is constant in an equilibrium state, and $h_r = 1 - h_s - h_e - h_i$. Then, the system given in Model 3.3 is equivalent to a non-linear system of five differential equations

$$\begin{aligned}
\frac{dm_e}{dt} &= \beta_m h_i(1 - m_e - m_i) - (\theta_m + \mu_m)m_e \\
\frac{dm_i}{dt} &= \theta_m m_e - \mu_m m_i \\
\frac{dh_s}{dt} &= \mu_h - \beta_h m_i h_s - \mu_h h_s \\
\frac{dh_e}{dt} &= \beta_h m_i h_s - (\theta_h + \mu_h)h_e \\
\frac{dh_i}{dt} &= \theta_h h_e - (\gamma_h + \mu_h)h_i
\end{aligned} \tag{6.3}$$

The equilibrium points of Equation (6.3) are the disease-free states $P_0 = (0, 0, 1, 0, 0)$, in which there is no population of exposed or infected mosquitoes and the entire human population is considered susceptible, and the endemic equilibrium $P_1 = (\hat{m}_e, \hat{m}_i, \hat{h}_s, \hat{h}_e, \hat{h}_i)$, where

$$\begin{aligned}
\hat{m}_e &= \frac{\beta_m \mu_m \hat{h}_i}{(\theta_m + \mu_m)(\beta_m \hat{h}_i + \mu_m)} \\
\hat{m}_i &= \frac{\beta_m \theta_m \hat{h}_i}{(\beta_m \hat{h}_i + \mu_m)\mu_m(\theta_m + \mu_m)} \\
\hat{h}_s &= \frac{\mu_h(\theta_m + \mu_m)(\mu_m + \beta_m \hat{h}_i)}{\beta_h \beta_m \theta_m \hat{h}_i + \mu_h(\theta_m + \mu_m)(\mu_m + \beta_m \hat{h}_i)} \\
\hat{h}_e &= \frac{(\gamma_h + \mu_h)}{\theta_h} \hat{h}_i
\end{aligned} \tag{6.4}$$

where

$$\hat{h}_i = \frac{\mu_h \mu_m (\theta_m + \mu_m)}{\beta_m \beta_h \theta_m + \mu_h \beta_m (\theta_m + \mu_m)} (R_0^2 - 1)$$

with R_0 given by Equation (3.11).

Theorem 6.4.1. *The Jacobian matrix around each equilibrium point of the polynomial system in Equation (6.3) is a Hurwitz matrix.*

Proof. The Jacobian matrix at any point $P = (m_e, m_i, h_s, h_e, h_i)$ is given by

$$J = \begin{bmatrix} -\beta_m h_i - (\theta_m + \mu_m) & -\beta_m h_i & 0 & 0 & \beta_m(1 - m_e - m_i) & \\ \theta_m & -\mu_m & 0 & 0 & 0 & \\ 0 & -\beta_h h_s & -\beta_h m_i - \mu_h & 0 & 0 & \\ 0 & \beta_h h_s & \beta_h m_i & -(\theta_h + \mu_h) & 0 & \\ 0 & 0 & 0 & 0 & \theta_h & -(\gamma_h + \mu_h) \end{bmatrix}$$

At $P_0 = (0, 0, 1, 0, 0)$, the characteristic equation is $p_0(\lambda) = -(\lambda + \mu_h) q_0(\lambda)$, where $q_0(\lambda) = \lambda^4 + a_3\lambda^3 + a_2\lambda^2 + a_1\lambda + a_0$, with

$$a_3 = (\gamma_h + \mu_h) + (\theta_h + \mu_h) + (\theta_m + \mu_m) + \mu_m$$

$$a_2 = (\gamma_h + \mu_h)(\theta_h + \mu_h) + ((\gamma_h + \mu_h) + (\theta_h + \mu_h))((\theta_m + \mu_m) + \mu_m) + (\theta_m + \mu_m)\mu_m)$$

$$a_1 = (\gamma_h + \mu_h)(\theta_h + \mu_h)((\theta_m + \mu_m) + \mu_m) + ((\gamma_h + \mu_h) + (\theta_h + \mu_h))(\theta_m + \mu_m)\mu_m$$

$$a_0 = (\gamma_h + \mu_h)(\theta_h + \mu_h)(\theta_m + \mu_m)\mu_m[1 - R_0^2]$$

The condition in which the real parts of the eigenvalues are negative is equivalent to that in which the coefficients of q_0 satisfy the Routh-Hurwitz criterion for a polynomial of degree four, namely, $a_3 > 0$, $a_1 > 0$, $a_0 > 0$, and $a_1 a_2 a_3 > a_1^2 + a_0 a_3^2$ [24]. After several calculations, we can see that these conditions are fulfilled for $R_0^2 < 1$. Hence, the matrix $J(P_0)$ is Hurwitz.

At $P_1 = (\hat{m_e}, \hat{m_i}, \hat{h_s}, \hat{h_e}, \hat{h_i})$, the characteristic equation $p_1(\lambda) = -\lambda^5 - b_4\lambda^4 -$

$b_3\lambda^3 - b_2\lambda^2 - b_1\lambda - b_0$, with

$$
\begin{aligned}
b_4 &= \beta_m\hat{h}_i + \theta_m + 2\mu_m + w_1\\
b_3 &= (\theta_m + \mu_m)(\beta_m\hat{h}_i + \mu_m) + w_1(\beta_m\hat{h}_i + \theta_m + 2\mu_m) + w_2\\
b_2 &= w_1(\theta_m + \mu_m)(\beta_m\hat{h}_i + \mu_m) + w_2(\beta_m\hat{h}_i + \theta_m + 2\mu_m) + w_3\\
b_1 &= w_2(\theta_m + \mu_m)(\beta_m\hat{h}_i + \mu_m) + w_3(\beta_m\hat{h}_i + \theta_m + 2\mu_m) + \beta_m\beta_h\theta_m\theta_h(1 - \hat{m}_e - \hat{m}_i)\hat{h}_s\\
b_0 &= (\theta_m + \mu_m)(\beta_m\hat{h}_i + \mu_m) + \beta_m\beta_h\theta_m\theta_h\mu_h(1 - \hat{m}_e - \hat{m}_i)\hat{h}_s
\end{aligned}
$$

where

$$
\begin{aligned}
w_1 &= \beta_h\hat{m}_i + \mu_h + (\theta_h + \mu_h) + (\gamma_h + \mu_h)\\
w_2 &= (\beta_h\hat{m}_i + \mu_h)((\theta_h + \mu_h) + (\gamma_h + \mu_h)) + (\theta_h + \mu_h)(\gamma_h + \mu_h)\\
w_3 &= (\beta_h\hat{m}_i + \mu_h)(\theta_h + \mu_h)(\gamma_h + \mu_h)
\end{aligned}
$$

In this case, we apply the Routh-Hurwitz criterion for a polynomial of degree five. After several calculations, we prove that these conditions are fulfilled for $R_0^2 > 1$. Hence, the matrix $J(P_1)$ is Hurwitz.

□

Theorem 6.4.2. *When $R_0 \leq 1$, the diseases free-point $P_0 = (0, 0, 1, 0, 0)$ is globally asymptotically stable.*

Proof. We move the disease-free point P_0 to the origin. The system in Equation (6.3) becomes

$$
\begin{aligned}
\frac{dx_1}{dt} &= \beta_m x_5 - \beta_m x_1 x_5 - \beta_m x_2 x_5 - (\theta_m + \mu_m)x_1\\
\frac{dx_2}{dt} &= \theta_m x_1 - \mu_m x_2\\
\frac{dx_3}{dt} &= -\beta_h x_2 - \beta_h x_2 x_3 - \mu_h x_3\\
\frac{dx_4}{dt} &= \beta_h x_2 x_3 + \beta_h x_2 - (\theta_h + \mu_h)x_4\\
\frac{dx_5}{dt} &= \theta_h x_4 - (\gamma_h + \mu_h)x_5
\end{aligned}
\tag{6.5}
$$

where $x_1 = m_e$, $x_2 = m_i$, $x_3 = h_s - 1$, $x_4 = h_e$, and $x_5 = h_i$. With $0 \leq x_1, x_2, x_4, x_5 \leq 1$ and $-1 \leq x_3 \leq 0$. To look for a Lyapunov function $\mathcal{V}$, we will use the general expression of a polynomial in x_1, x_2, x_3, x_4 and x_5 of degree two with no constant or linear terms (because $\mathcal{V}(0) = 0$, and $\mathcal{V}$ has to be positive definite). We use a matrix representation for clarity.

$$\mathcal{V}(x) = \begin{bmatrix} x_1 \\ x_2 \\ x_3 \\ x_4 \\ x_5 \end{bmatrix}^T \begin{bmatrix} p_{11} & p_{12} & p_{13} & p_{14} & p_{15} \\ p_{12} & p_{22} & p_{23} & p_{24} & p_{25} \\ p_{13} & p_{23} & p_{33} & p_{34} & p_{35} \\ p_{14} & p_{24} & p_{34} & p_{44} & p_{45} \\ p_{15} & p_{25} & p_{35} & p_{45} & p_{55} \end{bmatrix} \begin{bmatrix} x_1 \\ x_2 \\ x_3 \\ x_4 \\ x_5 \end{bmatrix} \tag{6.6}$$

For the orbital derivative $\dot{\mathcal{V}} = \langle \nabla \mathcal{V}, \dot{\mathbf{x}} \rangle$, from Equations (6.5) and (6.6) we have

$$\begin{aligned}
\dot{\mathcal{V}}(x) = -2[&(p_{11}(\theta_m + \mu_m) + p_{12}\theta_m)x_1^2 \\
&+ (p_{12}((\theta_m + \mu_m) + \mu_m) + p_{13}\beta_h - p_{14}\beta_h - p_{22}\theta_m)x_1x_2 \\
&+ (p_{13}((\theta_m + \mu_m) + \mu_h) - p_{23}\theta_m)x_1x_3 \\
&+ (p_{14}((\theta_m + \mu_m) + (\theta_h + \mu_h)) - p_{15}\theta h - p_{24}\theta_m)x_1x_4 \\
&+ (p_{15}((\theta_m + \mu_m) + (\gamma_h + \mu_h)) - p_{11}\beta_m - p_{25}\theta_m)x_1x_5 \\
&+ (p_{23}\beta_h - p_{24}\beta_h + p_{22}\mu_m)x_2^2 + p_{33}\mu_h x_3^2 \\
&+ (p_{33}\beta_h - p_{34}\beta_h + p_{23}(\mu_m + \mu_h))x_2x_3 + p_{15}\beta_m x_1x_5^2 \\
&+ (p_{24}((\theta_h + \mu_h) + \mu_m) + p_{34}\beta_h - p_{44}\beta_h)x_2x_4 \\
&+ (p_{25}((\gamma_h + \mu_h) + \mu_m) - p_{12}\beta_m + p_{35}\beta_h - p_{45}\beta_h)x_2x_5 \\
&+ (p_{34}((\theta_h + \mu_h) + \mu_h) - p_{35}\theta_h)x_3x_4 + p_{15}\beta_m x_2x_5^2 \\
&+ (p_{35}((\gamma_h + \mu_h) + \mu_h) - p_{13}\beta_m)x_3x_5 + p_{13}\beta_m x_1x_3x_5 \\
&+ (p_{44}(\theta_h + \mu_h) - p_{45}\theta_h)x_4^2 + (p_{13}\beta_h - p_{14}\beta_h)x_1x_2x_3 \\
&+ (p_{45}((\theta_h + \mu_h) + (\gamma_h + \mu_h)) - p_{14}\beta_m - p_{55}\theta_h)x_4x_5
\end{aligned}$$

$$
\begin{aligned}
&+ (p_{55}(\gamma_h + \mu_h) - p_{15}\beta_m)x_5^2 + p_{11}\beta_m x_1^2 x_5 + p_{12}\beta_m x_2^2 x_5 \\
&+ (p_{11}\beta_m + p_{12}\beta_m)x_1 x_2 x_5 + p_{14}\beta_m x_1 x_4 x_5 + p_{14}\beta_m x_2 x_4 x_5 \\
&+ (p_{13}\beta_m + p_{35}\beta_h - p_{45}\beta_h)x_2 x_3 x_5 + (p_{34}\beta_h + p_{44}\beta_h)x_2 x_3 x_4 \\
&+ (p_{33}\beta_h - p_{34}\beta_h)x_2 x_3^2 + (p_{23}\beta_h - p_{24}\beta_h)x_2^2 x_3]
\end{aligned}
$$

We obtain after some algebra that $\dot{\mathcal{V}} = -w^T Q w$, where

$$
w^T = [x_1 \ x_2 \ x_3 \ x_4 \ x_5 \ x_1 x_5 \ x_2 x_3 \ x_2 x_5],
$$

and Q as in Equation (6.7). □

Theorem 6.4.3. *When $R_0 > 1$, the endemic point $E_1 = (\hat{m}_e, \hat{m}_i, \hat{h_s}, \hat{h_e}, \hat{h_i})$ is globally asymptotically stable.*

Proof. To prove this, first we move the endemic equilibrium point P_1 to the origin so that the system in Equation (6.3) becomes

$$
\begin{aligned}
\frac{dx_1}{dt} &= -(\beta_m \hat{h}_i + (\theta_m + \mu_m))x_1 - \beta_m x_1 x_5 - \beta_m x_2 x_5 - \beta_m \hat{h}_i x_2 \\
&\quad + \beta_m(1 - \hat{m}_e - \hat{m}_i)x_5 \\
\frac{dx_2}{dt} &= \theta_m x_1 - \mu_m x_2 \\
\frac{dx_3}{dt} &= -\beta_h \hat{h}_s x_2 - \beta_h x_2 x_3 - (\beta_h \hat{m}_i + \mu_h)x_3 \\
\frac{dx_4}{dt} &= \beta_h x_2 x_3 + \beta_h \hat{h}_s x_2 + \beta_h \hat{m}_i x_3 - (\theta_h + \mu_h)x_4 \\
\frac{dx_5}{dt} &= \theta_h x_4 - (\gamma_h + \mu_h)x_5
\end{aligned}
\tag{6.8}
$$

where $x_1 = m_e - \hat{m}_e$, $x_2 = m_i - \hat{m}_i$, $x_3 = h_s - \hat{h}_s$, $x_4 = h_e - \hat{h}_e$, and $x_5 = h_i - \hat{h}_i$. Similarly, to look for a Lyapunov function, we will use the general expression in Equation (6.6). In this case the orbital derivative is given by:

$$
\dot{\mathcal{V}}(x) = -2[(p_{11}(\beta_m \hat{h}_i + (\theta_m + \mu_m)) - p_{12}\theta_m)x_1^2
$$

$$Q = \begin{bmatrix} 2p_{11}(\theta_m+\mu_m)+p_{12}\theta_m & p_{12}K_1+(p_{13}-p_{14})\beta_h-p_{22}\theta_m & p_{13}K_2-p_{13}\theta_m & p_{14}K_3-p_{15}\theta_h-p_{24}\theta_m & p_{15}K_4-p_{11}\beta_m-p_{25}\theta_m & p_{11}\beta_m & (p_{13}-p_{14})\beta_h & (p_{11}+p_{12})\beta_m \\ p_{12}K_1+(p_{13}-p_{14})\beta_h-p_{22}\theta_m & 2(p_{23}-p_{24})\beta_h+p_{22}\mu_m & (p_{33}-p_{34})\beta_h+p_{23}(\mu_m+\mu_h) & p_{24}K_5+(p_{34}-p_{44})\beta_h & p_{25}K_6+(p_{35}-p_{12}-p_{45})\beta_h & (p_{11}+p_{12})\beta_m & (p_{23}-p_{24})\beta_h & p_{12}\beta_m \\ p_{13}K_2-p_{13}\theta_m & (p_{33}-p_{34})\beta_h+p_{23}(\mu_m+\mu_h) & 2p_{33}\mu_h & p_{34}K_7-p_{35}\theta_h & p_{35}K_8-p_{13}\beta_m & p_{13}\beta_m & (p_{33}-p_{34})\beta_h & (p_{13}\beta_m+(p_{35}-p_{45})\beta_h) \\ p_{14}K_3-p_{15}\theta_h-p_{24}\theta_m & p_{24}K_5+(p_{34}-p_{44})\beta_h & p_{34}K_7-p_{35}\theta_h & 2p_{44}(\theta_h+\mu_h)-p_{45}\theta_h & p_{45}K_9-p_{14}\beta_m-p_{55}\theta_h & p_{14}\beta_m & (p_{34}+p_{44})\beta_h & p_{14}\beta_m \\ p_{15}K_4-p_{11}\beta_m-p_{25}\theta_m & p_{25}K_6+(p_{35}-p_{12}-p_{45})\beta_h & p_{35}K_8-p_{13}\beta_m & p_{45}K_9-p_{14}\beta_m-p_{55}\theta_h & 2(p_{55}(\gamma_h+\mu_h)-p_{15}\beta_m) & p_{15}\beta_m & p_{13}\beta_m+(p_{35}-p_{45})\beta_h & p_{15}\beta_m \\ p_{11}\beta_m & 0 & p_{13}\beta_m & p_{14}\beta_m & p_{15}\beta_m & 0 & 0 & 0 \\ (p_{13}-p_{14})\beta_h & (p_{23}-p_{24})\beta_h & (p_{33}-p_{34})\beta_h & (p_{34}+p_{44})\beta_h & p_{13}\beta_m+(p_{35}-p_{45})\beta_h & 0 & 0 & 0 \\ (p_{11}+p_{12})\beta_m & p_{12}\beta_m & (p_{13}\beta_m+(p_{35}-p_{45})\beta_h) & p_{14}\beta_m & p_{15}\beta_m & 0 & 0 & 0 \end{bmatrix} \tag{6.7}$$

where

$$\begin{aligned} K_1 &= (\theta_m+\mu_m)+\mu_m \\ K_2 &= (\theta_m+\mu_m)+\mu_h \\ K_3 &= (\theta_m+\mu_m)+(\theta_h+\mu_h) \\ K_4 &= (\theta_m+\mu_m)+(\gamma_h+\mu_h) \\ K_5 &= (\theta_h+\mu_h)+\mu_m \\ K_6 &= (\gamma_h+\mu_h)+\mu_m \\ K_7 &= (\theta_h+\mu_h)+\mu_h \\ K_8 &= (\gamma_h+\mu_h)+\mu_h \\ K_9 &= (\theta_h+\mu_h)+(\gamma_h+\mu_h) \end{aligned}$$

$$
\begin{aligned}
&+ (p_{11}\beta_m\hat{h}_i + p_{12}((\theta_m+\mu_m)+\mu_m+\beta_m\hat{h}_i) + \beta_h\hat{h}_s(p_{13}-p_{14}) - p_{22}\theta_m)x_1x_2\\
&+ (p_{13}((\theta_m+\mu_m)+\beta_m\hat{h}_i+\beta_m\hat{m}_i+\mu_h) - p_{14}\beta_h\hat{m}_i - p_{23}\theta_m)x_1x_3\\
&+ (p_{14}((\theta_m+\mu_m)+(\theta_h+\mu_h)+\beta_h\hat{h}_i) - p_{15}\theta_h - p_{24}\theta_m)x_1x_4\\
&+ (p_{15}((\theta_m+\mu_m)+(\gamma_h+\mu_h)+\beta_m\hat{h}_i) - p_{11}\beta_m(1-\hat{m}_e-\hat{m}_i) - p_{25}\theta_m)x_1x_5\\
&+ (p_{12}\beta_m\hat{h}_i + p_{23}\beta_h\hat{h}_s + p_{22}\mu_m - p_{24}\beta_h\hat{h}_s)x_2^2\\
&+ (p_{13}\beta_m\hat{h}_i + p_{23}(\beta_m\hat{m}_i+\mu_h+\mu_m) - p_{24}\beta_h\hat{m}_i + p_{33}\beta_h\hat{h}_s - p_{34}\beta_h\hat{h}_s)x_2x_3\\
&+ (p_{14}\beta_m\hat{h}_i + p_{24}((\theta_h+\mu_h)+\mu_m) - p_{25}\theta_h + \beta_h\hat{h}_s(p_{34}-p_{44}))x_2x_4\\
&+ (p_{15}\beta_m\hat{h}_i - p_{12}\beta_m(1-\hat{m}_e-\hat{m}_i) + p_{25}((\gamma_h+\mu_h)+\mu_m)\\
&+ (p_{33}(\beta_m\hat{m}_i+\mu_h) - p_{34}\beta_h\hat{m}_i)x_3^2 + (p_{35}-p_{45})\beta_h\hat{h}_s)x_2x_5\\
&+ (p_{34}(\beta_m\hat{m}_i+(\theta_h+\mu_h)+\mu_h) - p_{35}\theta_h - p_{44}\beta_h\hat{m}_i)x_3x_4\\
&+ (p_{35}((\gamma_h+\mu_h)+\beta_m\hat{m}_i+\mu_h) - p_{45}\beta_h\hat{m}_i - p_{13}\beta_m(1-\hat{m}_e-\hat{m}_i))x_3x_5\\
&+ (p_{44}(\theta_h+\mu_h) - p_{45}\theta_h)x_4^2\\
&+ (p_{45}((\theta_h+\mu_h)+(\gamma_h+\mu_h)) - p_{14}\beta_m(1-\hat{m}_e-\hat{m}_i) - p_{55}\theta_h)x_4x_5\\
&+ (p_{55}(\gamma_h+\mu_h) - p_{15}\beta_m(1-\hat{m}_e-\hat{m}_i))x_5^2\\
&+ ((p_{13}-p_{14})\beta_h)x_1x_2x_3 + ((p_{11}+p_{12})\beta_m)x_1x_2x_5 + p_{14}\beta_m x_2x_4x_5\\
&+ p_{13}\beta_m x_1x_3x_5 + p_{14}\beta_m x_1x_4x_5 + ((p_{34}+p_{44})\beta_h)x_2x_3x_4\\
&+ ((p_{35}-p_{45})\beta_h + p_{13}\beta_m)x_2x_3x_5 + p_{15}\beta_m x_1x_5^2 + ((p_{23}-p_{24})\beta_h)x_2^2x_3\\
&+ ((p_{33}-p_{34})\beta_h)x_2x_3^2 + p_{11}\beta_m x_1^2x_5 + p_{12}\beta_m x_2^2x_5 + p_{15}\beta_m x_2x_5^2]
\end{aligned}
$$

In this case the matrix, Q of the orbital derivative is given by Equation (6.9). □

Remark. To identify whether one should consider the system given by Equation (6.5) or Equation (6.8), we must know the R_0's value. Figure 6.1 shows the regions in which each equilibrium point emerges according to the values of R_{0_M} and R_{0_H}.

Figures 6.2 and 6.3 present the regions defined by the ranges of the param-

$$Q = \begin{bmatrix}
2p_{11}K_1 - p_{12}\theta_m & (p_{11}\beta_m\hat{h}_i + p_{12}K_2 + \beta_h\hat{h}_s(p_{13} - p_{14}) - p_{22}\theta_m) & (p_{13}K_3 - p_{14}\beta_h\hat{m}_i - p_{23}\theta_m) & (p_{14}K_4 - p_{15}\theta_h - p_{24}\theta_m) & (p_{15}K_5 - p_{11}\beta_m K_0 - p_{25}\theta_m) & p_{11}\beta_m & (p_{13} - p_{14})\beta_h & (p_{11} + p_{12})\beta_m \\
(p_{11}\beta_m\hat{h}_i + p_{12}K_2 + \beta_h\hat{h}_s(p_{13} - p_{14}) - p_{22}\theta_m) & (p_{12}\beta_m\hat{h}_i + p_{22}\mu_m(p_{23} - p_{24}\beta_h\hat{h}_s) & (p_{13}\beta_m\hat{h}_i + p_{23}K_6 - p_{24}\beta_h\hat{m}_i + (p_{33} - p_{34})\beta_h\hat{h}_s) & (p_{14}\beta_m\hat{h}_i + p_{24}K_7 - p_{25}\theta_h + \beta_h\hat{h}_s(p_{34} - p_{44})) & (p_{15}\beta_m\hat{h}_i - p_{12}\beta_m K_0 + p_{25}K_8 + (p_{35} - p_{45})\beta_h\hat{h}_s) & (p_{11} + p_{12}\beta_m) & (p_{23} - p_{24})\beta_h & p_{12}\beta_m \\
(p_{13}K_3 - p_{14}\beta_h\hat{m}_i - p_{23}\theta_m) & (p_{13}\beta_m\hat{h}_i + p_{23}K_6 - p_{24}\beta_h\hat{m}_i + (p_{33} - p_{34})\beta_h\hat{h}_s) & (p_{33}(\beta_m\hat{m}_i + \mu_h) - p_{34}\beta_h\hat{m}_i) & (p_{34}K_9 - p_{35}\theta_h - p_{44}\beta_h\hat{m}_i) & (p_{35}K_{10} - p_{45}\beta_h\hat{m}_i - p_{13}\beta_m K_0) & p_{13}\beta_m & (p_{33} - p_{34})\beta_h & (p_{13}\beta_m + (p_{35} - p_{45})\beta_h) \\
(p_{14}K_4 - p_{15}\theta_h - p_{24}\theta_m) & (p_{14}\beta_m\hat{h}_i + p_{24}K_7 - p_{25}\theta_h + \beta_h\hat{h}_s(p_{34} - p_{44})) & (p_{34}K_9 - p_{35}\theta_h - p_{44}\beta_h\hat{m}_i) & (p_{44}(\theta_h + \mu_h) - p_{45}\theta_h) & (p_{45}K_{11} - p_{14}\beta_m K_0 - p_{55}\theta_h) & p_{14}\beta_m & (p_{34} + p_{44})\beta_h & p_{14}\beta_m \\
(p_{15}K_5 - p_{11}\beta_m K_0 - p_{25}\theta_m) & (p_{15}\beta_m\hat{h}_i - p_{12}\beta_m K_0 + p_{25}K_8 + (p_{35} - p_{45})\beta_h\hat{h}_s) & (p_{35}K_{10} - p_{45}\beta_h\hat{m}_i - p_{13}\beta_m K_0) & (p_{45}K_{11} - p_{14}\beta_m K_0 - p_{55}\theta_h) & (p_{55}(\gamma_h + \mu_h) - p_{15}K_0) & p_{15}\beta_m & p_{13}\beta_m + (p_{35} - p_{45})\beta_h & p_{15}\beta_m \\
p_{11}\beta_m & (p_{11} + p_{12}\beta_m) & p_{13}\beta_m & p_{14}\beta_m & p_{15}\beta_m & 0 & 0 & 0 \\
(p_{13} - p_{14})\beta_h & (p_{23} - p_{24})\beta_h & (p_{33} - p_{34})\beta_h & (p_{34} + p_{44})\beta_h & p_{13}\beta_m + (p_{35} - p_{45})\beta_h & 0 & 0 & 0 \\
(p_{11} + p_{12})\beta_m & p_{12}\beta_m & (p_{13}\beta_m + (p_{35} - p_{45})\beta_h) & p_{14}\beta_m & p_{15}\beta_m & 0 & 0 & 0
\end{bmatrix} \tag{6.9}$$

where

$$\begin{aligned}
K_0 &= 1 - \hat{m}_e - \hat{m}_i \\
K_1 &= \beta_m\hat{h}_i + (\theta_m + \mu_m) \\
K_2 &= (\theta_m + \mu_m) + \mu_m + \beta_m\hat{h}_i \\
K_3 &= (\theta_m + \mu_m) + \beta_m\hat{h}_i + \beta_m\hat{m}_i + \mu_h \\
K_4 &= (\theta_m + \mu_m) + (\theta_h + \mu_h) + \beta_h\hat{h}_i \\
K_5 &= (\theta_m + \mu_m) + (\gamma_h + \mu_h) + \beta_m\hat{h}_i \\
K_6 &= \beta_m\hat{m}_i + \mu_h + \mu_m \\
K_7 &= (\theta_h + \mu_h) + \mu_m \\
K_8 &= (\gamma_h + \mu_h) + \mu_h \\
K_9 &= \beta_m\hat{m}_i + (\theta_h + \mu_h) + \mu_h \\
K_{10} &= (\gamma_h + \mu_h) + \beta_m\hat{m}_i + \mu_h \\
K_{11} &= (\theta_h + \mu_h) + (\gamma_h + \mu_h)
\end{aligned}$$

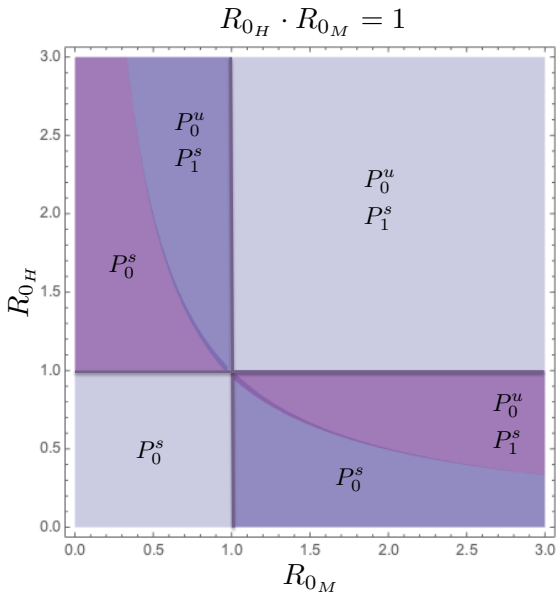

Figure 6.1 – In Figure 6.1 we plot $R_0 = 1$. P_0 corresponds to the steady-state regarding the disease-free point. P_1 corresponds to the steady-state regarding the endemic point. The superscripts s and u stand for, respectively, stable and unstable.

eters given in Table 3.1 and the region obtained after discarding incompatible regions with the reported data (see Equations (5.9) and (5.10)). Then we consider the values for R_{0_M} and R_{0_H} in each region for Neiva and Itagüí, respectively. The biological region defined by the parameters values in Table 3.1 is the same for both municipalities. Figure 6.2 shows that for Itagüí the input region, Z for Algorithm 2 consider values for both R_{0_M} and R_{0_H} greater and less than one. While Figure 6.3 shows that for Neiva the input region, Z for Algorithm 2 consider only parameters values such that $R_{0_M} < 1$ and $R_{0_H} > 1$.

Example 6.4.1. Consider the system given by Equation (6.5). For Itagüí, we consider the parameters values $\theta_m = 0.6$, $\theta_h = 1.3$, $\mu_h = 0.00023$, $\beta_m = 0.18$, $\beta_h = 1.78$, $\mu_m = 0.23$, and $\gamma_h = 1.71$. For these values, $R_0 = 0.77$, $R_{0_H} = 1.02$, and $R_{0_M} = 0.75$. After replacing these values in the matrices P and Q in Theorem 6.4.2, we

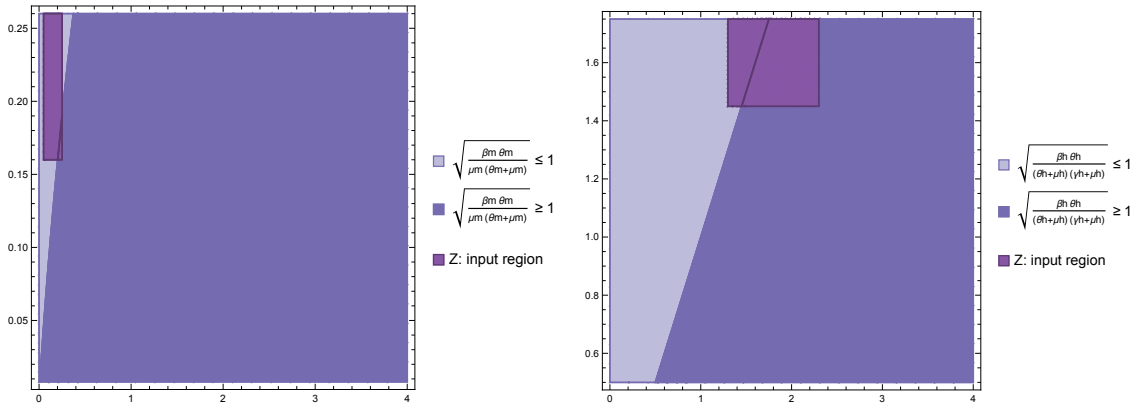

(a) (b)

Figure 6.2 – In Figure 6.2(a), the horizontal axis corresponds to β_m range, while the vertical axis corresponds to θ_m range. In Figure 6.2(b), the horizontal axis corresponds to β_h range, while the vertical axis corresponds to θ_h range. The small rectangle correspond to the input region, Z for Algorithm 2. These regions correspond to parameter values for Itagüí municipality.

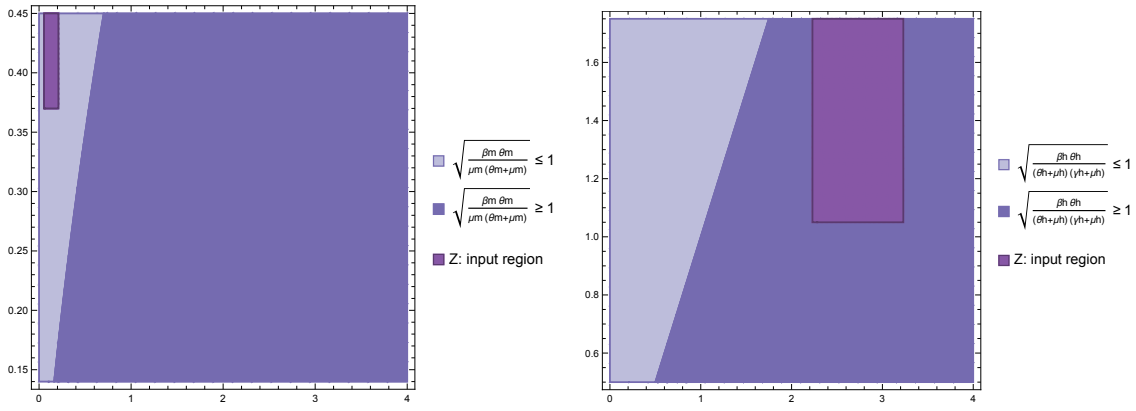

(a) (b)

Figure 6.3 – In Figure 6.3(a), the horizontal axis corresponds to β_m range, while the vertical axis corresponds to θ_m range. In Figure 6.3(b), the horizontal axis corresponds to β_h range, while the vertical axis corresponds to θ_h range. The small rectangle correspond to the input region, Z for Algorithm 2. These regions correspond to parameter values for Neiva municipality.

apply Sylvester's criterion to find the Lyapunov function

$$\begin{aligned}\mathcal{V}(x) = 30.4448[&x_1^2 + 0.992037x_1x_2 + 1.25254x_1x_3 + 0.856998x_1x_4\\ &+ 0.600645x_1x_5 + 0.855158x_2^2 + 0.833685x_2x_3 + 0.560394x_2x_4\\ &+ 0.447515x_2x_5 + 0.885896x_3^2 + 1.30045x_3x_4 + 0.69718x_3x_5\\ &+ 0.539584x_4^2 + 0.562744x_4x_5 + 0.36002x_5^2]\end{aligned}$$

For Neiva the Lyapunov function is given by

$$\begin{aligned}\mathcal{V}(x) = 30.2278[&x_1^2 + 1.14689x_1x_2 + 1.2623x_1x_3 + 0.951502x_1x_4\\ &+ 0.688759x_1x_5 + 1.03729x_2^2 + 0.907342x_2x_3 + 0.688296x_2x_4\\ &+ 0.563226x_2x_5 + 0.986879x_3^2 + 1.58359x_3x_4 + 0.850995x_3x_5\\ &+ 0.694854x_4^2 + 0.720839x_4x_5 + 0.466534x_5^2]\end{aligned}$$

when parameters values are $\theta_m = 0.8$, $\theta_h = 1.3$, $\mu_h = 0.00011$, $\beta_m = 0.17$, $\beta_h = 2.6$, $\mu_m = 0.44$, and $\gamma_h = 1.65$. For these values, $R_0 = 0.63$, $R_{0_H} = 1.26$, and $R_{0_M} = 0.5$.

On the other hand, to illustrate the case when $R_0 > 1$ we define the parameters values as $\theta_m = 0.8$, $\theta_h = 1.3$, $\mu_h = 0.000011$, $\beta_m = 0.3$, $\beta_h = 2$, $\mu_m = 0.23$, and $\gamma_h = 1.65$. For these values, $R_0 = 1.11$, $R_{0_H} = 1.1$, and $R_{0_M} = 1.01$. In this case, we have to consider the system given by Equation (6.8) and the equilibrium point in Equation (6.4). Then, the Lyapunov function is

$$\begin{aligned}\mathcal{V}(x) = 28.0968[&x_1^2 + 1.14173x_1x_2 + 1.3848x_1x_3 + 0.965742x_1x_4\\ &+ 0.737869x_1x_5 + 0.88792x_2^2 + 0.962711x_2x_3 + 0.663323x_2x_4\\ &+ 0.553299x_2x_5 + 1.0006x_3^2 + 1.48918x_3x_4 + 0.828466x_3x_5\\ &+ 0.625036x_4^2 + 0.698833x_4x_5 + 0.432214x_5^2]\end{aligned}$$

6.5 Discussion and conclusion

This chapter presented a strategy to construct new Lyapunov functions in addition to the classical functions used in mathematical epidemiology. To apply it, first, we must verify that the system is polynomial and exponentially stable. As an example of using this approach, we considered Model 3.3.

In [35], the author proposed to perform a preliminary transformation to the space of state variables to construct Lyapunov functions for population models. This transformation should map the positive orthant into the whole space ($\mathbb{R}^n$). Thus, the Lyapunov function would be biologically meaningful. This strategy has also been applied to epidemiological models [105, 48]. In contrast to this approach, in this work, we exploit the fact that the system is bounded to construct and prove that the matrices are positive definite.

As we computed in Chapter 3, Model 3.3 has two equilibrium points, the disease-free point, and the endemic point. The R_0 value tells us which equilibrium point emerges. For Itagüí and Neiva, we calculated the regions where R_{0_H} and R_{0_M} are greater than or equal to one (See Fig 1 and 2). Additionally, Figure 6.1 shows the regions where each equilibrium point emerged according to the R_0 value. As for the interval parameters estimated by PISA, R_0 is less than one, and there exists a unique equilibrium point for Model 3.3, the disease-free point, which is globally stable.

Nevertheless, it is important to note again that the value of R_0 depends on the strategy followed to calculate it, as explained by [99]. For instance, in [54], the authors show that in some cities where dengue outbreaks occur, the parameter values that fit the data well can produce a R_0 value less than one. However, in our case study, there are always intervals where R_{0_H} is greater than one, and this parameter is the one that finally reflects the transmission in humans.

It is worth mentioning that the stability analysis is critical because it permits

us to define the stability region of each equilibrium point. In this way, it is confident that the model trajectories will have the same behavior when considering initial conditions in this region. This fact is valuable when one considers uncertain initial conditions.

Bibliography of the current chapter

[24] Leah Edelstein-Keshet. Mathematical models in biology. Vol. 46. Siam, 1988 (cit. on p. 152).

[34] Peter Giesl and Sigurdur Hafstein. Review on computational methods for Lyapunov functions. Discrete and Continuous Dynamical Systems-Series B 20.8 (2015), pp. 2291–2331 (cit. on p. 148).

[35] BS Goh. Global stability in a class of prey-predator models. Bulletin of Mathematical Biology 40.4 (1978), pp. 525–533 (cit. on p. 162).

[36] BS Goh. Global stability in many-species systems. The American Naturalist 111.977 (1977), pp. 135–143 (cit. on p. 148).

[37] BS Goh. Global stability in two species interactions. Journal of Mathematical Biology 3.3-4 (1976), pp. 313–318 (cit. on p. 148).

[48] Andrei Korobeinikov and Graeme C Wake. Lyapunov functions and global stability for SIR, SIRS, and SIS epidemiological models. Applied Mathematics Letters 15.8 (2002), pp. 955–960 (cit. on pp. 148, 162).

[50] Shu Liao and Jin Wang. Global stability analysis of epidemiological models based on Volterra–Lyapunov stable matrices. Chaos, Solitons & Fractals 45.7 (2012), pp. 966–977 (cit. on p. 148).

[54] Diana Paola Lizarralde-Bejarano, Daniel Rojas-Díaz, Sair Arboleda-Sánchez, and María Eugenia Puerta-Yepes. Sensitivity, uncertainty and identifiability analyses to define a dengue transmission model with real data of an endemic municipality of Colombia. PLoS ONE 15.3 (2020), e0229668. DOI: https://doi.org/10.1371/journal.pone.0229668 (cit. on pp. 58, 81, 131, 162).

[83] Pablo A Parrilo. Semidefinite programming relaxations for semialgebraic problems. Mathematical programming 96.2 (2003), pp. 293–320 (cit. on pp. 148–150).

[84] Pablo A Parrilo. Structured semidefinite programs and semialgebraic geometry methods in robustness and optimization. California Institute of Technology, 2000 (cit. on pp. 12, 148–150).

[85] Matthew M Peet. Exponentially stable nonlinear systems have polynomial Lyapunov functions on bounded regions. IEEE Transactions on Automatic Control 54.5 (2009), pp. 979–987 (cit. on pp. 148, 149).

[97] Zhisheng Shuai and Pauline van den Driessche. Global stability of infectious disease models using Lyapunov functions. SIAM Journal on Applied Mathematics 73.4 (2013), pp. 1513–1532 (cit. on p. 148).

[99] Robert J. Smith, Jing Li, and Daniel Blakeley. The failure of R_0. Computational and Mathematical Methods in Medicine 2011 (2011). DOI: https://doi.org/10.1155/2011/527610 (cit. on pp. 25, 162).

[105] P Van den Driessche, M Li, and J Muldowney. Global stability of SEIRS models in epidemiology. Canadian Applied Mathematics Quarterly 7 (1999), pp. 409–425 (cit. on pp. 148, 162).

Conclusions and future work

The purpose of the current research was to apply the theory of interval analysis to include uncertainty in the ODEs that simulate dengue transmission. As a case study, we considered two outbreaks of different magnitudes that occurred in 2016 in two endemic municipalities of Colombia, Itagüí and Neiva.

In the formulation of dengue transmission models, we focused on the fitting data problem. To do so, the limited available information was (i) the number of reported dengue cases per epidemiological week; (ii) the results from experimental assays with mosquito population; and (iii) the information from the WHO to define the ranges of parameters that simulate the transition between infectious states and recovery states in humans (θ_m, θ_h, and γ_h).

The main difference between the proposed models is how we included the vector's development stages to explain its entry into the adult population and the beginning of the dengue transmission cycle. Thus, the complexity in terms of the number of parameters and state variables is different between the models.

Before estimating the parameter's models, we calculated the elasticity of the basic reproductive number (R_0) for each parameter and we performed the structural identifiability analysis to each model. These analyses allowed us to identify which parameters influenced more new dengue cases and if it is possible to estimate them uniquely when we assumed noise-free data. The elasticity's results of R_0 depend on the parameter values, except for the elasticity concerning the transmission probabilities (β_m and β_h) that are constant (see Table 3.3).

However, as the R_0 is the same for the three models, elasticities do not change between models. On the other hand, Table 3.5 showed that our proposed models are unidentifiable. Moreover, it is important to notice that the unidentifiable parameters are precisely those that simulate the transitions and mortality in the vector's developmental stages. The unidentifiable initial conditions correspond to all the vector's initial conditions. The previous observation suggests that we need more information about the mosquito population to have structural identifiable models.

In the posterior analysis, we only consider Model 3.3. This model is the only one that does not consider the vector's development stages. Therefore, we only have to fix the value of one unidentifiable parameter to make it locally structural identifiable. Furthermore, Model 3.3 has a lower dimension and fewer parameters propagating error in intermediate integration steps than the other models; hence it is computationally faster.

We proposed a method to include uncertainty in parameters and initial conditions through the application of interval analysis. Later on, we formulated an algorithm to estimate interval parameters. Then, we detected how much noise in the data could explain this estimation from a compatibility measure.

To select the uncertain parameters and initial conditions that we included in the formulation of the interval systems, we used the elasticity and structural identifiability analysis results. We did that because of the high number of parameters and the high dimensions of the system.

To estimate parameters, we have to solve the direct problem, i.e. we need to solve the formulated model for each given parameter and initial condition. For the models proposed here, these solutions are obtained numerically.

This study was interested in obtaining mathematically and computationally verified solutions when considered uncertainty in parameter and initial conditions. After reviewing the algorithms and software available to solve interval

ODEs, we found that the VSPODE software (Validating Solver for Parametric ODEs) was the most suitable tool that fulfilled our needs. As far as we know, VSPODE is the only software in which parameters can be defined as real closed intervals without increasing the dimension of the ODEs. Furthermore, VSPODE has been applied to obtain rigorous enclosures for psychological, ecological, and epidemiological models that compare its results against Monte Carlo simulations exhibiting a better performance, see [26, 27, 25].

With VSPODE as our chosen tool for solving interval systems, we addressed our primary concern, the fitting data problem. To achieve this goal, we formulated a novel algorithm based on modifying the best-first search algorithm jointly constraining our case study to delete sub-boxes where we do not find reasonable solutions systematically. Algorithm 2 allows us to compute narrow enclosures. Here, we established the width of the boxes as one of the stopping criteria for the algorithm. Moreover, an interesting result of our approach is that depending on the number of nodes allowed for further refinements; it is possible to find disconnected regions where the objective function value does not differ significantly in each region. It would be up to the modeller to decide which estimation they use. This characteristic is beneficial in biological applications, where there are certain multiple minima.

To evaluate the error level that can explain the estimations obtained, we added noise to the data that follows a uniform distribution, and then we calculate the strong compatibility measure. Next, we consider two scenarios. In the first scenario, we obtained that the four parameters' estimated can explain up to 30% of the under-reporting in reported cases of dengue. While in the second scenario, we obtained that the uncertain initial conditions can explain up to 40% of the under-reporting. However, neither the estimated parameters nor the estimated initial conditions belong to the tolerable set.

The method proposed here contributes to the modeling uncertainty in epi-

demiological models without making any additional assumptions about the available information. Here, we exploited the characteristics and knowledge that we have about our case study to define criteria that allow the algorithm to converge to coherent biological solutions. The aforementioned method highlights the potential usefulness of interval analysis theory to obtain rigorous solutions in epidemiological models using real data.

Further research might explore solutions to the parameter estimation problem for other types of models through interval uncertainty for parameters and initial conditions for other types of models. For instance, discrete models or models based on systems of differential algebraic equations (DAEs) with index[3] greater than one. This future work implies the developing an interval solver for this kind of systems with equiparable quality of existing interval ODE solvers, as pointed out by Nedialkov for DAE solvers in [71]. Also, future studies should try to weaken the requirement for differentiability and continuity in the vector field to permit the application of interval arithmetic algorithms to a larger number of systems.

From the mathematical epidemiology perspective, as ODEs simulate many phenomena, it can be useful to design solvers for specific model characteristics. In this way, it is possible to exploit those characteristics to design better strategies that reduce the dependency problem and the wrapping effect, making the corresponding algorithm more efficient and capable of managing at the same time more uncertainty parameters and initial conditions for longer integration periods.

[3]The *index* is the minimum number of differentation steps required to transform a DAE into an ODE.

Bibliography of the current chapter

[25] Joshua Enszer and Mark Stadtherr. Verified Solution Method for Population Epidemiology Models with Uncertainty. International Journal of Applied Mathematics and Computer Science 19.3 (2009), pp. 501–512. DOI: https://doi.org/10.2478/v10006-009-0040-4 (cit. on pp. 46, 90, 92, 110, 168).

[26] Joshua A Enszer and Mark A Stadtherr. Verified Solution and Propagation of Uncertainty in Physiological Models. Reliable Computing 15.3 (2011), pp. 168–178 (cit. on pp. 90, 168).

[27] Joshua A. Enszer, D. Andrei Măces, and Mark A. Stadtherr. Probability bounds analysis for nonlinear population ecology models. Mathematical Biosciences 267 (2015), pp. 97–108. DOI: https://doi.org/10.1016/j.mbs.2015.06.012 (cit. on pp. 90, 168).

[71] Nedialko S Nedialkov. Interval tools for ODEs and DAEs. In: 12th GAMM-IMACS International Symposium on Scientific Computing, Computer Arithmetic and Validated Numerics (SCAN 2006). IEEE. 2006, pp. 4–4 (cit. on pp. 143, 169).

Bibliography

[1] Ben Adams and Michael Boots. How important is vertical transmission in mosquitoes for the persistence of dengue? Insights from a mathematical model. Epidemics 2.1 (2010), pp. 1–10 (cit. on p. 27).

[2] Roy M Anderson. The role of mathematical models in the study of HIV transmission and the epidemiology of AIDS. Journal of Acquired Immune Deficiency Syndromes 1.3 (1988), pp. 241–256 (cit. on p. 20).

[3] Mathieu Andraud, Niel Hens, Christiaan Marais, and Philippe Beutels. Dynamic epidemiological models for dengue transmission: a systematic review of structural approaches. PloS one 7.11 (2012), e49085 (cit. on p. 21).

[4] Richard C Aster, Brian Borchers, and Clifford H Thurber. Parameter estimation and inverse problems. Elsevier, 2018 (cit. on pp. 7, 119).

[5] Frank Ball et al. Seven challenges for metapopulation models of epidemics, including households models. Epidemics 10 (2015), pp. 63–67 (cit. on p. 22).

[6] L. C. Barros, R. C. Bassanezi, R. Z. G. Oliveira, and M. B. F. Leite. A disease evolution model with uncertain parameters. In: Proceedings Joint 9th IFSA World Congress and 20th NAFIPS International Conference (Cat. No. 01TH8569). Vol. 3. IEEE. 2001, pp. 1626–1630. DOI: https://doi.org/10.1109/NAFIPS.2001.943794 (cit. on pp. 46, 47, 110).

[7] L.C.DE Barros, M.B.Ferreira Leite, and R.C Bassanezi. The SI epidemiological models with a fuzzy transmission parameter. Computers & Mathematics with Applications 45.10 (2003), pp. 1619–1628. DOI: https://doi.org/10.1016/S0898-1221(03)00141-X (cit. on pp. 46, 110).

[8] Giuseppina Bellu, Maria Pia Saccomani, Stefania Audoly, and Leontina D'Angiò. DAISY: A new software tool to test global identifiability of biological and physiological systems. Computer Methods and Programs in Biomedicine 88.1 (2007), pp. 52–61. DOI: https://doi.org/10.1016/j.cmpb.2007.07.002 (cit. on p. 80).

[9] Samir Bhatt et al. The global distribution and burden of dengue. Nature 496.7446 (2013), pp. 504–507. DOI: https://doi.org/10.1038/nature12060 (cit. on pp. 103, 111).

[10] Oliver J Brady et al. Modelling adult Aedes aegypti and Aedes albopictus survival at different temperatures in laboratory and field settings. Parasites & Vectors 6.1 (2013), p. 351. DOI: 10.1186/1756-3305-6-351 (cit. on p. 18).

[11] Fred Brauer. Mathematical epidemiology: Past, present, and future. Infectious Disease Modelling 2.2 (2017), pp. 113–127. DOI: https://doi.org/10.1016/j.idm.2017.02.001 (cit. on pp. 19, 23, 24).

[12] Tom Britton and David Lindenstrand. Epidemic modelling: Aspects where stochasticity matters. Mathematical Biosciences 222.2 (2009), pp. 109–116. DOI: https://doi.org/10.1016/j.mbs.2009.10.001 (cit. on pp. 46, 47, 110).

[13] JS Brownstein, E Hett, and SL ONeill. The potential of virulent Wolbachia to modulate disease transmission by insects. Journal of invertebrate pathology 84.1 (2003), pp. 24–29 (cit. on p. 27).

[14] Alexandra Catano-Lopez, Daniel Rojas-Diaz, Henry Laniado, Sair Arboleda-Sánchez, María Eugenia Puerta-Yepes, and Diana Paola Lizarralde-Bejarano. An alternative model to explain the vectorial capacity using as example *Aedes aegypti* case in dengue transmission. Heliyon 5.10 (2019), e02577. DOI: https://doi.org/10.1016/j.heliyon.2019.e02577 (cit. on p. 111).

[15] Oana-Teodora Chis, Julio R Banga, and Eva Balsa-Canto. Structural Identifiability of systems biology models: A critical comparison of methods. PLoS ONE 6.11 (2011), e27755. DOI: https://doi.org/10.1371/journal.pone.0027755 (cit. on p. 80).

[16] Oana Chiş, Julio R. Banga, and Eva Balsa-Canto. GenSSI: A software toolbox for structural identifiability analysis of biological models. Bioinformatics 27.18 (2011), pp. 2610–2611. DOI: https://doi.org/10.1093/bioinformatics/btr431 (cit. on p. 80).

[17] Laurent Coudeville and Geoff P Garnett. Transmission dynamics of the four dengue serotypes in southern Vietnam and the potential impact of vaccination. PloS one 7.12 (2012), e51244 (cit. on pp. 27, 81).

[18] Hend Dawood. Interval mathematics as a potential weapon against uncertainty. In: Mathematics of uncertainty modeling in the analysis of engineering and science problems. IGI Global, 2014, pp. 1–38 (cit. on p. 53).

[19] Michel De Lara and Lilian Sofia Sepulveda Salcedo. Viable control of an epidemiological model. Mathematical biosciences 280 (2016), pp. 24–37 (cit. on pp. 26, 81).

[20] Sara Del Valle, Herbert Hethcote, James M Hyman, and Carlos Castillo-Chavez. Effects of behavioral changes in a smallpox attack model. Mathematical biosciences 195.2 (2005), pp. 228–251 (cit. on p. 20).

[21] Yamille Del Valle, Ganesh Kumar Venayagamoorthy, Salman Mohagheghi, Jean-Carlos Hernandez, and Ronald G Harley. Particle swarm optimization: basic concepts, variants and applications in power systems. IEEE Transactions on evolutionary computation 12.2 (2008), pp. 171–195 (cit. on p. 7).

[22] O. Diekmann, J. A.P. Heesterbeek, and J. A.J. Metz. On the definition and the computation of the basic reproduction ratio R_0 in models for infectious diseases in heterogeneous populations. Journal of Mathematical Biology 28.4 (1990), pp. 365–382. DOI: https://doi.org/10.1007/BF00178324 (cit. on pp. 25, 83).

[23] O. Diekmann, J.A.P. Heesterbeek, and M.G. Roberts. The construction of next-generation matrices for compartmental epidemic models. Journal of the Royal Society Interface 7.47 (2010), pp. 873–885. DOI: https://doi.org/10.1098/rsif.2009.0386 (cit. on pp. 25, 83).

[24] Leah Edelstein-Keshet. Mathematical models in biology. Vol. 46. Siam, 1988 (cit. on p. 152).

[25] Joshua Enszer and Mark Stadtherr. Verified Solution Method for Population Epidemiology Models with Uncertainty. International Journal of Applied Mathematics and Computer Science 19.3 (2009), pp. 501–512. DOI: https://doi.org/10.2478/v10006-009-0040-4 (cit. on pp. 46, 90, 92, 110, 168).

[26] Joshua A Enszer and Mark A Stadtherr. Verified Solution and Propagation of Uncertainty in Physiological Models. Reliable Computing 15.3 (2011), pp. 168–178 (cit. on pp. 90, 168).

[27] Joshua A. Enszer, D. Andrei Măces, and Mark A. Stadtherr. Probability bounds analysis for nonlinear population ecology models. Mathematical Biosciences 267 (2015), pp. 97–108. DOI: https://doi.org/10.1016/j.mbs.2015.06.012 (cit. on pp. 90, 168).

[28] Lourdes Esteva and Cristobal Vargas. A model for dengue disease with variable human population. Journal of Mathematical Biology 38.3 (1999), pp. 220–240. DOI: https://doi.org/10.1007/s002850050147 (cit. on pp. 27, 59).

[29] Lourdes Esteva and Cristobal Vargas. Analysis of a dengue disease transmission model. Mathematical Biosciences 150.2 (1998), pp. 131–151. DOI: https://doi.org/10.1016/S0025-5564(98)10003-2 (cit. on pp. 27, 62).

[30] Lourdes Esteva and Cristobal Vargas. Coexistence of different serotypes of dengue virus. Journal of Mathematical Biology 46.1 (2003), pp. 31–47 (cit. on pp. 27, 83).

[31] Lourdes Esteva and Cristobal Vargas. Influence of vertical and mechanical transmission on the dynamics of dengue disease. Mathematical biosciences 167.1 (2000), pp. 51–64 (cit. on p. 27).

[32] Lourdes Esteva and Hyun Mo Yang. Assessing the effects of temperature and dengue virus load on dengue transmission. Journal of Biological Systems 23.04 (2015), p. 1550027. DOI: https://doi.org/10.1142/S0218339015500278 (cit. on pp. 27, 83).

[33] Zhilan Feng and Jorge X Velasco-Hernández. Competitive exclusion in a vector-host model for the dengue fever. Journal of mathematical biology 35.5 (1997), pp. 523–544 (cit. on pp. 20, 27).

[34] Peter Giesl and Sigurdur Hafstein. Review on computational methods for Lyapunov functions. Discrete and Continuous Dynamical Systems-Series B 20.8 (2015), pp. 2291–2331 (cit. on p. 148).

[35] BS Goh. Global stability in a class of prey-predator models. Bulletin of Mathematical Biology 40.4 (1978), pp. 525–533 (cit. on p. 162).

[36] BS Goh. Global stability in many-species systems. The American Naturalist 111.977 (1977), pp. 135–143 (cit. on p. 148).

[37] BS Goh. Global stability in two species interactions. Journal of Mathematical Biology 3.3-4 (1976), pp. 313–318 (cit. on p. 148).

[38] Jack K Hale and Hüseyin Koçak. Dynamics and bifurcations. Vol. 3. Springer Science & Business Media, 2012 (cit. on p. 38).

[39] Eldon Hansen and G William Walster. Global optimization using interval analysis: revised and expanded. Vol. 264. CRC Press, 2003 (cit. on pp. 7, 143).

[40] J A P Heesterbeek. A brief history of R_0 and a recipe for its calculation. Acta Biotheoretica 50.3 (2002), pp. 189–204. DOI: https://doi.org/10.1023/A:1016599411804 (cit. on p. 25).

[41] J.C. Helton, J.D. Johnson, and W.L. Oberkampf. An exploration of alternative approaches to the representation of uncertainty in model predictions. Reliability Engineering $&$ System Safety 85.1 (2004), pp. 39–71. DOI: https://doi.org/10.1016/j.ress.2004.03.025 (cit. on p. 110).

[42] Herbert W Hethcote. The basic epidemiology models: models, expressions for R_0, parameter estimation, and applications. In: Mathematical understanding of infectious disease dynamics. World Scientific, 2009, pp. 1–61. DOI: https://doi.org/10.1142/9789812834836_0001 (cit. on pp. 18, 45, 79).

[43] Harriet Hughes and Nicholas F Britton. Modelling the use of Wolbachia to control dengue fever transmission. Bulletin of mathematical biology 75.5 (2013), pp. 796–818 (cit. on p. 27).

[44] Michael A Johansson, Joachim Hombach, and Derek AT Cummings. Models of the impact of dengue vaccines: a review of current research and potential approaches. Vaccine 29.35 (2011), pp. 5860–5868 (cit. on pp. 21, 27).

[45] Johan Karlsson, Milena Anguelova, and Mats Jirstrand. An Efficient Method for Structural Identifiability Analysis of Large Dynamic Systems. 16th IFAC Symposium on System Identification. IFAC Proceedings Volumes 45.16 (2012), pp. 941–946. DOI: https://doi.org/10.3182/20120711-3-BE-2027.00381 (cit. on pp. 80, 81).

[46] William O Kermack and Anderson G McKendrick. A contribution to the mathematical theory of epidemics. In: Proceedings of the Royal Society of London A: Mathematical, Physical and Engineering Sciences. Vol. 115. 772. The Royal Society. 1927, pp. 700–721 (cit. on p. 20).

[47] Michel Kieffer and Eric Walter. Guaranteed estimation of the parameters of nonlinear continuous-time models: Contributions of interval analysis. International Journal of Adaptive Control and Signal Processing 25.3 (2011), pp. 191–207 (cit. on pp. 8, 143).

[48] Andrei Korobeinikov and Graeme C Wake. Lyapunov functions and global stability for SIR, SIRS, and SIS epidemiological models. Applied Mathematics Letters 15.8 (2002), pp. 955–960 (cit. on pp. 148, 162).

[49] Vladik Kreinovich and Sergey P Shary. Interval methods for data fitting under uncertainty: a probabilistic treatment (2015) (cit. on p. 51).

[50] Shu Liao and Jin Wang. Global stability analysis of epidemiological models based on Volterra–Lyapunov stable matrices. Chaos, Solitons & Fractals 45.7 (2012), pp. 966–977 (cit. on p. 148).

[51] Youdong Lin and Mark A. Stadtherr. Deterministic Global Optimization for Parameter Estimation of Dynamic Systems. Industrial & Engineering Chemistry Research 45.25 (Dec. 2006), pp. 8438–8448. DOI: 10.1021/ie0513907 (cit. on p. 143).

[52] Youdong Lin and Mark A. Stadtherr. Validated solutions of initial value problems for parametric ODEs. Applied Numerical Mathematics 57.10 (2007), pp. 1145–1162. DOI: https://doi.org/10.1016/j.apnum.2006.10.006 (cit. on pp. 4, 6, 11, 92, 117, 118, 143).

[53] Diana Paola Lizarralde-Bejarano, Sair Arboleda-Sánchez, and María Eugenia Puerta-Yepes. Understanding epidemics from mathematical models: Details of the 2010 dengue epidemic in Bello (Antioquia, Colombia). Applied Mathematical Modelling 43 (2017), pp. 566–578. DOI: https://doi.org/10.1016/j.apm.2016.11.022 (cit. on p. 66).

[54] Diana Paola Lizarralde-Bejarano, Daniel Rojas-Díaz, Sair Arboleda-Sánchez, and María Eugenia Puerta-Yepes. Sensitivity, uncertainty and identifiability analyses to define a dengue transmission model with real data of an endemic municipality of Colombia. PLoS ONE 15.3 (2020), e0229668. DOI: https://doi.org/10.1371/journal.pone.0229668 (cit. on pp. 58, 81, 131, 162).

[55] Rudolf J Lohner. On the ubiquity of the wrapping effect in the computation of error bounds. In: Perspectives on enclosure methods. Springer, 2001, pp. 201–216 (cit. on pp. 6, 36, 37, 90).

[56] Paula Mendes Luz, Cláudia Torres Codeço, Eduardo Massad, and Claudio José Struchiner. Uncertainties regarding dengue modeling in Rio de Janeiro, Brazil. Memórias do Instituto Oswaldo Cruz 98.7 (2003), pp. 871–878 (cit. on p. 46).

[57] Rafael Maciel-de-Freitas, Jacob C Koella, and Ricardo Lourenço-de-Oliveira. Lower survival rate, longevity and fecundity of Aedes aegypti (Diptera: Culicidae) females orally challenged with dengue virus serotype 2. Transactions of the Royal Society of Tropical Medicine and Hygiene 105.8 (2011), pp. 452–458 (cit. on p. 27).

[58] Kyoko Makino and Martin Berz. Remainder differential algebras and their applications. Computational Differentiation: Techniques, Applications and Tools (1996). Ed. by Martin Berz, Christian Bischof, George Corliss, and Andreas Griewank, pp. 63–74 (cit. on p. 94).

[59] Cecilia de Almeida Marques-Toledo et al. Dengue prediction by the web: Tweets are a useful tool for estimating and forecasting Dengue at country and city level. PLOS Neglected Tropical Diseases 11.7 (July 2017), pp. 1–20. DOI: https://doi.org/10.1371/journal.pntd.0005729 (cit. on p. 18).

[60] Maia Martcheva. Ch. 6: Fitting Models to Data in: An Introduction to Mathematical Epidemiology. Springer US, 2015, pp. 123–148. DOI: https://doi.org/10.1007/978-1-4899-7612-3_6 (cit. on p. 78).

[61] Maia Martcheva. "Ch.7: Analysis of Complex ODE Epidemic Models: Global Stability". In: *An Introduction to Mathematical Epidemiology*. Springer US, 2015, pp. 149–181. DOI: https://doi.org/10.1007/978-1-4899-7612-3_7 (cit. on p. 38).

[62] E Massad, FAB Coutinho, MN Burattini, and M Amaku. Estimation of R_0 from the initial phase of an outbreak of a vector-borne infection. Tropical medicine & international health 15.1 (2010), pp. 120–126 (cit. on p. 77).

[63] Eduardo Massad, Neli Regina Siqueira Ortega, Laecio Carvalho de Barros, and Claudio José Struchiner. Fuzzy Logic in Action: Applications in Epidemiology and Beyond. Springer Berlin Heidelberg, 2008. DOI: 10.1007/978-3-540-69094-8 (cit. on pp. 48, 49).

[64] Emanuele Massaro, Daniel Kondor, and Carlo Ratti. Assessing the interplay between human mobility and mosquito borne diseases in urban environments. Scientific Reports 9.1 (Nov. 2019). DOI: 10.1038/s41598-019-53127-z (cit. on p. 83).

[65] Wasim Maziak. Is uncertainty in complex disease epidemiology resolvable? Emerging Themes in Epidemiology 12.1 (2015), p. 7. DOI: https://doi.org/10.1186/s12982-015-0028-5 (cit. on p. 45).

[66] Nicolette Meshkat, Christine Er-zhen Kuo, and Joseph DiStefano. On finding and using identifiable parameter combinations in nonlinear dynamic systems biology models and COMBOS: A novel web implementation. PLoS ONE 9.10 (2014), e110261. DOI: https://doi.org/10.1371/journal.pone.0110261 (cit. on p. 80).

[67] Hongyu Miao, Xiaohua Xia, Alan S. Perelson, and Hulin Wu. On identifiability of nonlinear ODE models and applications in viral dynamics. SIAM review 53.1 (2011), pp. 3–39. DOI: https://doi.org/10.1137/090757009 (cit. on p. 80).

[68] Ramon E Moore, Fritz Bierbaum, and Klaus-Peter Schwiertz. Methods and applications of interval analysis. 2 (1979) (cit. on p. 29).

[69] Ramon E Moore, R Baker Kearfott, and Michael J Cloud. Introduction to Interval Analysis. Siam, 2009 (cit. on pp. 4, 29).

[70] SM Mousavi, R Tavakkoli-Moghaddam, H Hashemi, and SMH Mojtahedi. A novel approach based on non-parametric resampling with interval analysis for large engineering project risks. Safety science 49.10 (2011), pp. 1340–1348 (cit. on p. 48).

[71] Nedialko S Nedialkov. Interval tools for ODEs and DAEs. In: 12th GAMM-IMACS International Symposium on Scientific Computing, Computer Arithmetic and Validated Numerics (SCAN 2006). IEEE. 2006, pp. 4–4 (cit. on pp. 143, 169).

[72] Nedialko S Nedialkov, Kenneth R Jackson, and George F Corliss. Validated solutions of initial value problems for ordinary differential equations. Applied Mathematics and Computation 105.1 (1999), pp. 21–68 (cit. on pp. 6, 35, 90, 93, 110, 143).

[73] Markus Neher. From interval analysis to Taylor models-an Overview. In: Proc. IMACS. 2005 (cit. on p. 36).

[74] Markus Neher, Kenneth R Jackson, and Nedialko S Nedialkov. On Taylor model based integration of ODEs. SIAM Journal on Numerical Analysis 45.1 (2007), pp. 236–262 (cit. on pp. 6, 91).

[75] Arnold Neumaier. Complete search in continuous global optimization and constraint satisfaction. Acta Numerica 13 (May 2004), pp. 271–369. DOI: 10.1017/s0962492904000194 (cit. on p. 143).

[76] Hung T Nguyen. A note on the extension principle for fuzzy sets. Journal of Mathematical Analysis and Applications 64.2 (June 1978), pp. 369–380. DOI: 10.1016/0022-247x(78)90045-8 (cit. on p. 50).

[77] Hung T. Nguyen, Vladik Kreinovich, Berlin Wu, and Gang Xiang. Computing Statistics under Interval and Fuzzy Uncertainty. Springer Berlin Heidelberg, 2012. DOI: 10.1007/978-3-642-24905-1 (cit. on p. 48).

[78] Oms. Dengue y dengue grave. May 2016. URL: http://www.who.int/mediacentre/factsheets/fs117/es/ (cit. on p. 26).

[79] World Health Organization et al. Dengue: Guías para el diagnóstico, tratamiento, prevención y control: nueva edición. Tech. rep. Ginebra: Organización Mundial de la Salud, May 2009 (cit. on pp. 26, 66).

[80] Julio César Padilla, Diana Patricia Rojas, and Roberto Sáenz Gómez. Dengue en Colombia: epidemiología de la reemergencia a la hiperendemia. Guías de Impresión Ltda., 2012 (cit. on p. 26).

[81] Abhishek Pandey, Anuj Mubayi, and Jan Medlock. Comparing vector-host and SIR models for dengue transmission. Mathematical biosciences 246.2 (2013), pp. 252–259 (cit. on pp. 22, 26).

[82] Mayra Elizabeth Parra-Amaya, María Eugenia Puerta-Yepes, Diana Paola Lizarralde-Bejarano, and Sair Arboleda-Sánchez. Early detection for dengue using Local Indicator of Spatial Association (LISA) analysis. Diseases 4.2 (2016), p. 16. DOI: https://doi.org/10.3390/diseases4020016 (cit. on p. 18).

[83] Pablo A Parrilo. Semidefinite programming relaxations for semialgebraic problems. Mathematical programming 96.2 (2003), pp. 293–320 (cit. on pp. 148–150).

[84] Pablo A Parrilo. Structured semidefinite programs and semialgebraic geometry methods in robustness and optimization. California Institute of Technology, 2000 (cit. on pp. 12, 148–150).

[85] Matthew M Peet. Exponentially stable nonlinear systems have polynomial Lyapunov functions on bounded regions. IEEE Transactions on Automatic Control 54.5 (2009), pp. 979–987 (cit. on pp. 148, 149).

[86] M Peifer and J Timmer. Parameter estimation in ordinary differential equations for biochemical processes using the method of multiple shooting. IET Systems Biology 1.2 (2007), pp. 78–88 (cit. on p. 7).

[87] Víctor Hugo Peña-García, Omar Triana-Chávez, and Sair Arboleda-Sánchez. Estimating Effects of Temperature on Dengue Transmission in Colombian Cities. Annals of Global Health 83.3 (2017). Current Topics in Global Health, pp. 509–518. DOI: https://doi.org/10.1016/j.aogh.2017.10.011 (cit. on p. 18).

[88] Víctor Hugo Peña-García, Omar Triana-Chávez, Ana María Mejía-Jaramillo, Francisco J Díaz, Andrés Gómez-Palacio, and Sair Arboleda-Sánchez. Infection Rates by Dengue Virus in Mosquitoes and the Influence of Temperature May Be Related to Different Endemicity Patterns in Three Colombian Cities. International Journal of Environmental Research and Public Health 13.7 (2016), p. 734. DOI: https://doi.org/10.3390/ijerph13070734 (cit. on pp. 28, 111).

[89] Suani Tavares Rubim de Pinho, Claudia P Ferreira, Lourdes Esteva, FR Barreto, VC Morato e Silva, and MGL Teixeira. Modelling the dynamics of dengue real epidemics. Philosophical Transactions of the Royal Society A: Mathematical, Physical and Engineering Sciences 368.1933 (2010), pp. 5679–5693 (cit. on pp. 27, 81).

[90] Zhiping Qiu, Lihong Ma, and Xiaojun Wang. Non-probabilistic interval analysis method for dynamic response analysis of nonlinear systems with uncertainty. Journal of Sound and Vibration 319.1-2 (2009), pp. 531–540 (cit. on p. 48).

[91] Singiresu S Rao and L Berke. Analysis of uncertain structural systems using interval analysis. AIAA journal 35.4 (1997), pp. 727–735 (cit. on p. 46).

[92] Irfan A. Rather et al. Prevention and Control Strategies to Counter Dengue Virus Infection. Frontiers in Cellular and Infection Microbiology 7 (2017), p. 336. DOI: https://doi.org/10.3389/fcimb.2017.00336 (cit. on p. 111).

[93] Robert C Reiner et al. A systematic review of mathematical models of mosquito-borne pathogen transmission: 1970–2010. Journal of The Royal Society Interface 10.81 (2013), p. 20120921 (cit. on pp. 19, 21).

[94] Edward J Rothwell and Michael J Cloud. Automatic error analysis using intervals. IEEE Transactions on Education 55.1 (2012), pp. 9–15 (cit. on p. 48).

[95] Aymée de los Angeles Marrero Severo, Liuva M Pedroso Rodríguez, and Jorge Barrios Ginart. Algoritmos evolutivos en la solución de problemas de estimación de parámetros. Revista de Matemática: Teoría y Aplicaciones 13.2 (2006), pp. 139–150 (cit. on p. 7).

[96] Sergey P Shary. Weak and strong compatibility in data fitting problems under interval uncertainty. Advances in data science and adaptive analysis 12.1 (2020), p. 2050002 (cit. on pp. 117, 124).

[97] Zhisheng Shuai and Pauline van den Driessche. Global stability of infectious disease models using Lyapunov functions. SIAM Journal on Applied Mathematics 73.4 (2013), pp. 1513–1532 (cit. on p. 148).

[98] Boris Shulgin, Lewi Stone, and Zvia Agur. Pulse vaccination strategy in the SIR epidemic model. Bulletin of mathematical biology 60.6 (1998), pp. 1123–1148 (cit. on p. 21).

[99] Robert J. Smith, Jing Li, and Daniel Blakeley. The failure of R_0. Computational and Mathematical Methods in Medicine 2011 (2011). DOI: https://doi.org/10.1155/2011/527610 (cit. on pp. 25, 162).

[100] Luciano Stefanini and Barnabas Bede. Generalized Hukuhara differentiability of interval-valued functions and interval differential equations. Nonlinear Analysis: Theory, Methods and Applications 71.3-4 (2009), pp. 1311–1328 (cit. on p. 4).

[101] Anna M Stewart-Ibarra et al. Spatiotemporal clustering, climate periodicity, and social-ecological risk factors for dengue during an outbreak in Machala, Ecuador, in 2010. BMC Infectious Diseases 14.1 (2014), p. 610. DOI: https://doi.org/10.1186/s12879-014-0610-4 (cit. on p. 18).

[102] Khoa T. D. Thai et al. Age-Specificity of Clinical Dengue during Primary and Secondary Infections. PLoS Neglected Tropical Diseases 5.6 (June 2011). Ed. by Benedito A. Lopes da Fonseca, e1180. DOI: 10.1371/journal.pntd.0001180 (cit. on p. 83).

[103] Necibe Tuncer, Hayriye Gulbudak, Vincent L Cannataro, and Maia Martcheva. Structural and practical identifiability issues of immuno-epidemiological vector-host models with application to rift valley fever. Bulletin of mathematical biology 78.9 (2016), pp. 1796–1827 (cit. on p. 83).

[104] Necibe Tuncer, Maia Marctheva, Brian LaBarre, and Sabrina Payoute. Structural and practical identifiability analysis of Zika epidemiological models. Bulletin of mathematical biology 80.8 (2018), pp. 2209–2241 (cit. on p. 83).

[105] P Van den Driessche, M Li, and J Muldowney. Global stability of SEIRS models in epidemiology. Canadian Applied Mathematics Quarterly 7 (1999), pp. 409–425 (cit. on pp. 148, 162).

[106] Alejandro F. Villaverde, Antonio Barreiro, and Antonis Papachristodoulou. Structural Identifiability of Dynamic Systems Biology Models. PLoS Computational Biology 12.10 (2016), pp. 1–22. DOI: https://doi.org/10.1371/journal.pcbi.1005153 (cit. on p. 80).

[107] Éric Walter and Michel Kieffer. Guaranteed nonlinear parameter estimation in knowledge-based models. Journal of Computational and Applied Mathematics 199.2 (Feb. 2007), pp. 277–285. DOI: 10.1016/j.cam.2005.07.039 (cit. on p. 143).

[108] Liping Wang, Hongyong Zhao, Sergio Muniz Oliva, and Huaiping Zhu. Modeling the transmission and control of Zika in Brazil. Scientific Reports 7.1 (Aug. 2017). DOI: 10.1038/s41598-017-07264-y (cit. on p. 83).

[109] Tzai-Hung Wen, Neal H. Lin, Chun-Hung Lin, Chwan-Chuen King, and Ming-Daw Su. Spatial mapping of temporal risk characteristics to improve environmental health risk identification: A case study of a dengue epidemic in Taiwan. Science of the Total Environment 367.2 (2006), pp. 631–640. DOI: https://doi.org/10.1016/j.scitotenv.2006.02.009 (cit. on p. 18).

[110] Hyun Mo Yang and Cláudia Pio Ferreira. Assessing the effects of vector control on dengue transmission. Applied Mathematics and Computation 198.1 (2008), pp. 401–413 (cit. on pp. 21, 27).

[111] Hyun Mo Yang, Maria de Lourdes da Graca Macoris, Karen Cristina Galvani, and Maria Teresa Macoris Andrighetti. Follow up estimation of Aedes aegypti entomological parameters and mathematical modellings. Biosystems 103.3 (2011), pp. 360–371 (cit. on p. 27).

[112] Kenta Yashima and Akira Sasaki. Spotting Epidemic Keystones by R_0 Sensitivity Analysis: High-Risk Stations in the Tokyo Metropolitan Area. PLOS ONE 11.9 (Sept. 2016). Ed. by Hiroshi Nishiura, e0162406. DOI: 10.1371/journal.pone.0162406 (cit. on p. 83).

[113] H.-J. Zimmermann. An application-oriented view of modeling uncertainty. European Journal of Operational Research 122.2 (2000), pp. 190–198. DOI: https://doi.org/10.1016/S0377-2217(99)00228-3 (cit. on pp. 45, 110).

[114] H.-J. Zimmermann. The Extension Principle and Applications. In: Fuzzy Set Theory — and Its Applications. Springer Netherlands, 1991, pp. 53–67. DOI: 10.1007/978-94-015-7949-0_5 (cit. on p. 49).